

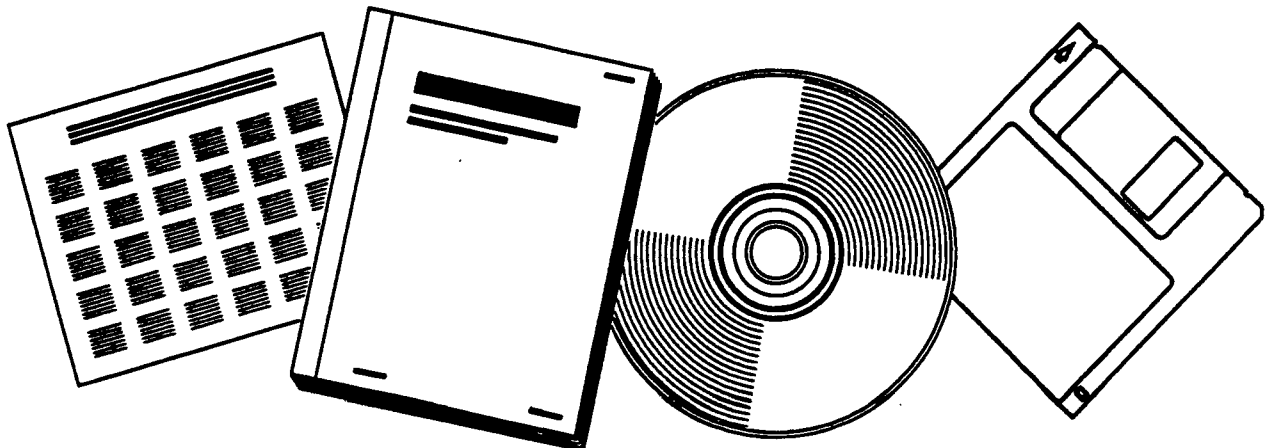


PB98-107022

NTIS[®]
Information is our business.

**PENDULUM TESTING OF FIXED-END W-BEAM
GUARDRAIL: FOIL TEST NUMBERS 96P001,
96P002, 96P003, 96P004, 96P005, AND
96P006**

JUL 97



U.S. DEPARTMENT OF COMMERCE
National Technical Information Service

Pendulum Testing of Fixed-End W-Beam Guardrail: FOIL Test

Numbers 96P001, 96P002, 96P003, 96P004, 96P005, and 96P006

PUBLICATION NO. FHWA-RD-97-078



PB98-107022

JULY 1997



U.S. Department of Transportation
Federal Highway Administration

Research and Development
Turner-Fairbank Highway Research Center
6300 Georgetown Pike
McLean, VA 22101-2296



REPRODUCED BY:
U.S. Department of Commerce
National Technical Information Service
Springfield, Virginia 22161

FOREWORD

This report documents the test procedures used and the test results from six pendulum crash tests conducted at the Federal Outdoor Impact Laboratory (FOIL) located in McLean, Virginia. The Federal Highway Administration (FHWA) has been evaluating advanced composite materials to be used in lieu of conventional materials used in the construction of roadside safety hardware. In particular, the FHWA has been investigating the use of fiber reinforced plastic (FRP) material in guardrail applications. The FRP material would be used in the design of a rail element as opposed to the conventional steel w-beam in use today. Baseline data on the dynamic properties of standard steel w-beam was needed to develop a design envelope for an FRP rail element. The FOIL's pendulum facility was used to conduct tests on steel w-beam rail elements rigidly anchored at both ends (a four-post configuration). The tests were conducted as part of an ongoing research effort to obtain baseline dynamic response data for standard w-beam guardrail.

This report (FHWA-RD-97-078) contains test data, photographs taken with high-speed film, and a summary of the test results. The weight of the FOIL pendulum with a rigid nose assembly was 912 kg. The tests were conducted at nominal speeds ranging from 20 km/h to 35 km/h.

This report will be of interest to all State departments of transportation; FHWA headquarters; region and division personnel; and highway safety researchers interested in the crashworthiness of roadside safety hardware.


A. George Ostensen, Director
Office of Safety and Traffic
Operations Research and Development

NOTICE

This document is disseminated under the sponsorship of the Department of Transportation in the interest of information exchange. The United States Government assumes no liability for its contents or use thereof. This report does not constitute a standard, specification, or regulation.

The United States Government does not endorse products or manufacturers. Trade and manufacturers' names appear in this report only because they are considered essential to the object of the document.

1. Report No. FHWA-RD-97-078		 PB98-107022		3. Recipient's Catalog No.	
4. Title and Subtitle PENDULUM TESTING OF FIXED-END W-BEAM GUARDRAIL: FOIL TEST NUMBERS 96P001, 96P002, 96P003, 96P004, 96P005, and 96P006		5. Report Date July 1997		6. Performing Organization Code	
		7. Author(s) Christopher M. Brown		8. Performing Organization Report No.	
9. Performing Organization Name and Address MiTech Incorporated 9430 Key West Avenue Suite 100 Rockville, MD 20850		10. Work Unit No. (TRAIS) 3A5F3142		11. Contract or Grant No. DTFH61-94-C-00008	
		12. Sponsoring Agency Name and Address Office of Safety and Traffic Operations R&D Federal Highway Administration 6300 Georgetown Pike McLean, VA 22101-2296		13. Type of Report and Period Covered Test Report, Feb/March 1996	
		14. Sponsoring Agency Code		15. Supplementary Notes Contracting Officer's Technical Representative (COTR)- Richard King, HSR-20	
16. Abstract This report contains the test setup and results from six pendulum crash tests performed at the Federal Outdoor Impact Lab (FOIL) located at the Turner-Fairbank Highway Research Center in McLean, Virginia. The tests were conducted on steel w-beam rail elements rigidly anchored at both ends (a four-post configuration). The tests were conducted as part of an ongoing research effort to obtain baseline data on the dynamic properties of standard steel w-beam in order to develop a design envelope for a fiber reinforced plastic rail element. The nominal weight of the FOIL pendulum with a rigid nose assembly was 912 kg. The tests were conducted at nominal speeds ranging from 20 km/h to 35 km/h. A 20-km/h and a 30-km/h test were conducted to observe the modified guardrail anchor cables attached to rigid anchor stanchions bolted to deep concrete foundations. These first two tests were conducted to observe their structural response before proceeding on to the 35-km/h tests. Four tests were conducted at 35 km/h. Results from the tests are presented as test summaries of data, graphs of data, and photographs taken before, during, and after the tests.					
17. Key Words FOIL, pendulum, rigid nose, w-beam, I-section, anchor stanchions			18. Distribution Statement No restrictions. This document is available to the public through the National Technical Information Service, Springfield, VA 22161.		
19. Security Classif. (of this report) Unclassified	20. Security Classif. (of this page) Unclassified	21. No. of Pages 86	22. Price		

SI* (MODERN METRIC) CONVERSION FACTORS

APPROXIMATE CONVERSIONS TO SI UNITS

APPROXIMATE CONVERSIONS FROM SI UNITS

Symbol	When You Know	Multiply By	To Find	Symbol	When You Know	Multiply By	To Find	Symbol
LENGTH								
in	inches	25.4	millimeters	mm	millimeters	0.039	inches	in
ft	feet	0.305	meters	m	meters	3.28	feet	ft
yd	yards	0.914	meters	m	kilometers	1.09	yards	yd
mi	miles	1.61	kilometers	km		0.621	miles	mi
AREA								
in ²	square inches	645.2	square millimeters	mm ²	square millimeters	0.0016	square inches	in ²
ft ²	square feet	0.093	square meters	m ²	square meters	10.764	square feet	ft ²
yd ²	square yards	0.836	square meters	m ²	square meters	1.195	square yards	yd ²
ac	acres	0.405	hectares	ha	hectares	2.47	acres	ac
mi ²	square miles	2.59	square kilometers	km ²	square kilometers	0.386	square miles	mi ²
VOLUME								
fl oz	fluid ounces	29.57	milliliters	mL	milliliters	0.034	fluid ounces	fl oz
gal	gallons	3.785	liters	L	liters	0.264	gallons	gal
ft ³	cubic feet	0.028	cubic meters	m ³	cubic meters	35.71	cubic feet	ft ³
yd ³	cubic yards	0.765	cubic meters	m ³	cubic meters	1.307	cubic yards	yd ³
NOTE: Volumes greater than 1000 l shall be shown in m ³ .								
MASS								
oz	ounces	28.35	grams	g	grams	0.035	ounces	oz
lb	pounds	0.454	kilograms	kg	kilograms	2.202	pounds	lb
T	short tons (2000 lb)	0.907	megagrams (or "metric ton")	Mg (or "t")	megagrams (or "metric ton")	1.103	short tons (2000 lb)	T
TEMPERATURE (exact)								
°F	Fahrenheit temperature	5(F-32)/9 or (F-32)/1.8	Celsius temperature	°C	Celsius temperature	1.8C + 32	Fahrenheit temperature	°F
ILLUMINATION								
fc	foot-candles	10.76	lux	lx	lux	0.0929	foot-candles	fc
fl	foot-Lamberts	3.426	candela/m ²	cd/m ²	candela/m ²	0.2919	foot-Lamberts	fl
FORCE and PRESSURE or STRESS								
lbf	poundforce	4.45	newtons	N	newtons	0.225	poundforce	lbf
lbf/in ²	poundforce per square inch	6.89	kilopascals	kPa	kilopascals	0.145	poundforce per square inch	lbf/in ²

* SI is the symbol for the International System of Units. Appropriate rounding should be made to comply with Section 4 of ASTM E380.

TABLE OF CONTENTS

BACKGROUND 1

SCOPE 1

TEST MATRIX 2

PENDULUM 2

TEST ARTICLE 3

DATA ACQUISITION 8

Speed Trap 8

Accelerometers 8

Strain gages 8

High-Speed Photography 10

DATA ANALYSIS 10

Speed trap 10

Accelerometers and strain gages 10

High-Speed Photography 11

RESULTS 11

CONCLUSION 13

APPENDIX A. DATA PLOTS OF DATA OBTAINED FROM ACCELEROMETERS
 AND STRAIN GAGES. 19

REFERENCES 79

LIST OF FIGURES

<u>Figure</u>	<u>Page</u>
1. Photographs of pendulum mass and rigid nose assembly . . .	4
2. Sketch of the steel anchor stanchions	5
3. Setup of pendulum test and high-speed camera placements .	6
4. Photographs of a typical test installation	7
5. Location of rosettes and single-gage strain gages	9
6. Pretest photographs, test 96P006	14
7. Post-test photographs, test 96P006	15
8. Test photographs during impact, test 96P006	17
9. Acceleration histories from tests 96P003, 96P004, and 96P006	18
10. Acceleration vs. time, test 96P001	19
11. Velocity vs. time, test 96P001	20
12. Displacement vs. time, test 96P001	21
13. Force vs. time, test 96P001	22
14. Force vs. displacement, test 96P001	23
15. Energy vs. displacement, test 96P001	24
16. Strain vs. time (left front), test 96P001	25
17. Strain vs. time (right front), test 96P001	26
18. Strain vs. time (left rear), test 96P001	27
19. Strain vs. time (right rear), test 96P001	28
20. Acceleration vs. time, test 96P002	29
21. Velocity vs. time, test 96P002	30
22. Displacement vs. time, test 96P002	31
23. Force vs. time, test 96P002	32
24. Force vs. displacement, test 96P002	33
25. Energy vs. displacement, test 96P002	34
26. Strain vs. time (left front), test 96P002	35
27. Strain vs. time (right front), test 96P002	36
28. Strain vs. time (left rear), test 96P002	37
29. Strain vs. time (right rear), test 96P002	38
30. Acceleration vs. time, test 96P003	39
31. Velocity vs. time, test 96P003	40
32. Displacement vs. time, test 96P003	41
33. Force vs. time, test 96P003	42
34. Force vs. displacement, test 96P003	43
35. Energy vs. displacement, test 96P003	44
36. Strain vs. time (left front), test 96P003	45
37. Strain vs. time (right front), test 96P003	46
38. Strain vs. time (left rear), test 96P003	47
39. Strain vs. time, (right rear), test 96P003	48
40. Acceleration vs. time, test 96P004	49
41. Velocity vs. time, test 96P004	50
42. Displacement vs. time, test 96P004	51
43. Force vs. time, test 96P004	52
44. Force vs. displacement, test 96P004	53
45. Energy vs. displacement, test 96P004	54
46. Strain vs. time (left front), test 96P004	55
47. Strain vs. time (right front), test 96P004	56
48. Strain vs. time (left rear), test 96P004	57
49. Strain vs. time (right rear), test 96P004	58

<u>Figure</u>	<u>Page</u>
50. Acceleration vs. time, test 96P005	59
51. Velocity vs. time, test 96P005	60
52. Displacement vs. time, test 96P005	61
53. Force vs. time, test 96P005	62
54. Force vs. displacement, test 96P005	63
55. Energy vs. displacement, test 96P005	64
56. Strain vs. time (left front), test 96P005	65
57. Strain vs. time (right front), test 96P005	66
58. Strain vs. time (left rear), test 96P005	67
59. Strain vs. time (right rear), test 96P005	68
60. Acceleration vs. time, test 96P006	69
61. Velocity vs. time, test 96P006	70
62. Displacement vs. time, test 96P006	71
63. Force vs. time, test 96P006	72
64. Force vs. displacement, test 96P006	73
65. Energy vs. displacement, test 96P006	74
66. Strain vs. time (left front), test 96P006	75
67. Strain vs. time (right front), test 96P006	76
68. Strain vs. time (left rear), test 96P006	77
69. Strain vs. time (right rear), test 96P006	78

LIST OF TABLES

<u>Table</u>	<u>Page</u>
1. Test matrix for pendulum testing four-post w-beam	2
2. Camera configuration and placement	10
3. Summary of pendulum testing of four-post w-beam rail . .	12

BACKGROUND

The Federal Highway Administration (FHWA) has been evaluating advanced composite materials to be used in lieu of conventional materials used in the construction of roadside safety hardware. In particular, the FHWA has been investigating the use of a fiber reinforced plastic (FRP) material in guardrail applications. The FRP material would be used in the design of a rail element, as opposed to the conventional steel w-beam in use today. Baseline data on the dynamic properties of standard steel w-beam was needed to develop a design envelope for an FRP rail element. The FHWA Federal Outdoor Impact Laboratory (FOIL) used its 820-kg pendulum facility to conduct seven dynamic impact tests on 1.9-m long steel w-beam rail elements attached to two standard steel I-section guardrail posts (a two-post configuration). The pendulum was fitted with a rigid nose to allow for complete energy absorption by the w-beam rail and I-section guardrail posts. The results from these pendulum tests are presented in the pending report *Pendulum Impact Testing of Steel W-Beam Guardrail*.⁽¹⁾ One conclusion from the two-post configuration testing was that the stiffness of the w-beam and I-section posts was not great enough to allow for peak loading of the w-beam rail element. The posts failed torsionally, allowing the pendulum to swing through and over the w-beam before achieving maximum loading of the rail. The testing was halted and pendulum modifications were made to facilitate better loading of the w-beam rail. In order to restrain the excessive deflections of the w-beam guardrail element and to better replicate the longitudinal tension found in actual guardrail installations, the w-beam element was semi-rigidly restrained in the longitudinal direction using cables attached at each end of the guardrail element. This was accomplished using a standard 25-mm guardrail anchor cable attached to rigid anchor stanchions. The anchor stanchions were constructed of steel box-sections and were bolted to deep concrete foundations. This report documents the testing performed on six cable anchored w-beam specimens.

SCOPE

This document contains the test setup and results from six pendulum crash tests conducted at the FHWA's FOIL facility located at the Turner-Fairbank Highway Research Center (TFHRC) in McLean, Virginia. The tests were conducted on steel w-beam rail elements rigidly anchored at both ends (a four-post configuration). The tests were conducted as part of an ongoing research effort to obtain baseline dynamic response data for standard w-beam guardrail. The nominal weight of the FOIL pendulum with a rigid nose assembly was 912 kg. The tests were conducted at nominal speeds ranging from 20 km/h to 35 km/h. A 20-km/h and a 30-km/h test were conducted to observe the new anchor stanchions' structural response before proceeding on to

the 35-km/h tests. Four tests were conducted at 35 km/h. The four 35-km/h tests were roughly equivalent to the National Cooperative Highway Research Program (NCHRP) Report 350, test 3-10, a small lightweight vehicle impacting a w-beam guardrail at a speed of 100 km/h and at an angle of 20°. ⁽²⁾ This was because, for test 3-10, the velocity component of the test vehicle perpendicular to the rail, was approximately 35 km/h. The perpendicular velocity component was the same as the higher-speed (35 km/h) pendulum tests. Also, the pendulum weight (912 kg) was that of a small, lightweight passenger sedan. Thus, the 35-km/h pendulum test as described in this report roughly approximates NCHRP Report 350, test 3-10. As such, this pendulum test can be used in the future to determine, in a preliminary manner, the structural adequacy of new guardrail/roadside barrier system.

TEST MATRIX

Six pendulum tests were conducted on steel w-beam rail anchored at both ends (four-post configuration). The mass of the pendulum was 912 kg for all tests. The first two tests were conducted at 20 and 30 km/h. This gradual speed increase was a precautionary measure to ensure that the structural integrity of the new stanchions would not be compromised during the higher speed tests. The highest level of strain observed during the two slow tests was 163 $\mu\epsilon$ during the 30-km/h test. This value is well below the limits for structural steel, therefore the 35-km/h tests were conducted. Table 1 is the matrix for the four-post w-beam pendulum testing. The highest strain observed during the 35-km/h tests was 186 $\mu\epsilon$, which is also well below the limits of structural steel.

Table 1. Test matrix for pendulum testing four-post w-beam.

Test Number	Test date	Test speed (km/h)	Impact location
96P001	02-21-96	20	center of w-beam rail
96P002	02-23-96	30	center of w-beam rail
96P003	02-26-96	35	center of w-beam rail
96P004	02-27-96	35	center of w-beam rail
96P005	03-06-96	35	center of w-beam rail
96P006	03-11-96	35	center of w-beam rail

PENDULUM

The test vehicle was the FOIL's 820-kg pendulum. The pendulum consisted of a reinforced concrete mass with steel end-plates suspended from a steel structure by four 25-mm steel

cables. The usual pendulum setup has a crushable nose inserted inside the concrete/steel body or mass. This nose was replaced with a rigid, solid oak nose. This was done so that the four-post w-beam specimen would be subject to all of the energy with no energy dissipation from deformation of the nose. Within the concrete mass were two aluminum guide sleeves, the wood nose was attached to two aluminum guide tubes which were inserted into the guide sleeves. Seven oak spacers (total length of 325 mm) were placed between the nose assembly and the pendulum mass. The spacers were necessary to allow for optimal contact between the w-beam specimen and the pendulum nose. This was determined during previous pendulum testing of the two-post w-beam setup. A thin rubber mat was attached to the pendulum nose to reduce the high frequency ring and inertial spike associated with contact between two rigid objects. The rigid nose assembly and wood spacers increased the mass of the pendulum from 820 kg to 912 kg. The vertical center of the pendulum was set at 533 mm above ground. This height corresponds to the height of the center of the w-beam specimens. Figure 1 is photographs of the pendulum mass and rigid nose assembly. The pendulum was setup the same for each test.

TEST ARTICLE

The w-beam rail consisted of three 1.9-m w-beam rails spliced end-to-end with the splices attached to standard guardrail strong posts (I-section) and blockouts. The post spacing between posts was 1 905 mm, which is standard for strong-post guardrail systems. The blockout-to-post connections were made using standard bolts in the same pattern that is in use on the national highway system (NHS). Standard post and rail heights of 710 mm and 685 mm respectively were used for setup of the four-post w-beam system. The two interior guardrail posts were rigidly clamped at the ground level. Thus, no energy dissipation associated with posts "plowing" and moving in the soil was present during testing. Because of this, all of the energy was absorbed solely by the guardrail sections and posts through bending, twisting, and tension loading. Each end of the three-panel system was semi-rigidly anchored using standard guardrail 25-mm-diameter steel cable. The cable was fastened to the w-beam using standard cable anchor brackets used on typical guardrail systems. The cables were passed through the anchor stanchions and fastened with a 25-mm cable-nut and washer. Standard rail-to-post bolts were used to fasten the ends of the w-beam to the anchor stanchions. Figure 2 is a sketch of the steel anchor stanchions. A birds-eye view of the test setup and high-speed camera placements is shown in figure 3. Photographs of a typical test installation are shown in figure 4. Tension was applied to the four-post w-beam systems prior to testing by tightening the anchor cables. An attempt was made to apply the same amount of rail tension to each tested rail. This was done by monitoring output from strain gages bonded to the w-beam rail. Prior to test 96P001, the cables were tightened to an arbitrary

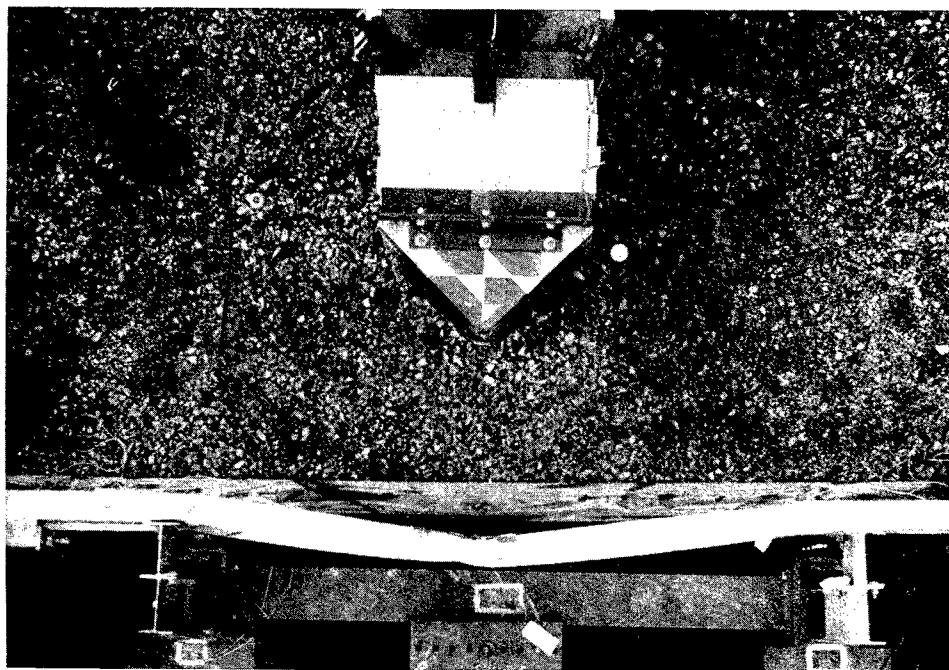
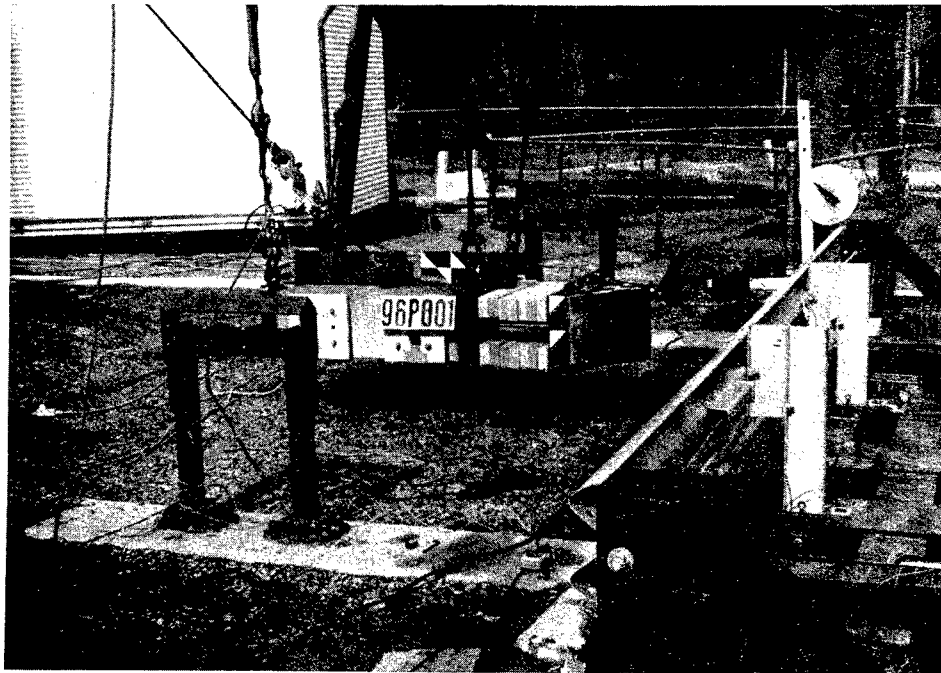
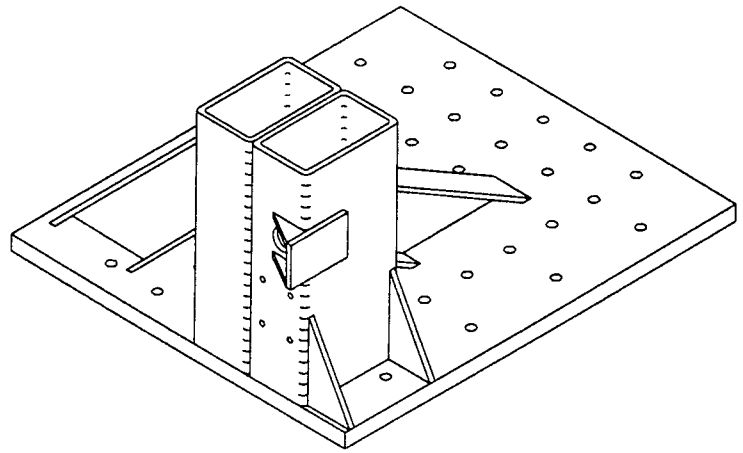
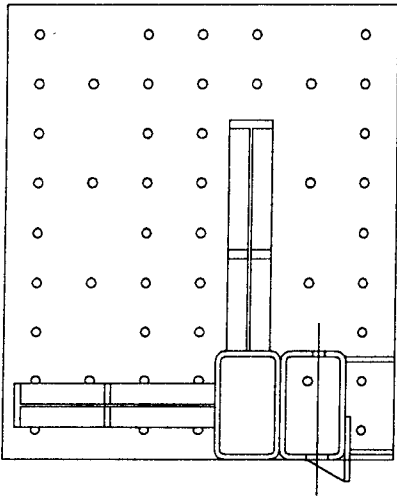
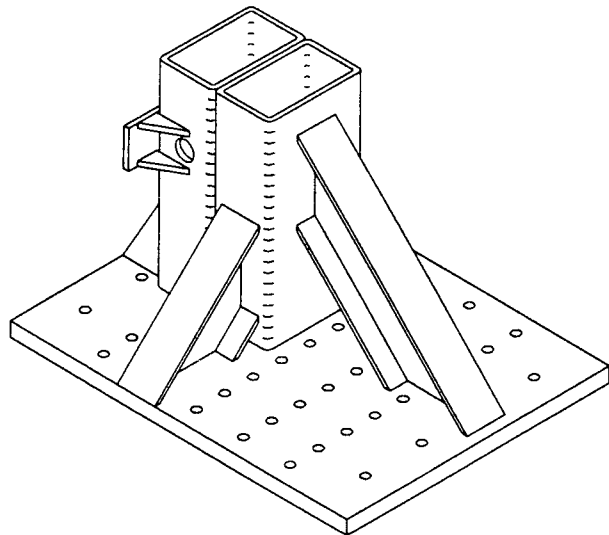
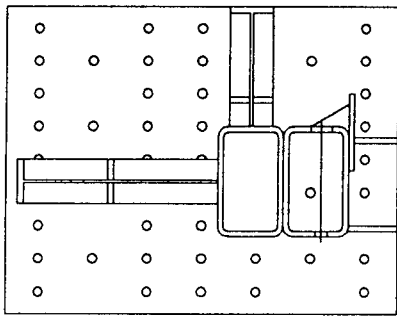


Figure 1. Photographs of pendulum mass and rigid nose assembly.



Right side anchor stanchion



Left side anchor stanchion

Figure 2. Sketch of the steel anchor stanchions.

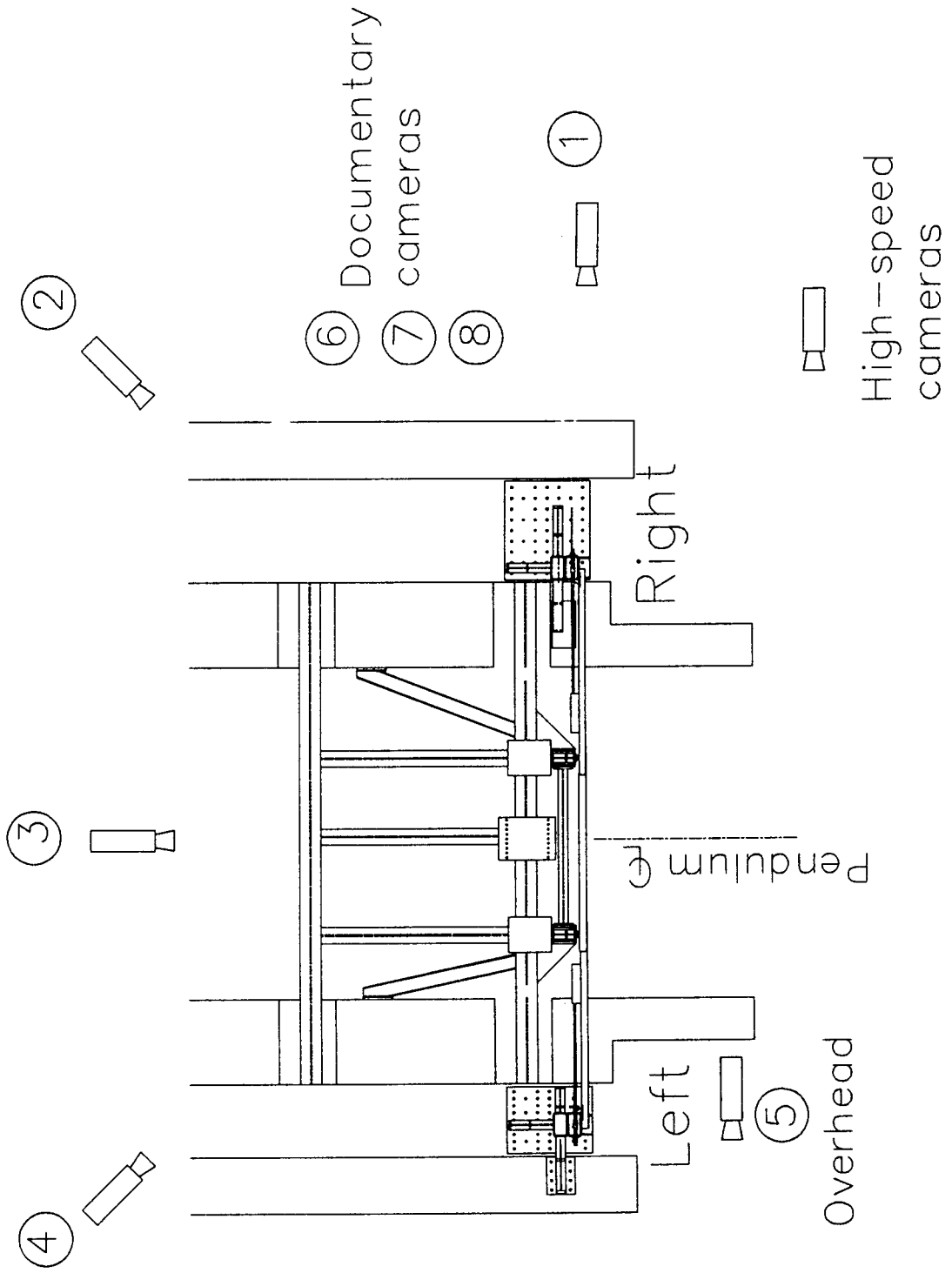


Figure 3. Setup of pendulum test and high-speed camera placements.

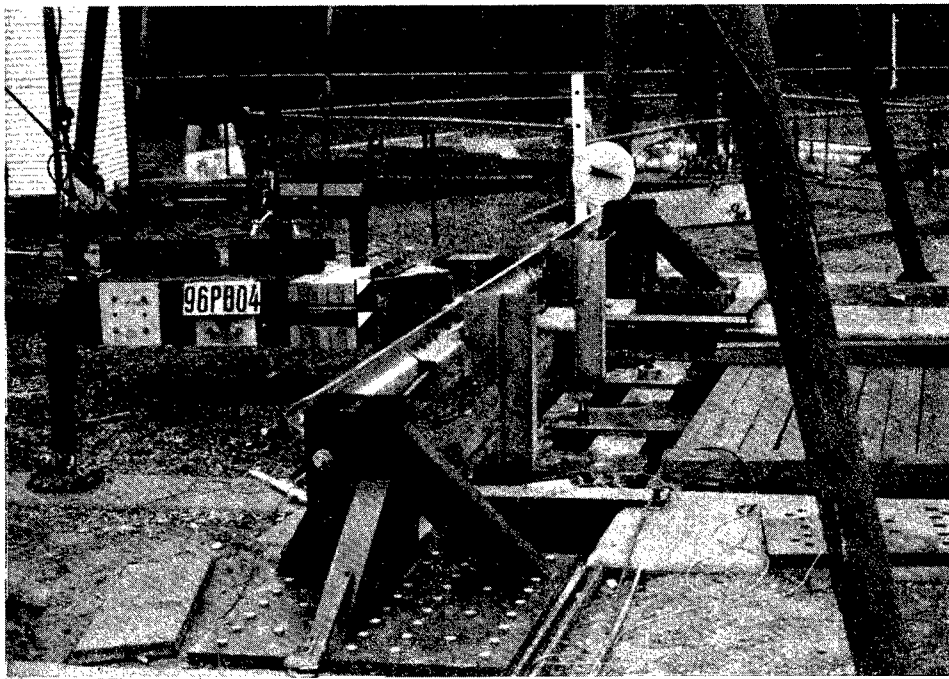
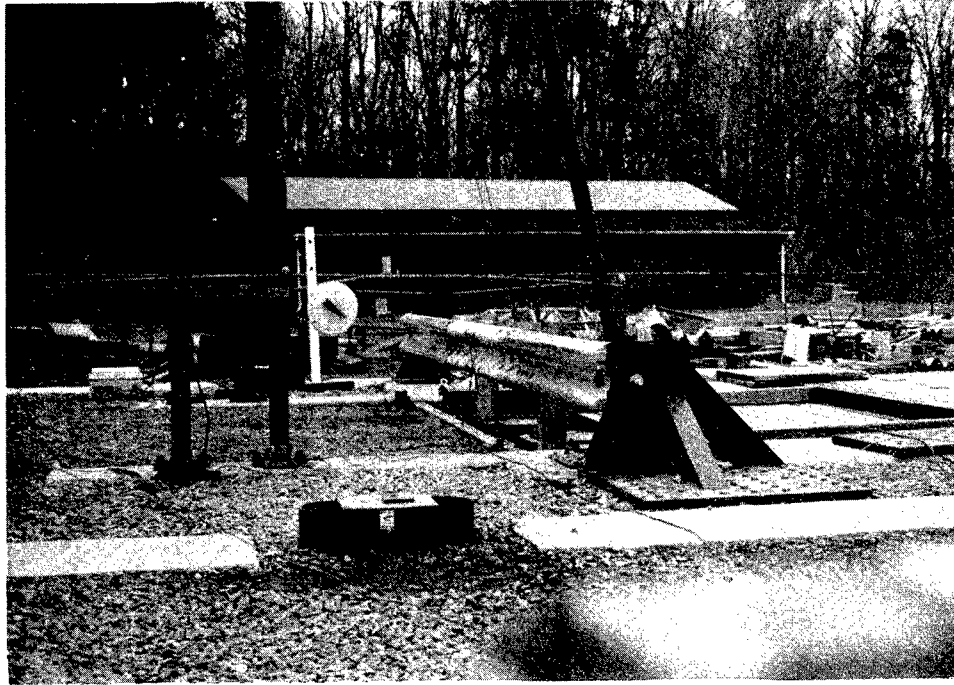


Figure 4. Photographs of a typical test installation.

tension (as tight as possible) and the voltages from two gages were read. For the remaining five tests, the cables were tightened until the same (as close as possible) gage output voltages were reached as in test 96P001.

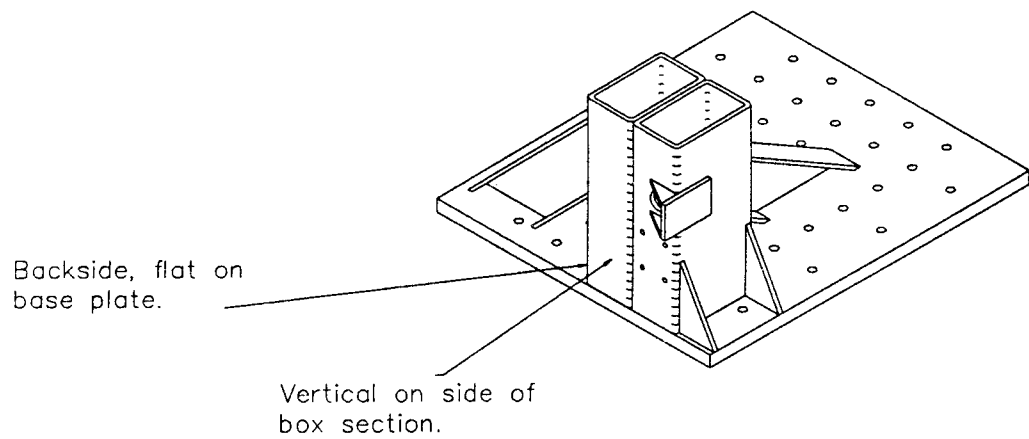
DATA ACQUISITION

For each pendulum test, a speed trap, accelerometers, strain gages, and high-speed film were used for data collection. Strain gages were placed on the w-beam rail elements and on one stanchion used for end-anchorage. The gages placed on the stanchion were precautionary; they were used to monitor stress in the steel structure to ensure that the newly fabricated stanchions would not fail during impact.

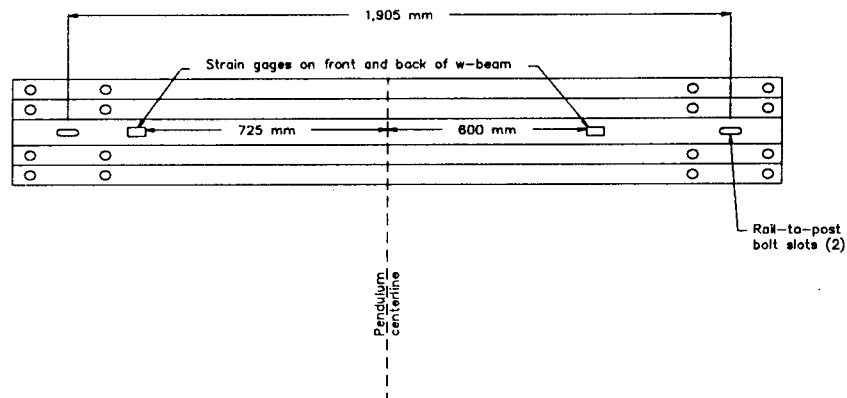
Speed Trap. The speed trap consisted of a set of four light emitting diode (LED) infrared emitter/receiver pairs fastened on opposite sides of the pendulum's swing path at 150-mm intervals. The scanner pairs were positioned before the impact area to measure the speed of the pendulum just prior to contact with the w-beam. Signals from the sensors were recorded on a Honeywell model 5600E analog tape recorder. The signals were stored on analog tape for future analysis.

Accelerometers. Two longitudinal (x-axis) 100-g accelerometers were mounted at the center of the rear face of the pendulum. The accelerometer signals were recorded by the FOIL on-board data acquisition system (ODAS) III/8. The ODAS III/8 is a self-contained data acquisition system providing transducer excitation, signal conditioning, 4000 Hz pre-filtering, 12,500 Hz digital sampling, and digital storage for up to eight channels. The data was collected, then downloaded to a portable computer.

Strain gages. Data from two three-gage rosettes and four single-gage strain gages were recorded during the pendulum tests. The rosettes were affixed to one of the end-anchorage stanchions to monitor the stress in the stanchion to ensure that the structural integrity would not be compromised during testing. The rosette strain gage signals were conditioned using Vishay model 2310 amplifiers and recorded on analog tape using a Honeywell 5600E tape recorder for later analysis. The four single-gage strain gages were attached to the w-beam specimen. Two gages were placed on the front and two gages were placed on the back of the guardrail. Each front and back pair was placed at the same location vertically and laterally. The gages were placed at the same locations for each test. The gages were positioned in the middle of the valley of the w-beam vertically, and midway between the impact point and the I-section strong-posts laterally. The w-beam strain gage data was recorded by the FOIL ODAS III system. Figure 5 shows the locations of the rosettes on the stanchions and the single-gage strain gages on the w-beam.



Right side anchor stanchion rosette strain gage locations.



Steel w-beam test specimen strain gage locations. Front of rail pictured.

Figure 5. Location of rosettes and single-gage strain gages.

High Speed Photography. The tests were photographed using five high-speed cameras, one real-time camera, and two 35-mm still cameras. All high-speed cameras were loaded with Kodak 2253 color daylight film and the real-time camera was loaded with Kodak 7239 color film. One 35-mm camera was loaded with black and white print film and the other with 35-mm color slide film. The camera placements are summarized in table 2. The camera numbers in table 2 are also shown back in figure 3.

Table 2. Camera configuration and placement.				
Camera Number	Type	Film Speed (frames/s)	Lens (mm)	Location
1	Locam II	500	50	90° to impact rt. side
2	Locam II	500	25	45° to impact rt. side
3	Locam II	500	75	180° to impact
4	Locam II	500	25	45° to impact left side
5	Locam II	500	25	overhead
6	Bolex	24	zoom	documentary
7	Canon A-1 (prints)	still	zoom	documentary
8	Canon A-1 (slides)	still	zoom	documentary

DATA ANALYSIS

For each pendulum test, a speed trap, accelerometers, strain gages, and high-speed film were used for data collection.

Speed trap. The speed trap consisted of a set of four LED infrared emitter/receiver pairs fastened on opposite sides of the pendulum's swing path at 150-mm intervals just prior the w-beam specimen. As the pendulum passed through the infrared scanners, electronic pulses were recorded on analog tape. The tape was played back through a Data Translation analog-to-digital (A/D) converter, and the time between pulses was determined. Time-displacement data was entered into a computer spreadsheet and a linear regression was performed on the data to determine the pendulum speed.

Accelerometers and strain gages. The data from the accelerometers and strain gages were digitally recorded and converted to the ASCII format. The sampling rate during data acquisition was 2000 Hz for data recorded via the FOIL umbilical cable (rosette strain gages) and 12,500 Hz for data recorded via the ODAS III on-board system (accelerometers and w-beam strain

gages). The ASCII files were processed, which included removal of zero-bias, storing the region of interest, and digitally filtering the data to 300 Hz (Class 180). The rosette data was filtered at 100 Hz. The data was imported into a spreadsheet for plotting and analysis.

High-Speed Photography. The crash event was recorded on 16-mm film by five high-speed cameras. Primarily, the overhead camera was the only camera used for high-speed film analysis. Analysis of the crash event was performed using an NAC Film Motion Analyzer model 160-F in conjunction with an IBM PC-AT. The motion analyzer digitized the 16-mm film, reducing the image to Cartesian coordinates. Using the Cartesian coordinate data, a time-displacement history of the test was obtained. The time-displacement data was then imported into a computer spreadsheet and a linear regression was performed to determine the impact velocity of the pendulum. Using the Cartesian coordinate data, the deflection of the rail could be measured directly. Film analysis data could be used in the event of electronic data channel failure. The speed trap data was used as the primary measurement for impact velocity.

RESULTS

For each test, the pendulum was accelerated to the target speed and made contact at the intended location on the w-beam. The first two tests were conducted at 20 and 30 km/h. This gradual speed increase was a precautionary measure to ensure that the structural integrity of the new stanchions would not be compromised during the higher speed tests. The highest level of strain observed during the two slow tests was $163 \mu\epsilon$ during the 30-km/h test. This value is well below the limits for structural steel; therefore, the 35-km/h tests were conducted. The highest strain observed during the 35-km/h tests was $186 \mu\epsilon$, which is also well below the limits of structural steel.

The response of the w-beam rail was similar during the four 35-km/h tests. The pendulum struck the w-beam, and the w-beam shape began to collapse. The forces built up in the rail, with the eventual torsional and bending failure of the two standard strong-posts at approximately 0.040 s after initial contact. The force relaxed until the cables engaged and stopped the pendulum (0.115 s). The pendulum rebounded with a small velocity. A portion of the rebound velocity may be attributed to the pendulum's natural return to equilibrium. During test 96P004, one rail-to-stanchion bolt failed, resulting in a slightly different deflection in the rail. The rail-to-stanchion bolts were upgraded to a grade five strength bolt for tests 96P005 and 96P006. However, the cables used in test 96P004 were reused in test 96P005, and one cable ruptured as a result during test 96P005. New cables were used for test 96P006. The data from the pendulum testing is summarized in table 3.

Table 3. Summary of pendulum testing of four-post w-beam rail.

Test Number	Speed (km/h)		E _i (kJ)	Rail Pre-tension (μe)		Peaks		Rail Deflection (mm)			Work F _o d (kJ)
	Trap	Film		Left gage	Right gage	g's	Force (1000 N)	Accel	Film	Static measure	
96P001	21.8	21.8	16.4	76	45	10.2	91	280	250	NA	16.3
96P002	30.0	29.8	31.7	70	70	13.9	124	471	390	305	31.3
96P003	35.1	34.9	43.3	25	67	16.1	144	610	501	406	43.2
96P004	35.1	34.9	43.3	99	61	14.9	134	600	532	445	43.2
96P005	35.0	35.1	43.1	80	63	23.9	214	820	762	597	42.9
96P006	35.3	35.2	43.8	69	68	14.8	133	630	595	425	43.6

Due to the similarities in testing, pretest and post-test photographs from one test (test 96P006, a 35-km/h test) are shown in figure 6 and 7, respectively. Photographs taken from high-speed film during one test (test 96P006) are shown in figure 8. Data plots of data obtained from the pendulum accelerometers and w-beam strain gages are shown in appendix A. The data from the rosette strain gages on the stanchion are not included in this report.

CONCLUSION

The data summarized in table 3 and shown in the data plots in Appendix A suggest a high degree of repeatability in the dynamic response of steel w-beam guardrail. Three similar tests, 96P003, 96P004, and 96P006, are comparable in peak force and rail deflection. These three tests should provide a design envelope for the design and fabrication of FRP composite rail elements. Test 96P005 was not included in the envelope due to the anchor cable failure. Acceleration histories from each of these 35-km/h tests are plotted together in figure 9. The plot demonstrates the similar loading characteristic. The two hump shape is a signature of the events during impact. The first hump may be attributed to the rise in force prior to buckling and torsional failure of the strong-posts and blockouts, while the second may be attributed to the load transfer to the anchor cables. This two-stage event should provide a target dynamic response to be replicated by an FRP system. The data also establishes that the energy from a pendulum with a mass of 912 kg and a velocity of 35 km/h is not enough to produce the forces necessary to load the w-beam element to failure. A heavier, faster pendulum is needed to generate sufficient forces to fail the steel w-beam rail.

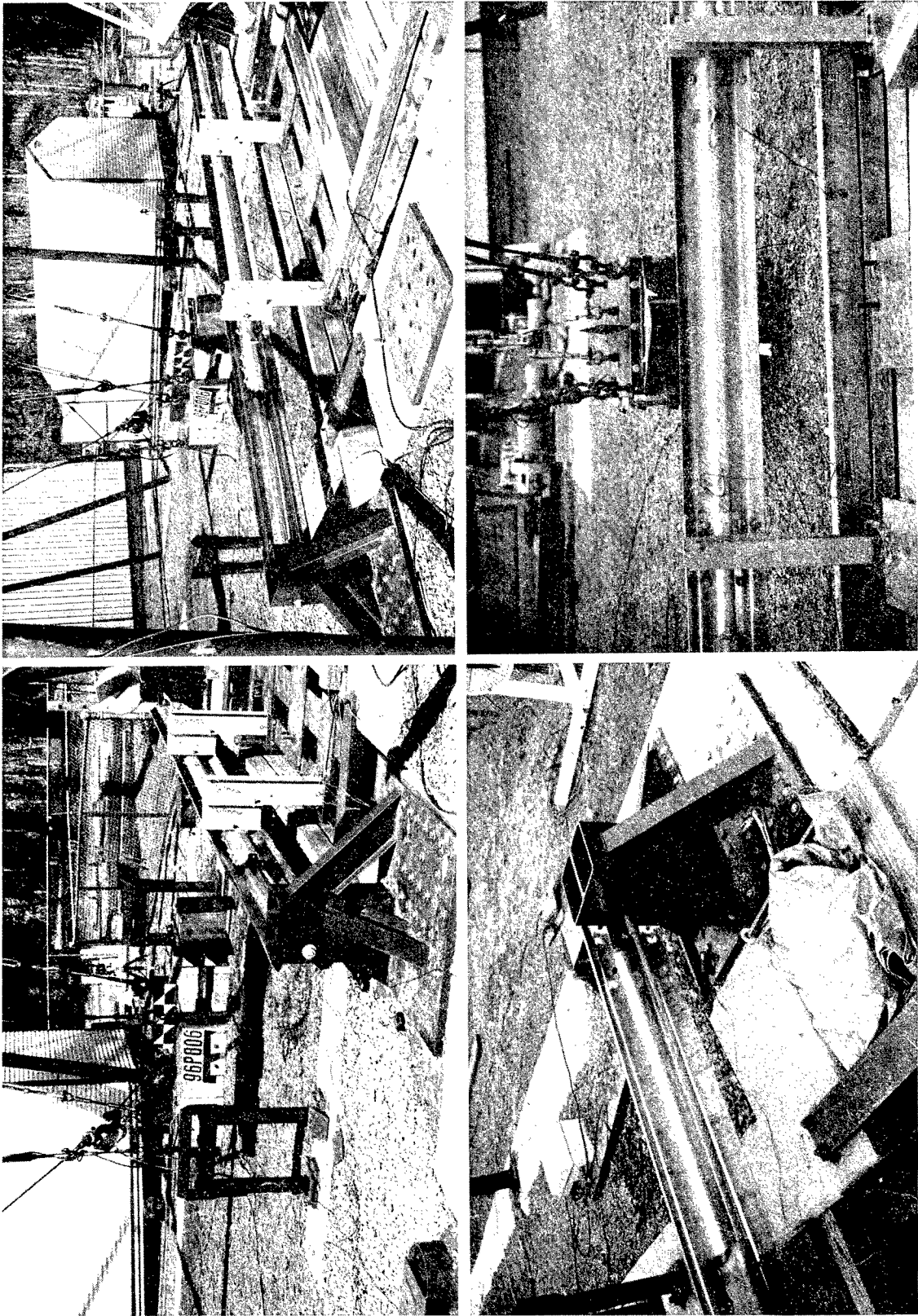


Figure 6. Pretest photographs, test 96P006.

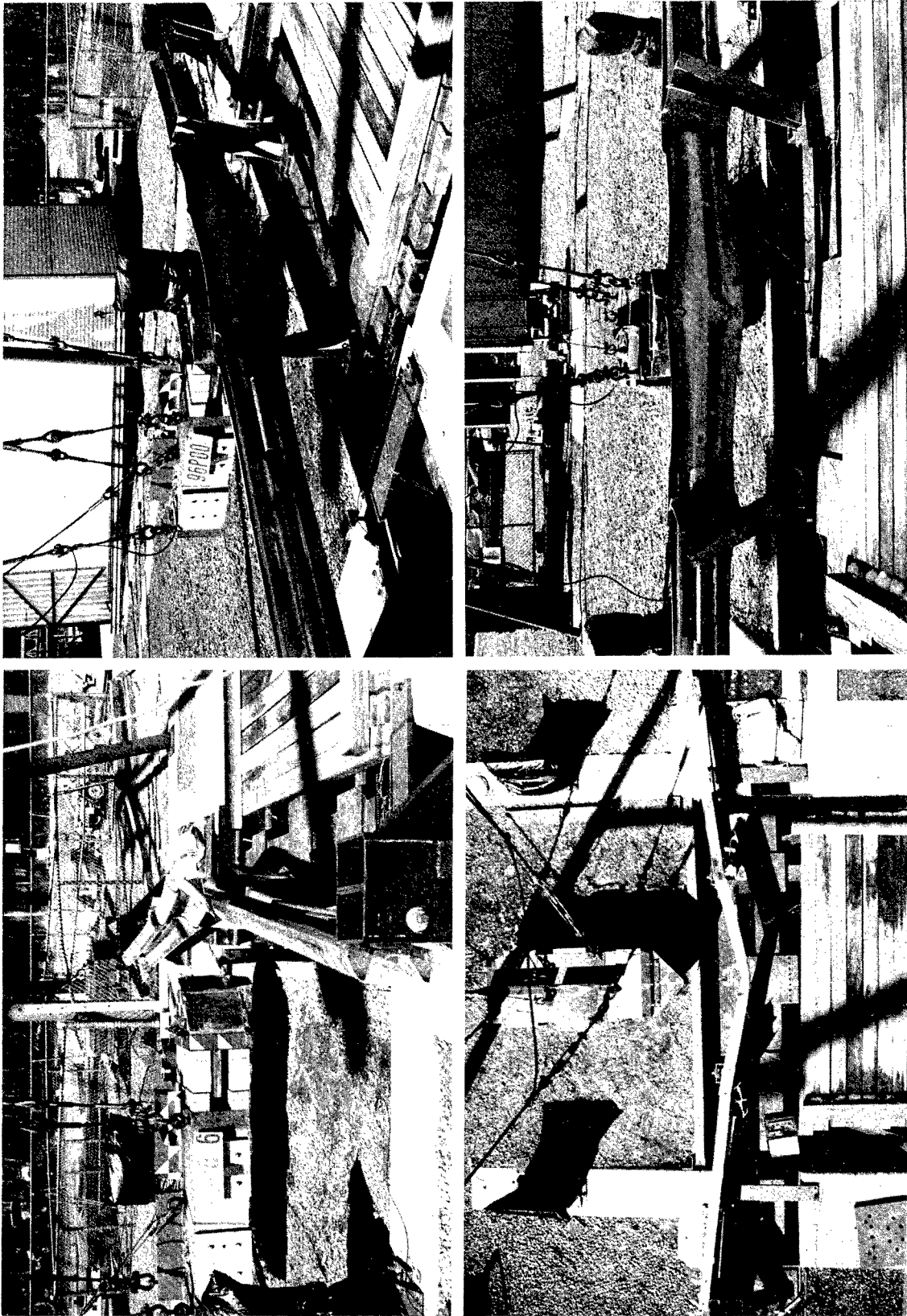


Figure 7. Post-test photographs, test 96P006.

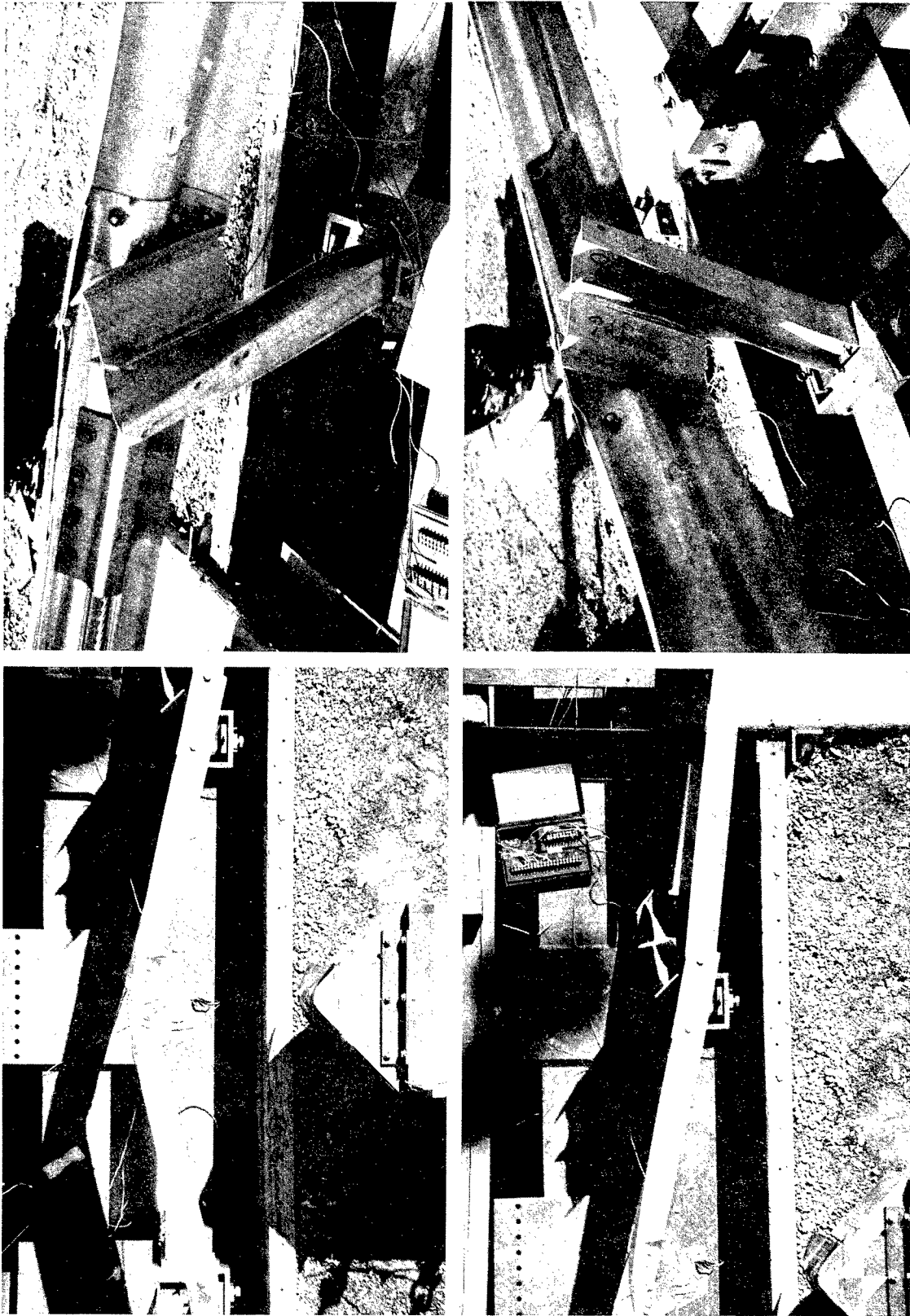
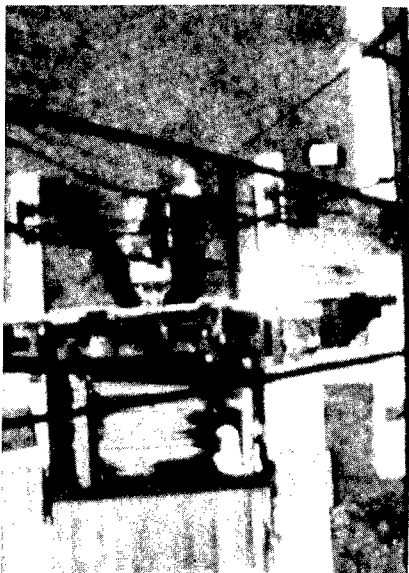
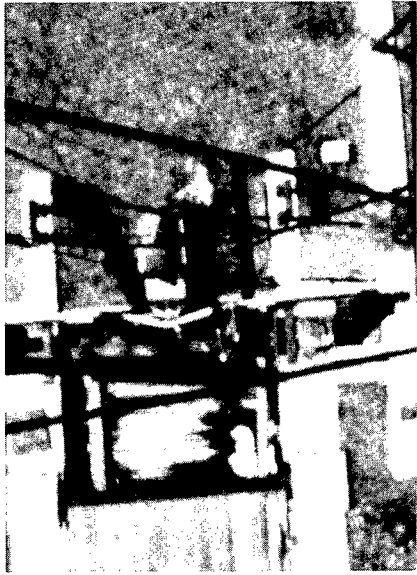


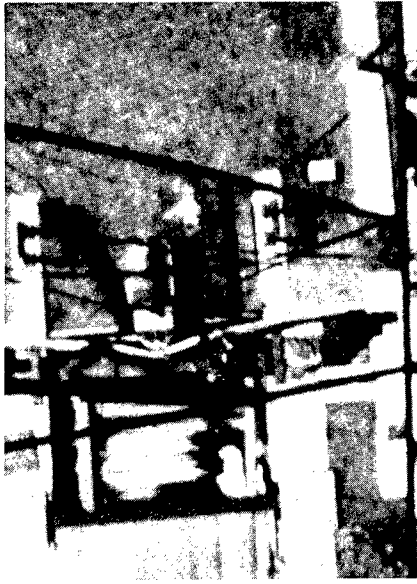
Figure 7. Post-test photographs, test 96P006 (continued).



0.000 s



0.032 s



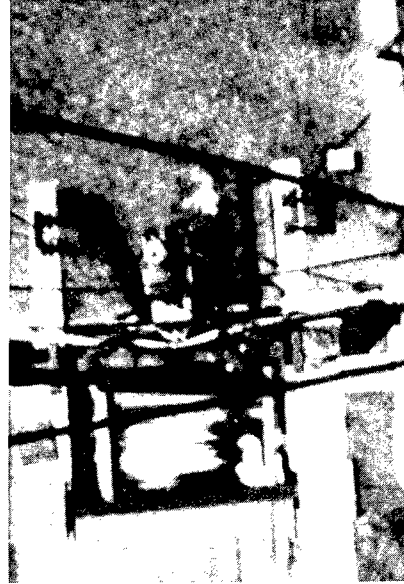
0.058 s



0.090 s



0.108 s



0.208 s

Figure 8. Test photographs during impact, test 96P006.

Acceleration vs. Time

96P003, 96P004, 96P006

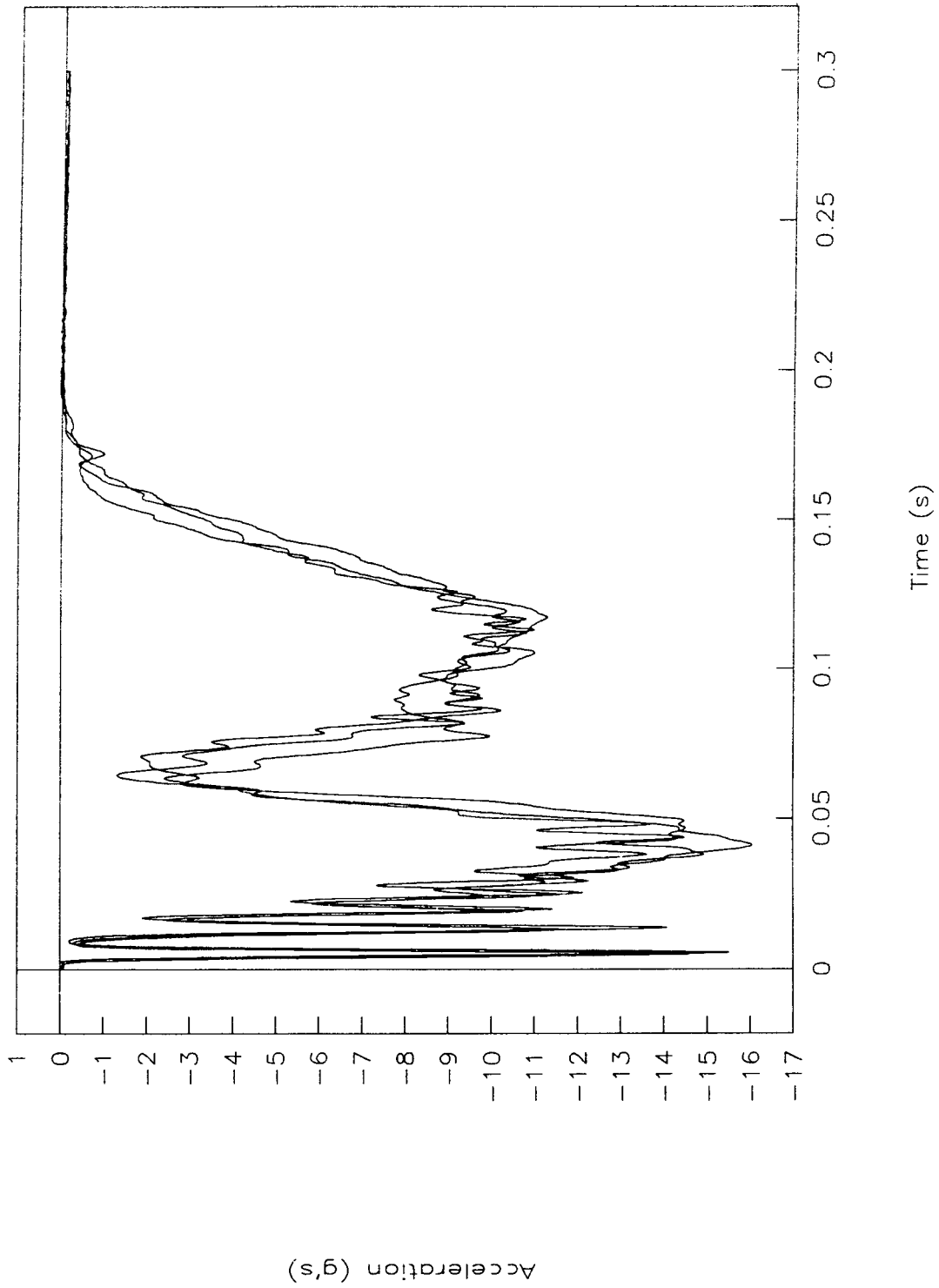


Figure 9. Acceleration histories from tests 96P003, 96P004, and 96P006.

APPENDIX A: DATA PLOTS OF DATA OBTAINED FROM
ACCELEROMETERS AND STRAIN GAGES

TEST NO. 96P001
Acceleration vs. time

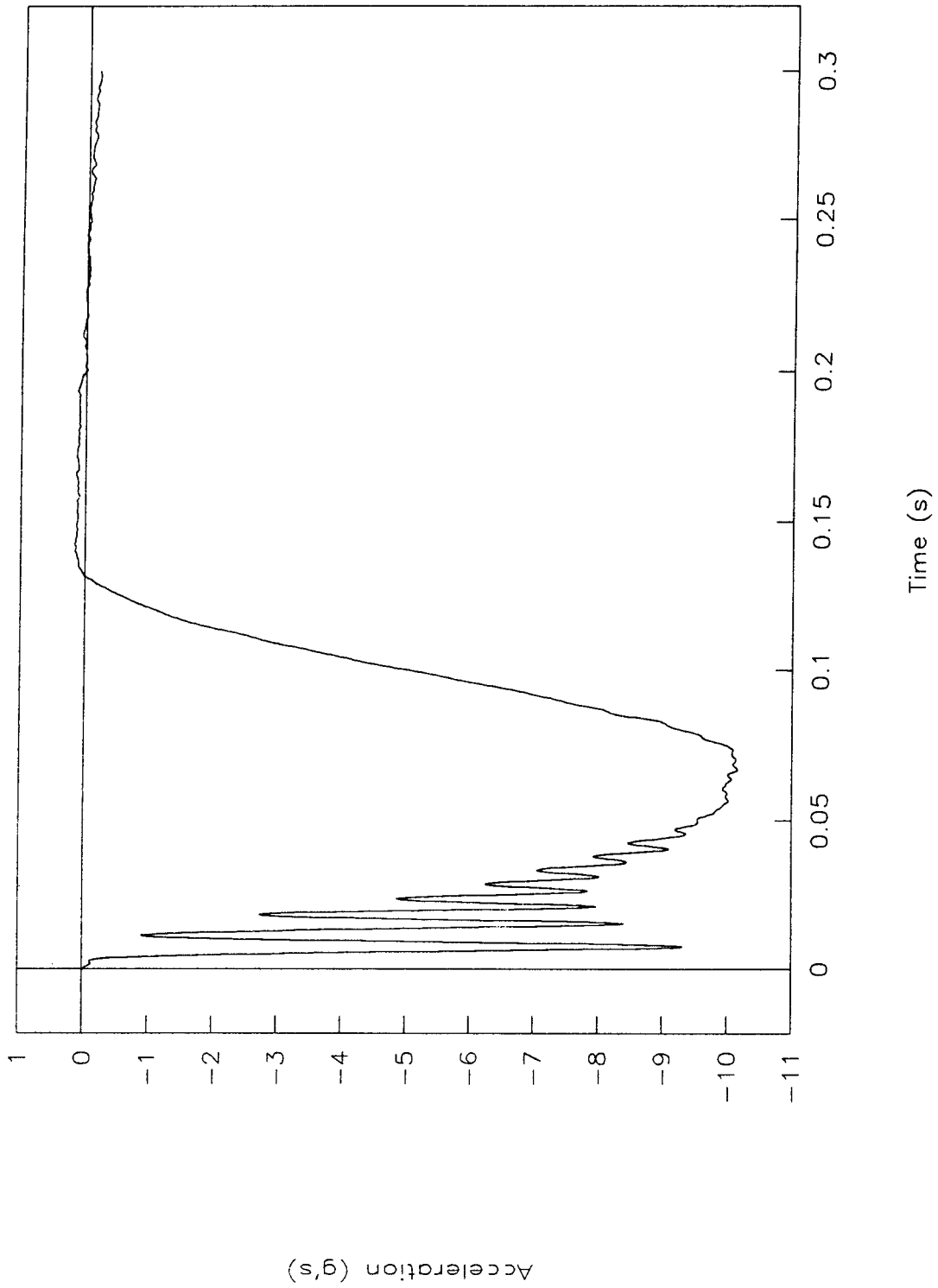


Figure 10. Acceleration vs. time, test 96P001.

TEST NO. 96P001

Velocity vs. time

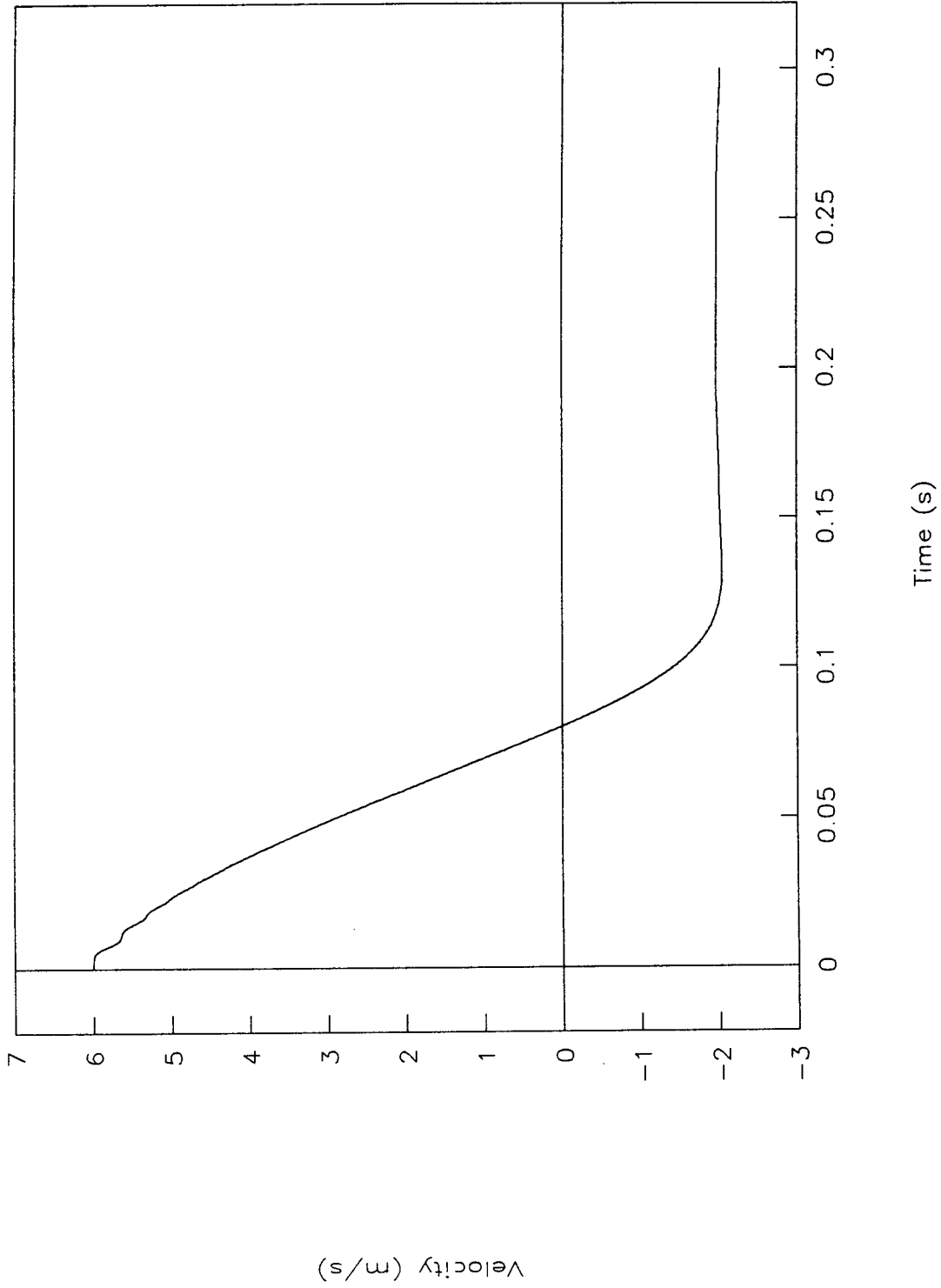


Figure 11. Velocity vs. time, test 96P001.

TEST NO. 96P001

Displacement vs. time

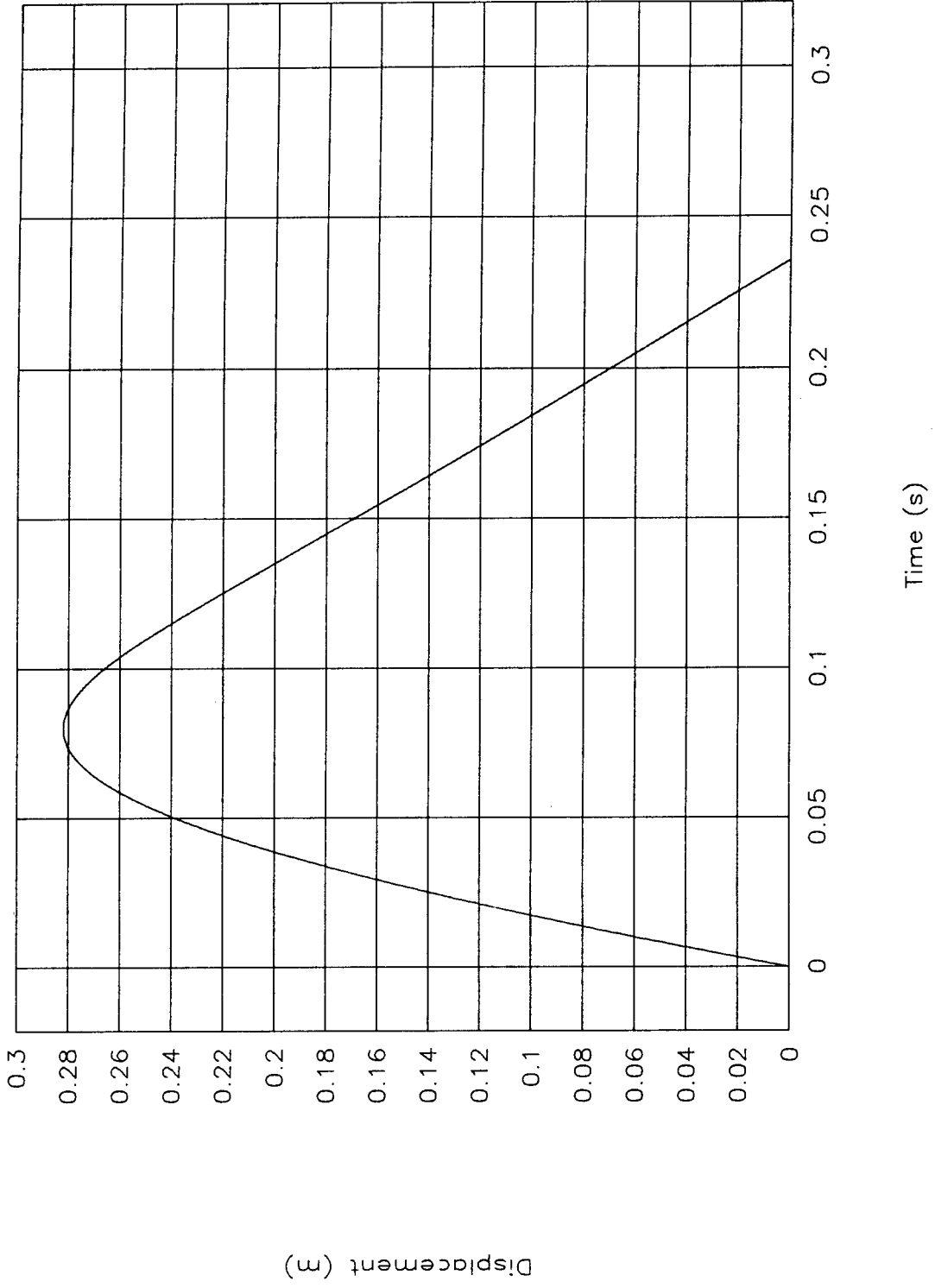


Figure 12. Displacement vs. time, test 96P001.

TEST NO. 96P001

Force vs. time

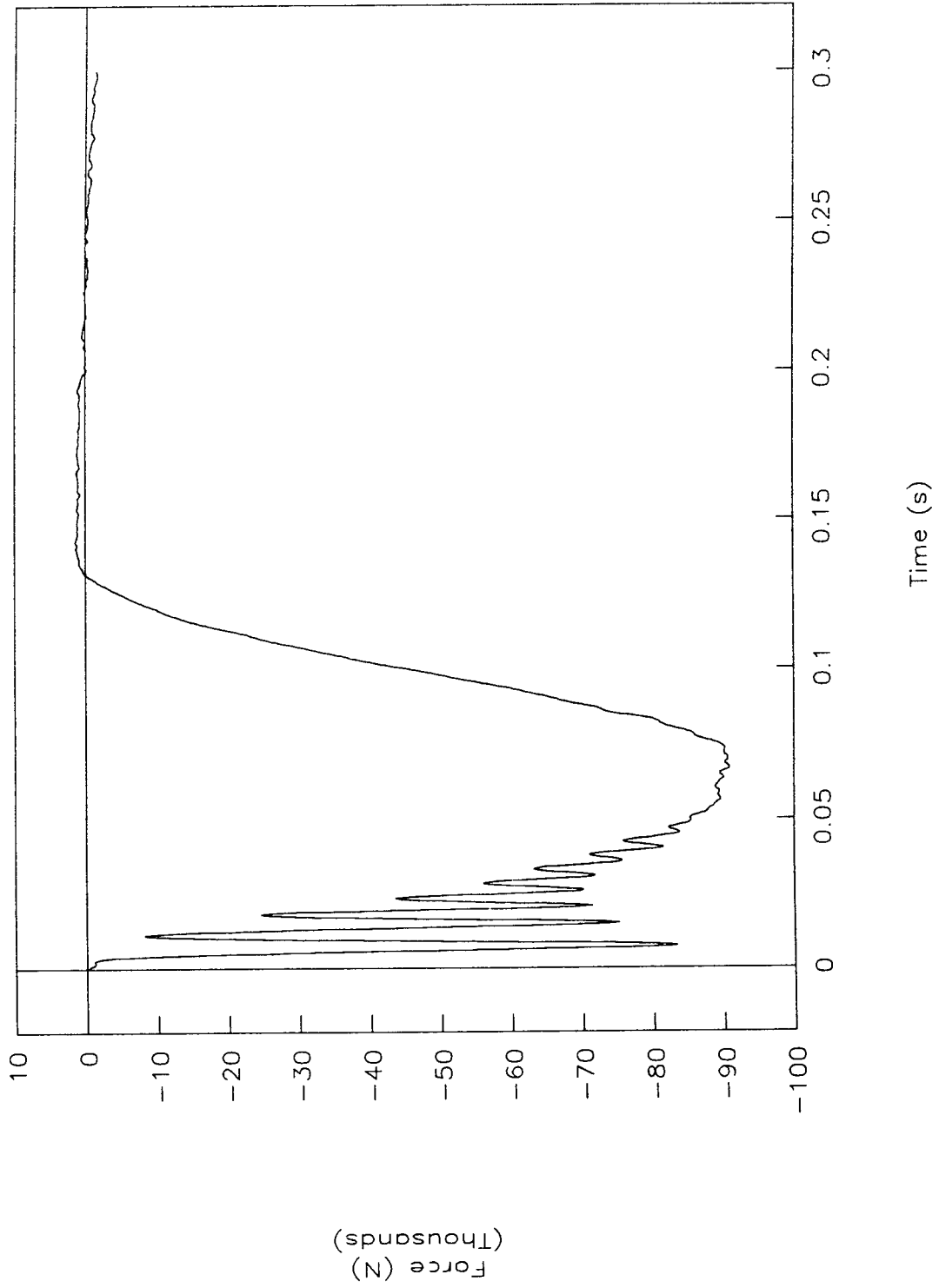


Figure 13. Force vs. time, test 96P001.

TEST NO. 96P001

Force vs. displacement

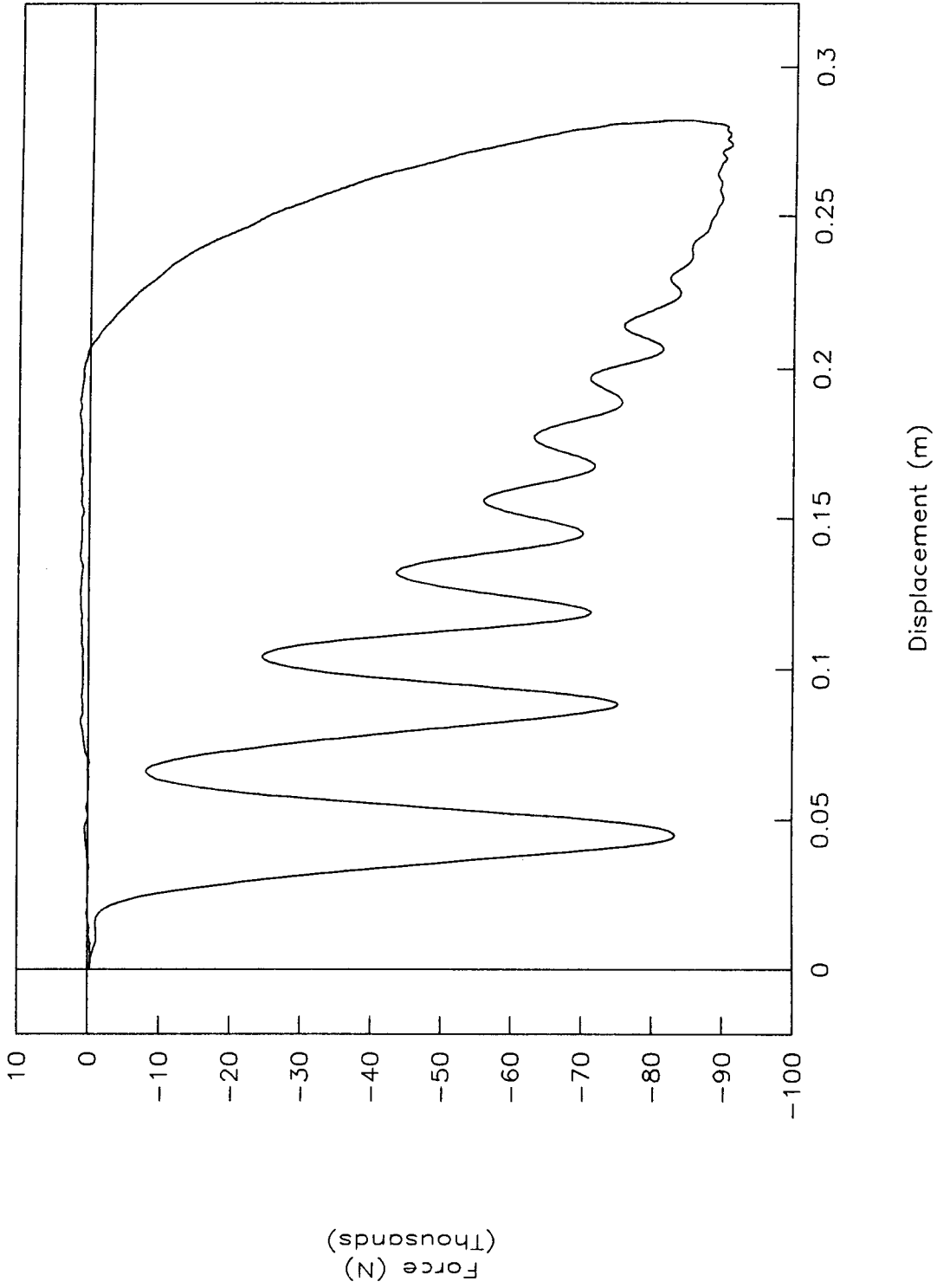


Figure 14. Force vs. displacement, test 96P001.

TEST NO. 96P001

Energy vs. displacement

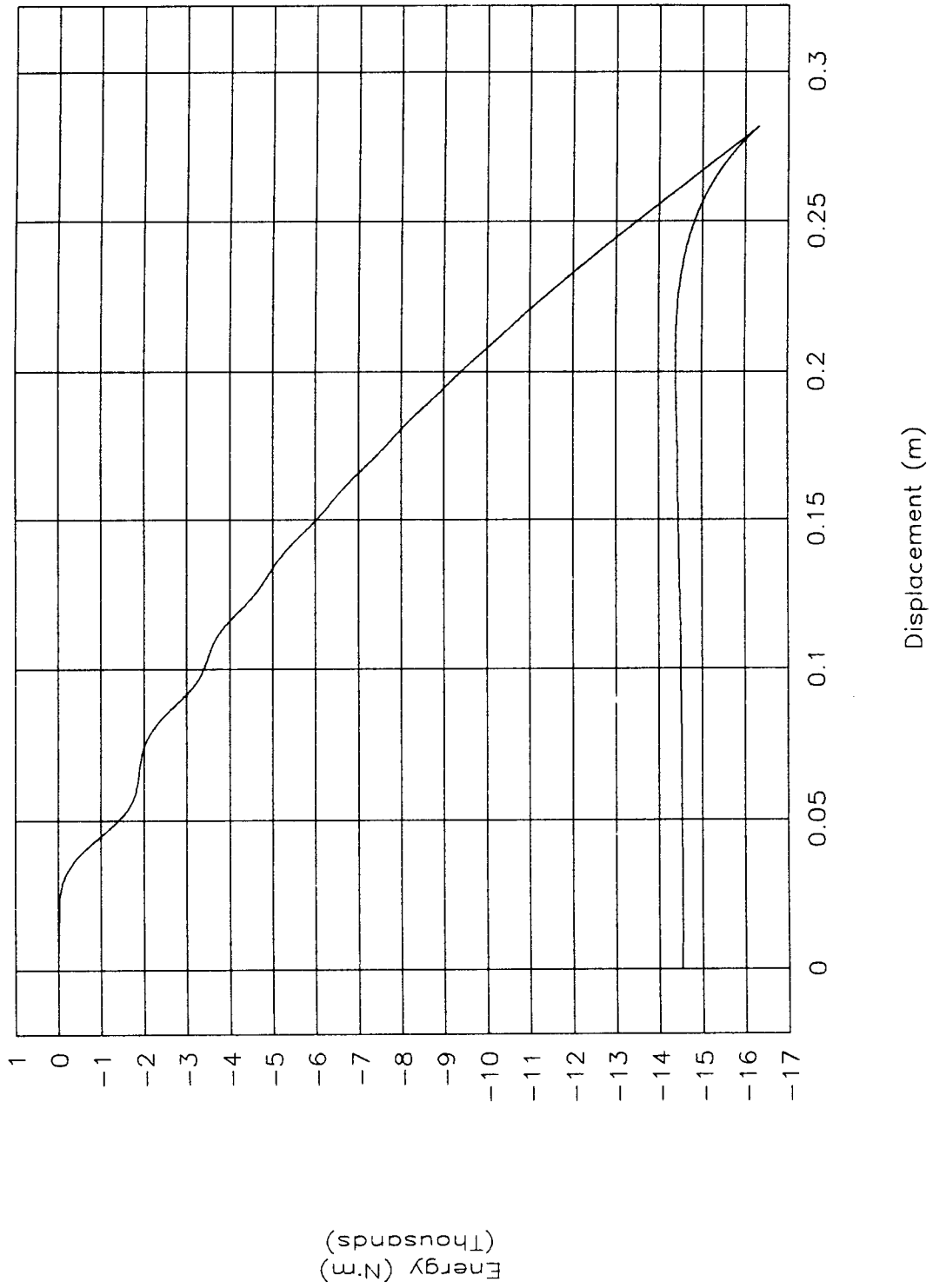


Figure 15. Energy vs. displacement, test 96P001.

TEST NO. 96P001

Strain vs. time (left front)

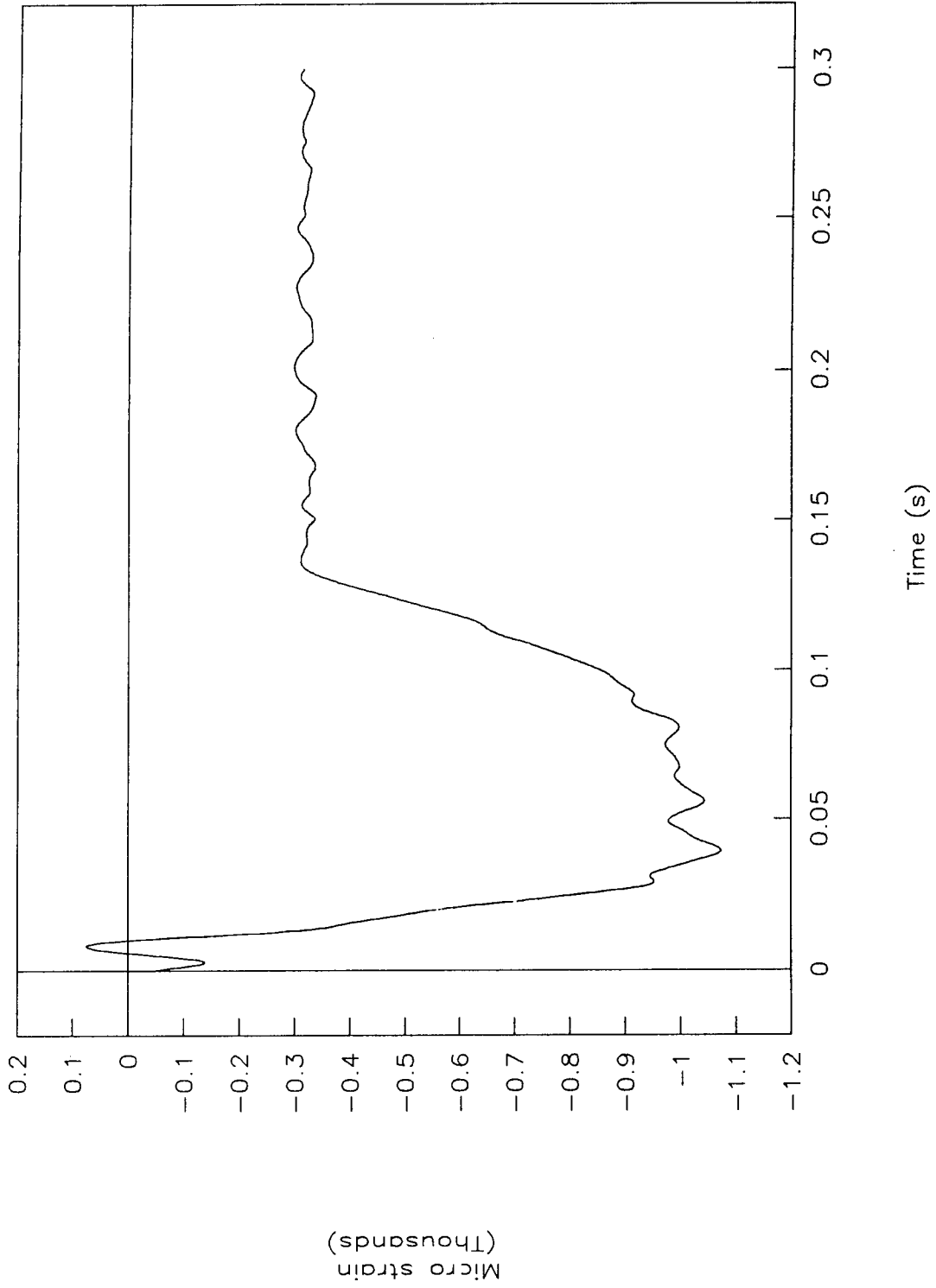


Figure 16. Strain vs. time (left front), test 96P001.

TEST NO. 96P001

Strain vs. time (right front)

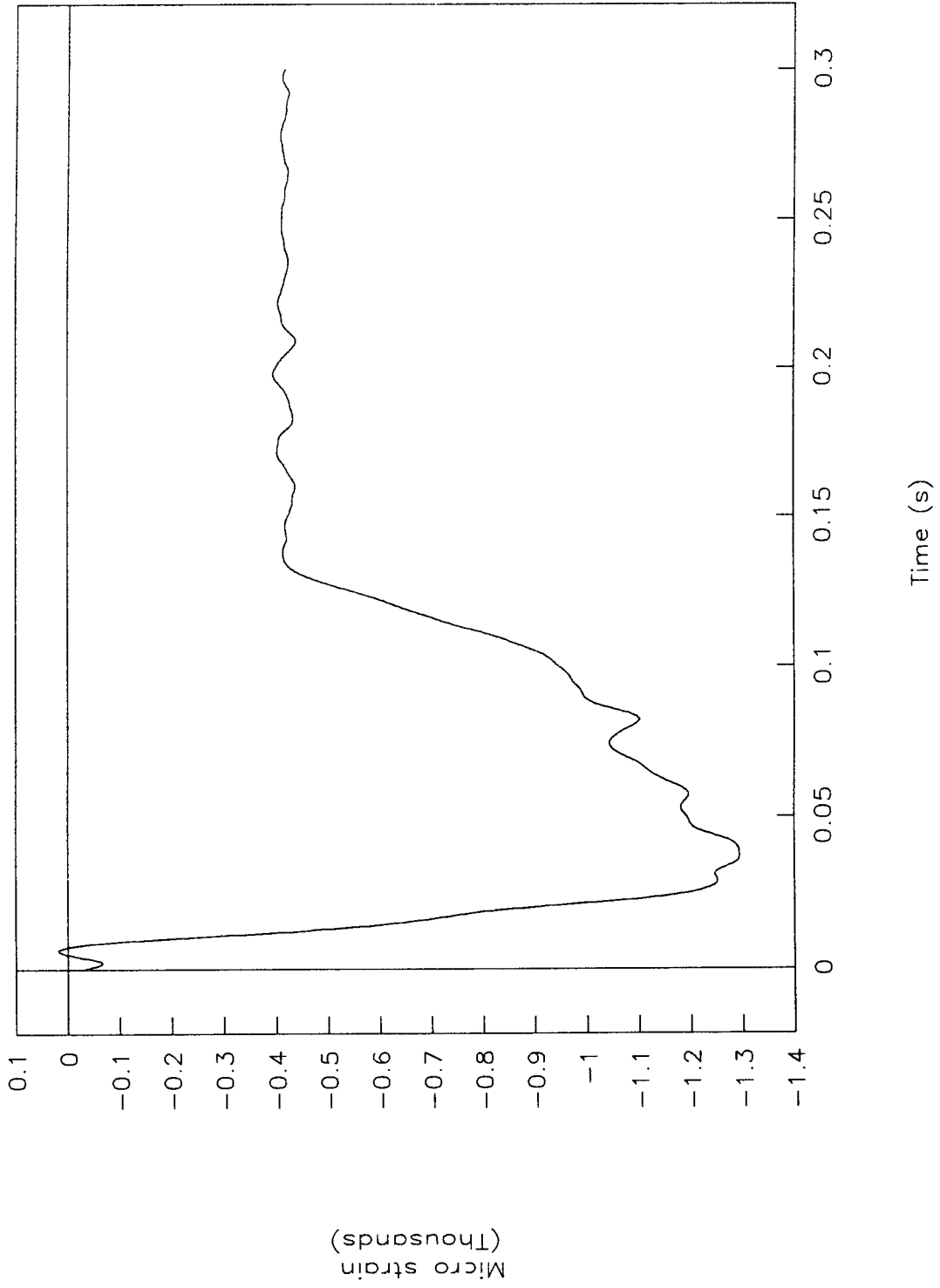


Figure 17. Strain vs. time (right front), test 96P001.

TEST NO. 96P001

Strain vs. time (left rear)

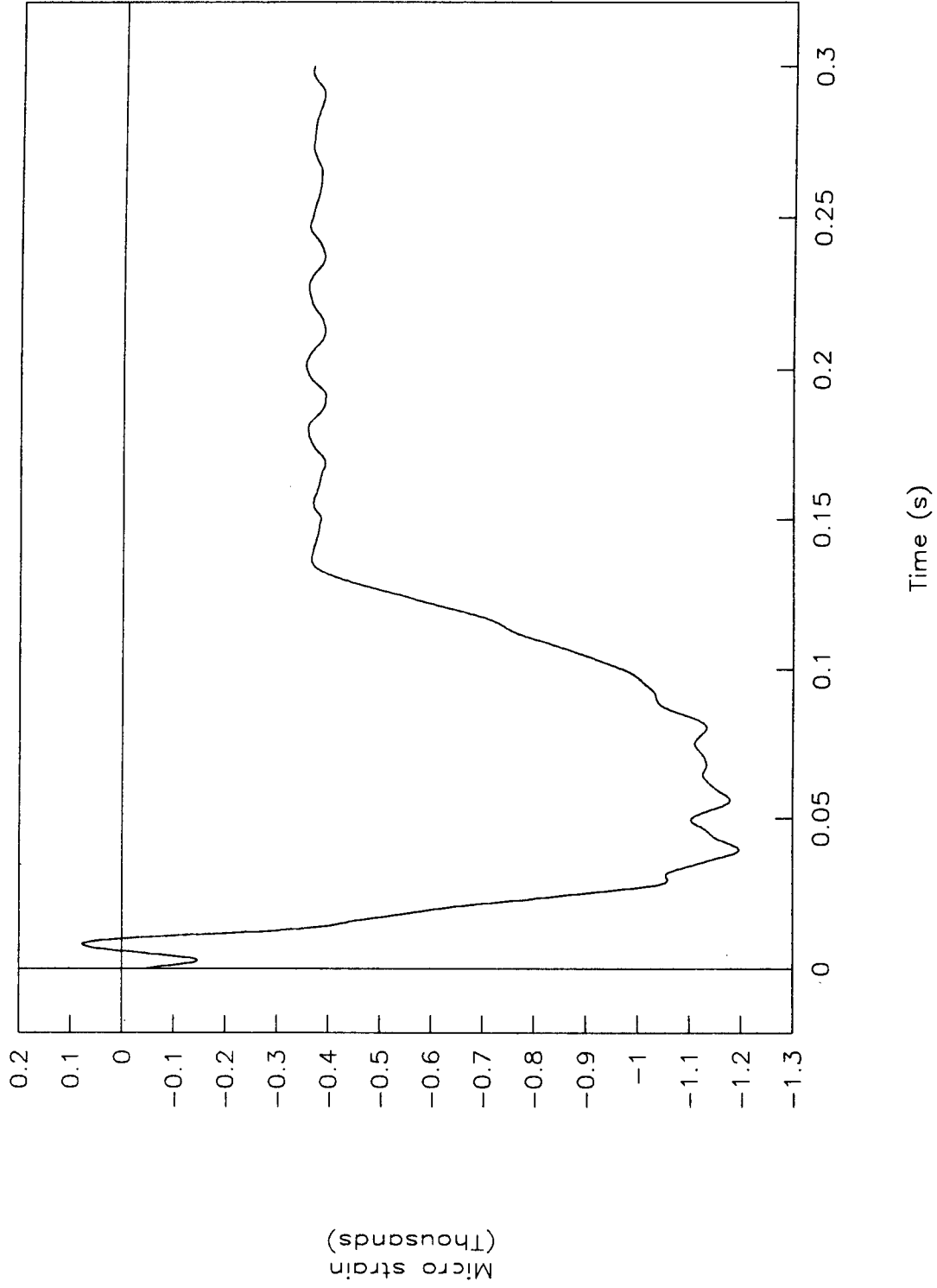


Figure 18. Strain vs. time (left rear), test 96P001.

TEST NO. 96P001

Strain vs. time (right rear)

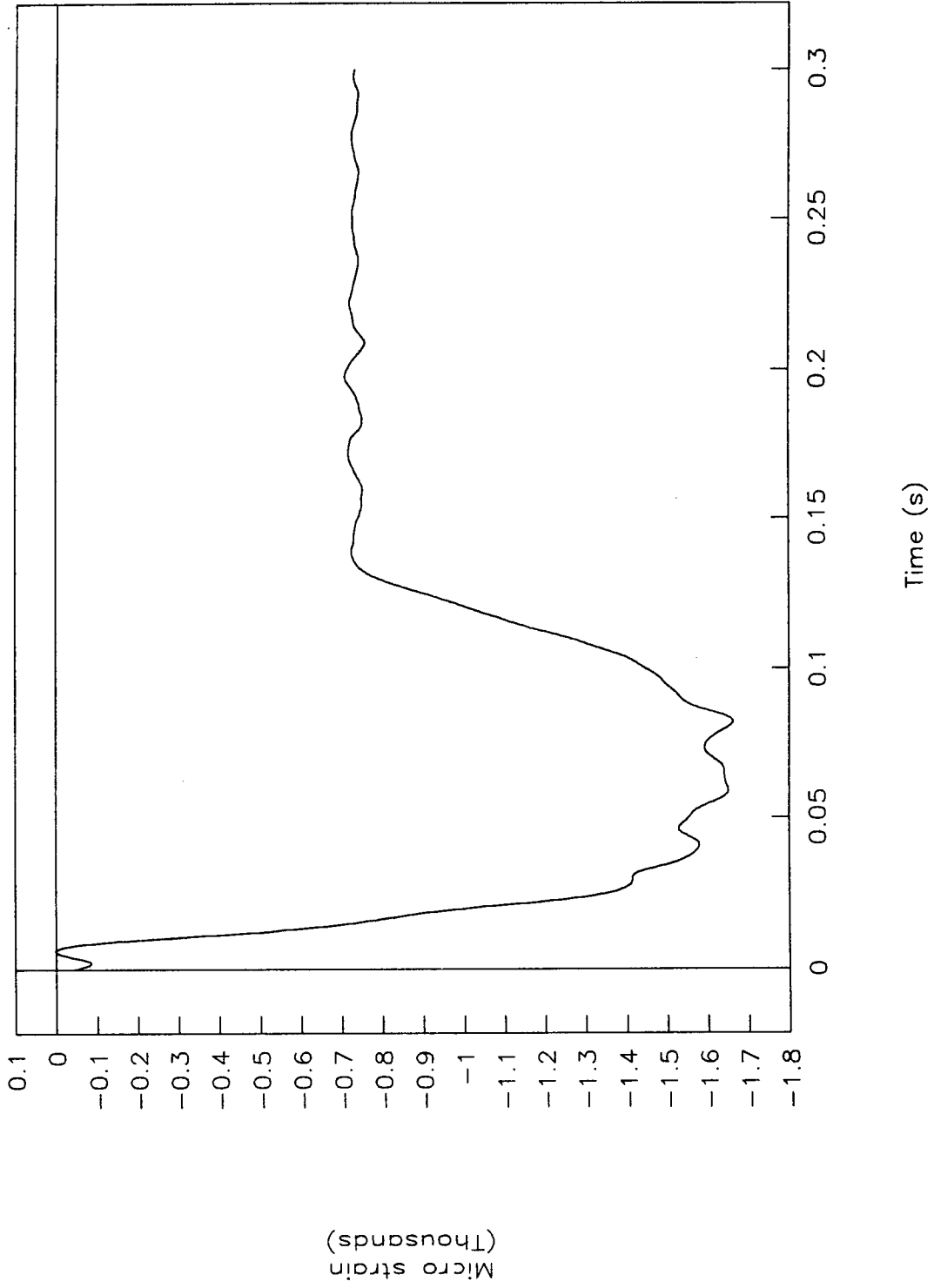


Figure 19. Strain vs. time (right rear), test 96P001.

TEST NO. 96P002

Acceleration vs. time

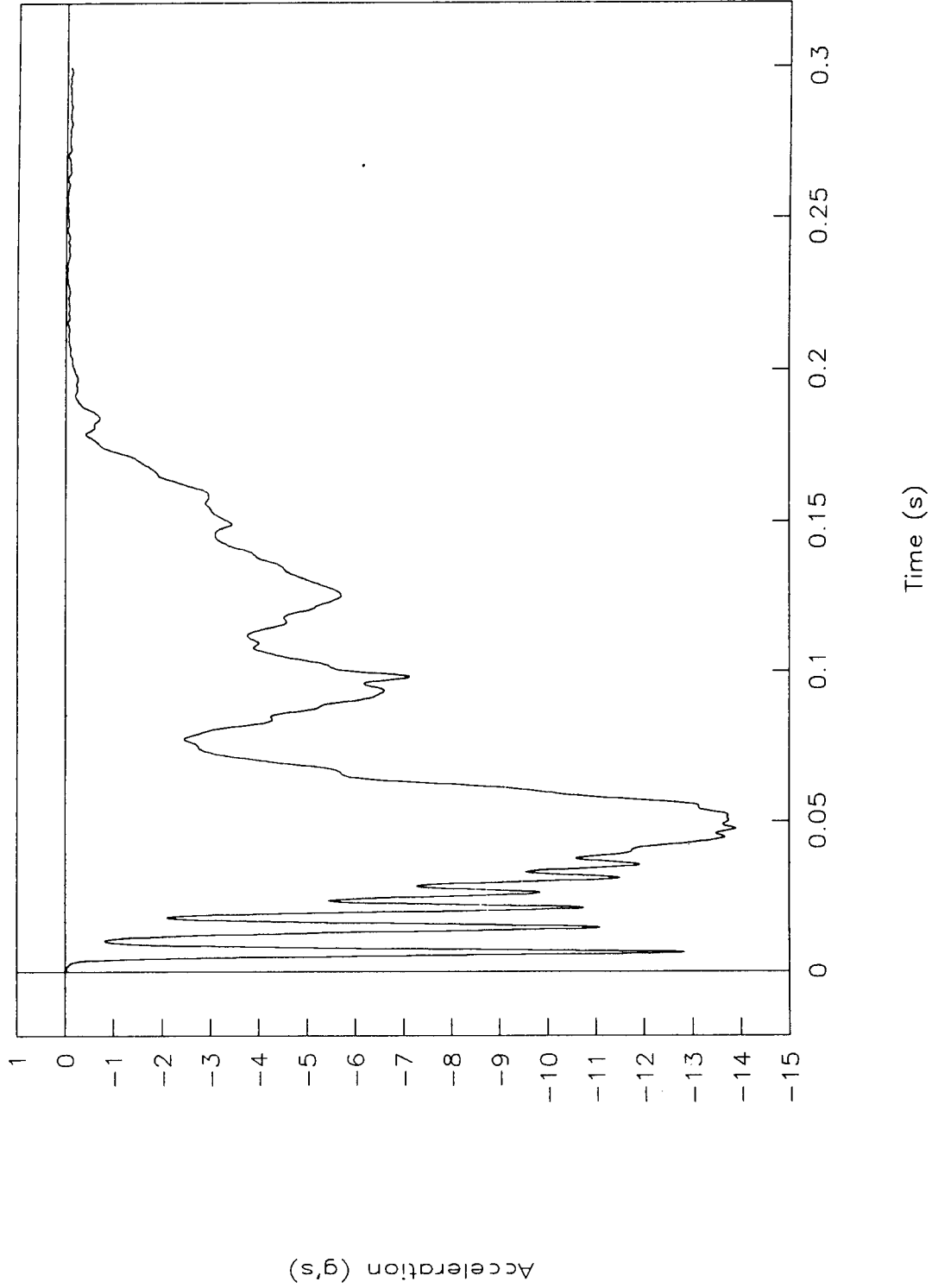


Figure 20. Acceleration vs. time, test 96P002.

TEST NO. 96P002

Velocity vs. time

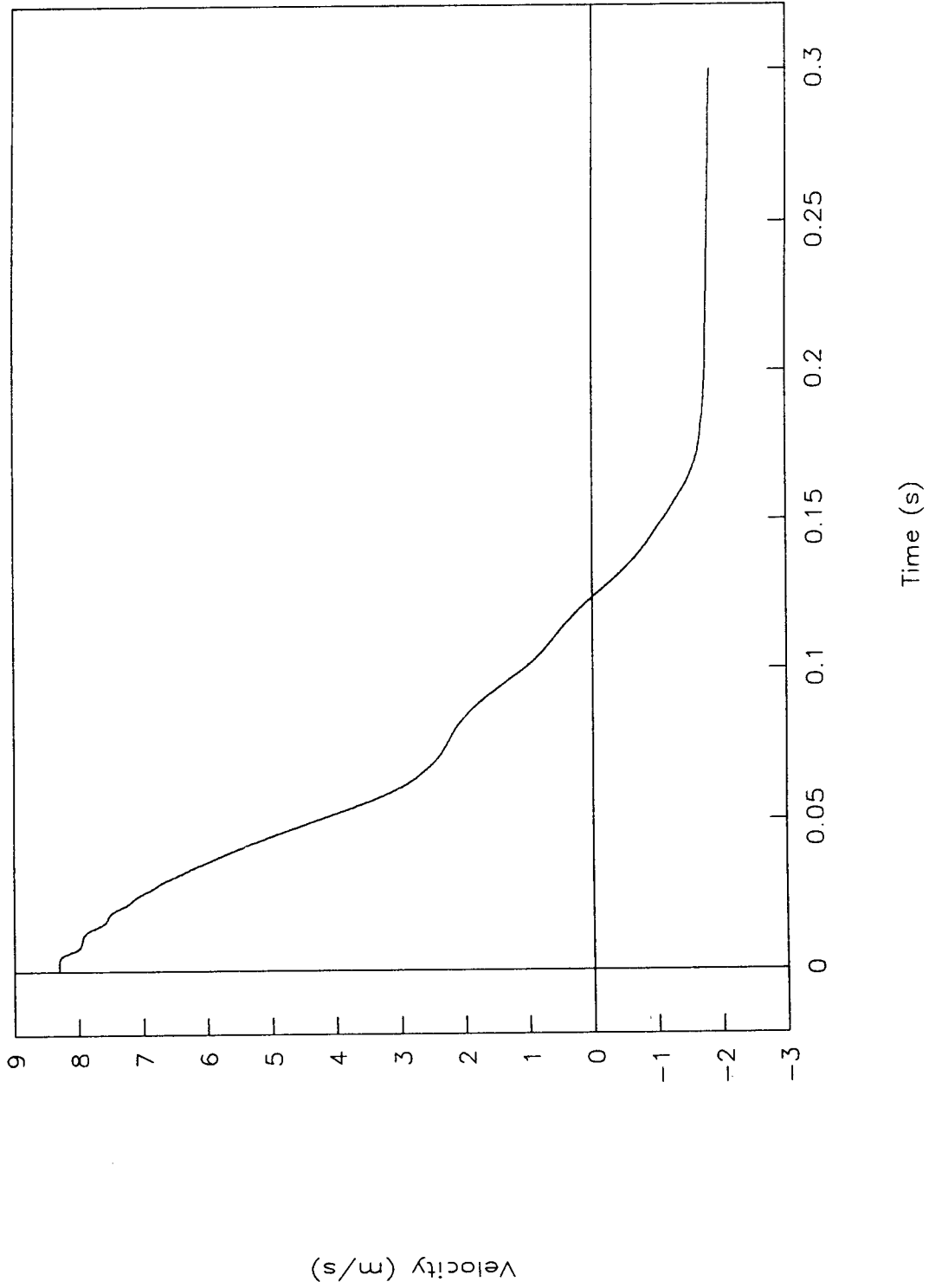


Figure 21. Velocity vs. time, test 96P002.

TEST NO. 96P002

Displacement vs. time

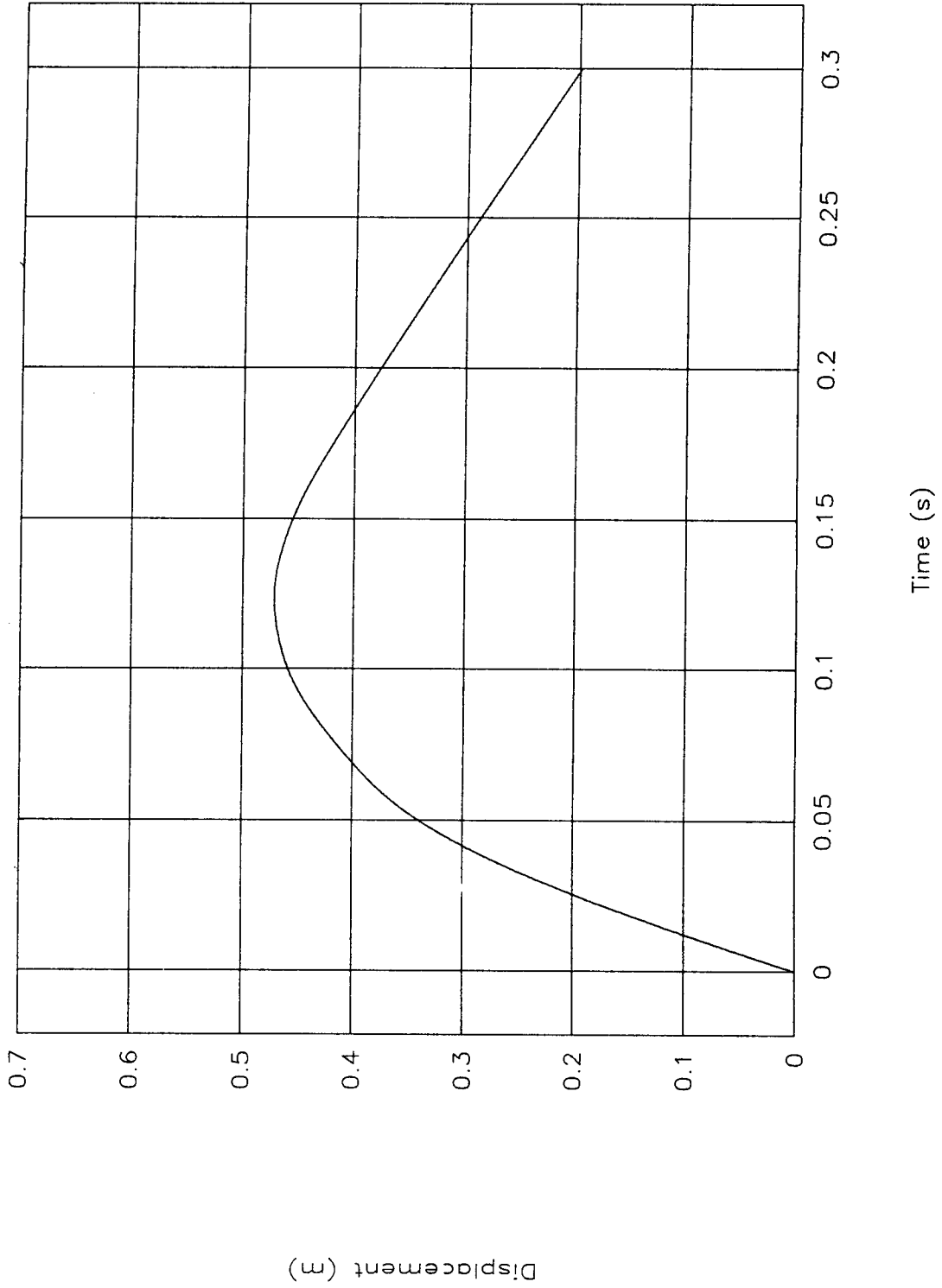


Figure 22. Displacement vs. time, test 96P002.

TEST NO. 96P002

Force vs. time

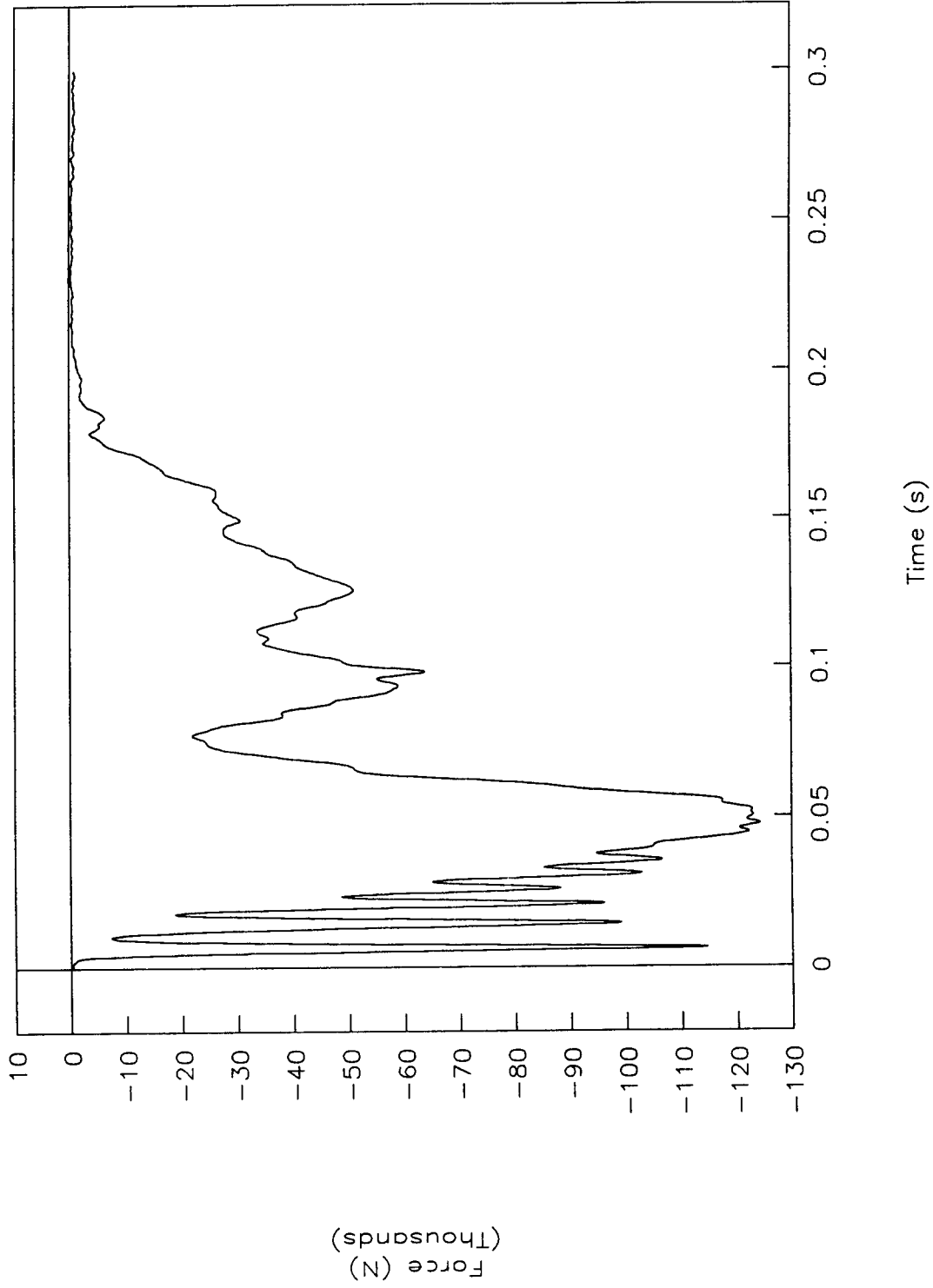


Figure 23. Force vs. time, test 96P002.

TEST NO. 96P002

Force vs. displacement

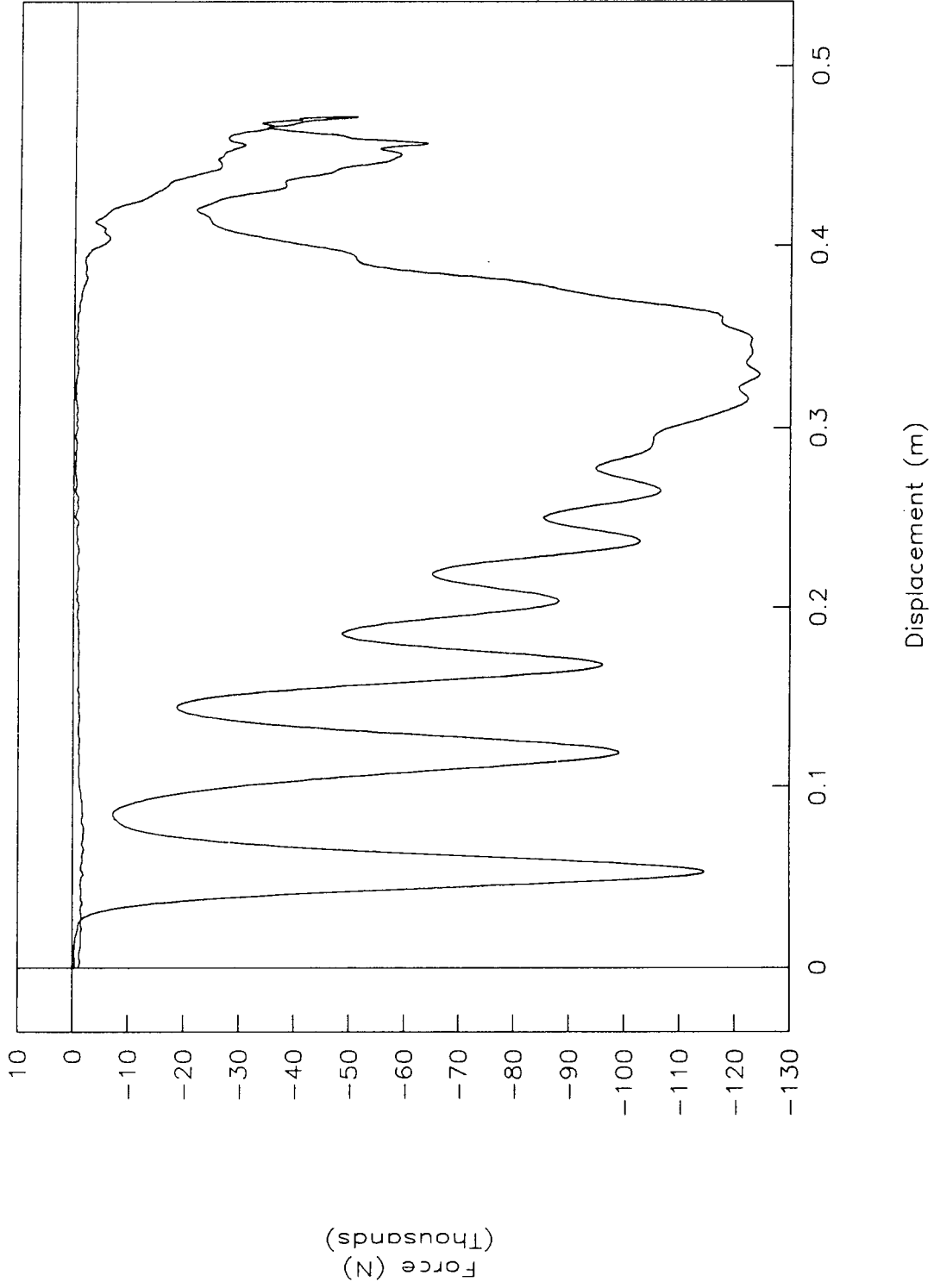


Figure 24. Force vs. displacement, test 96P002.

TEST NO. 96P002

Energy vs. displacement

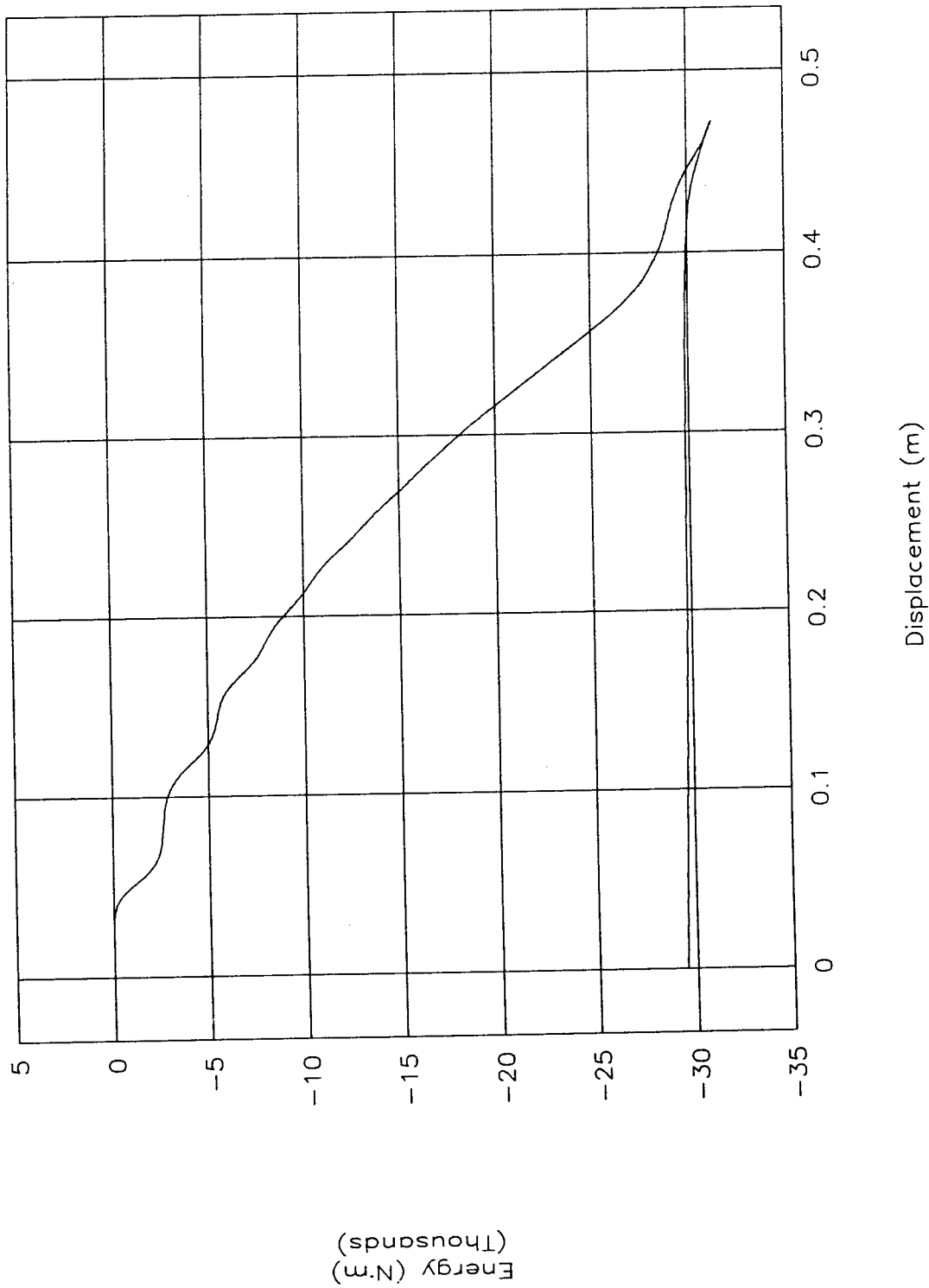


Figure 25. Energy vs. displacement, test 96P002.

TEST NO. 96P002

Strain vs. time (left front)

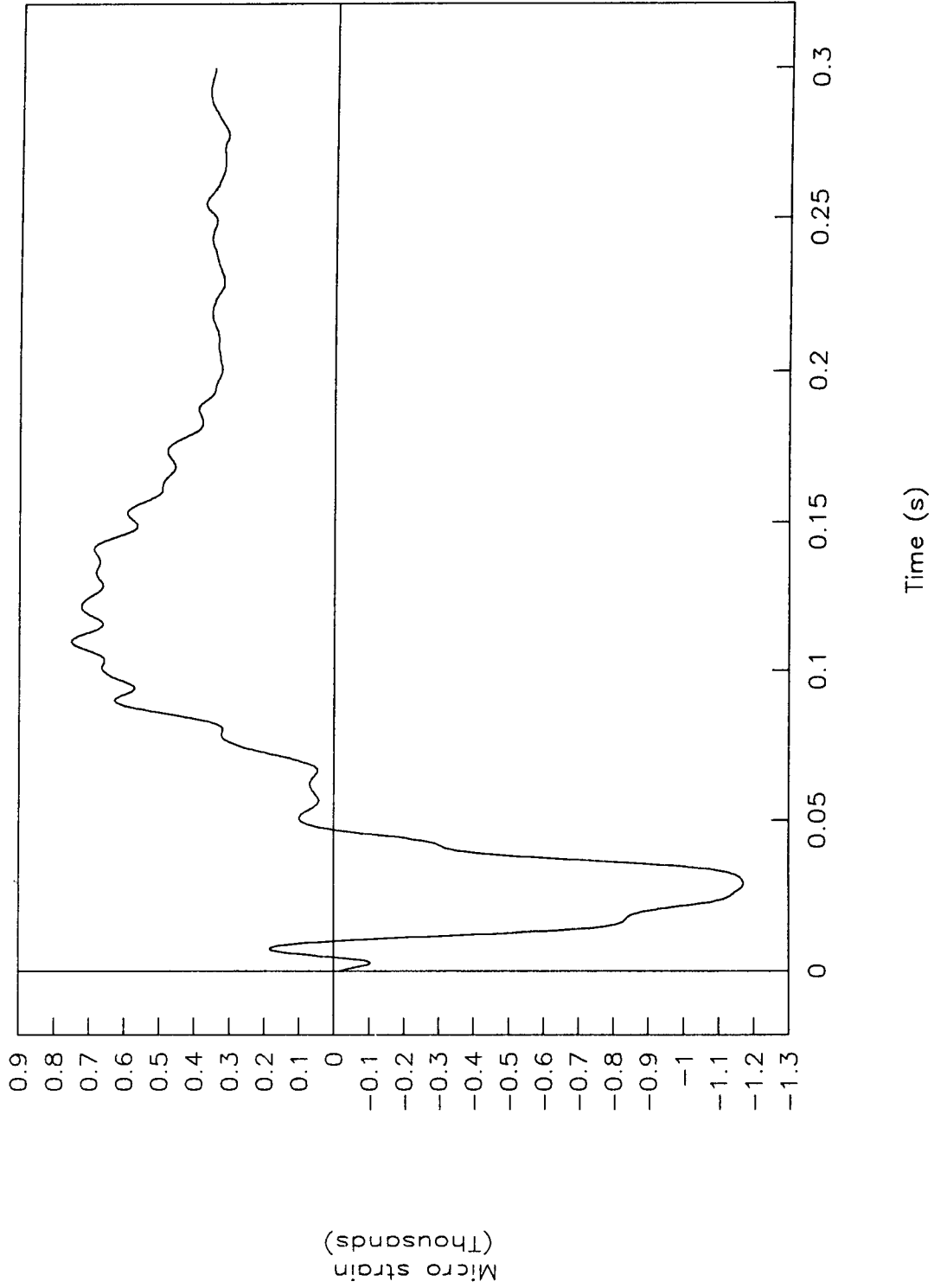


Figure 26. Strain vs. time (left front), test 96P002.

TEST NO. 96P002

Strain vs. time (right front)

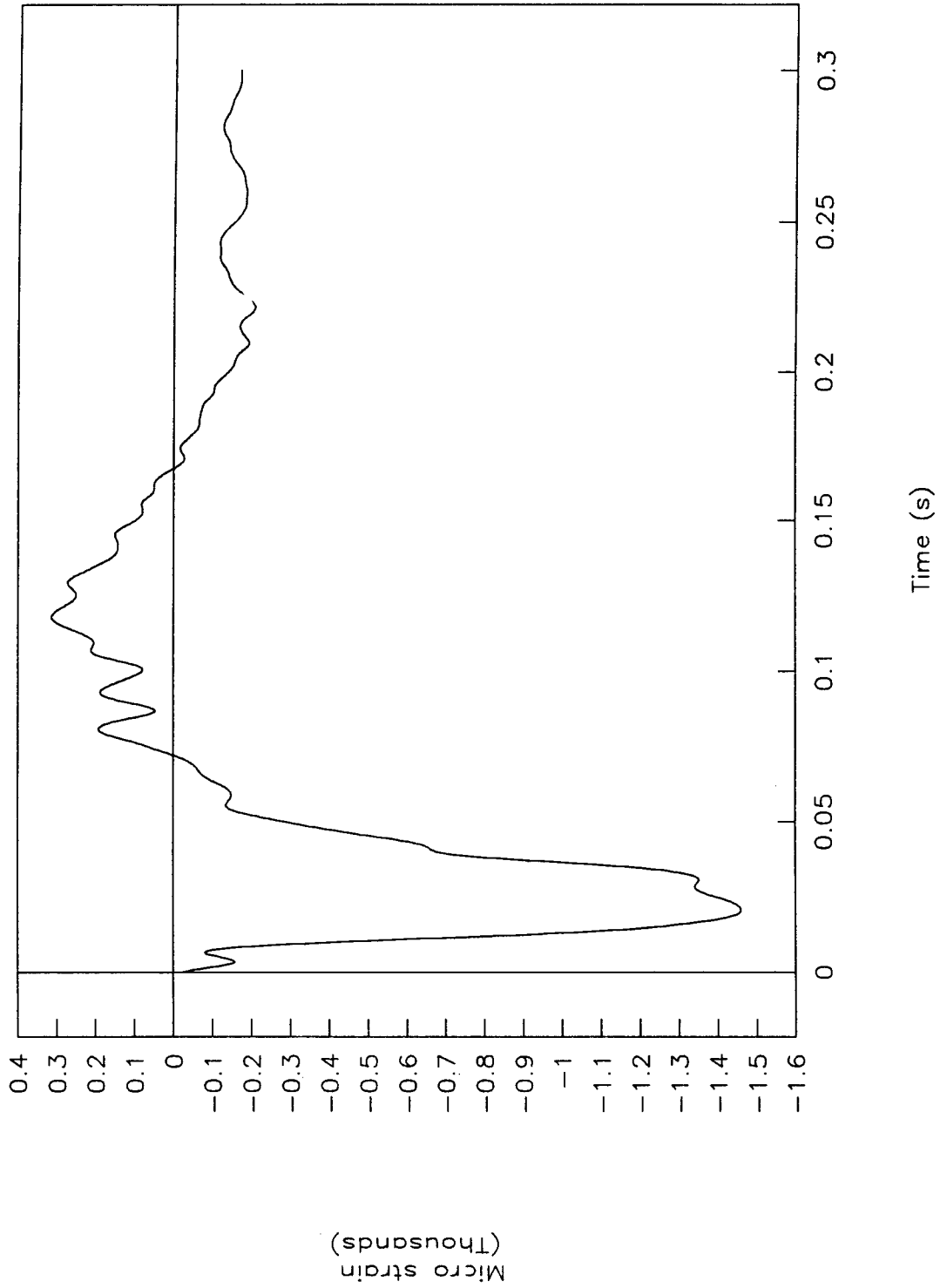


Figure 27. Strain vs. time (right front), test 96P002.

TEST NO. 96P002

Strain vs. time (left rear)

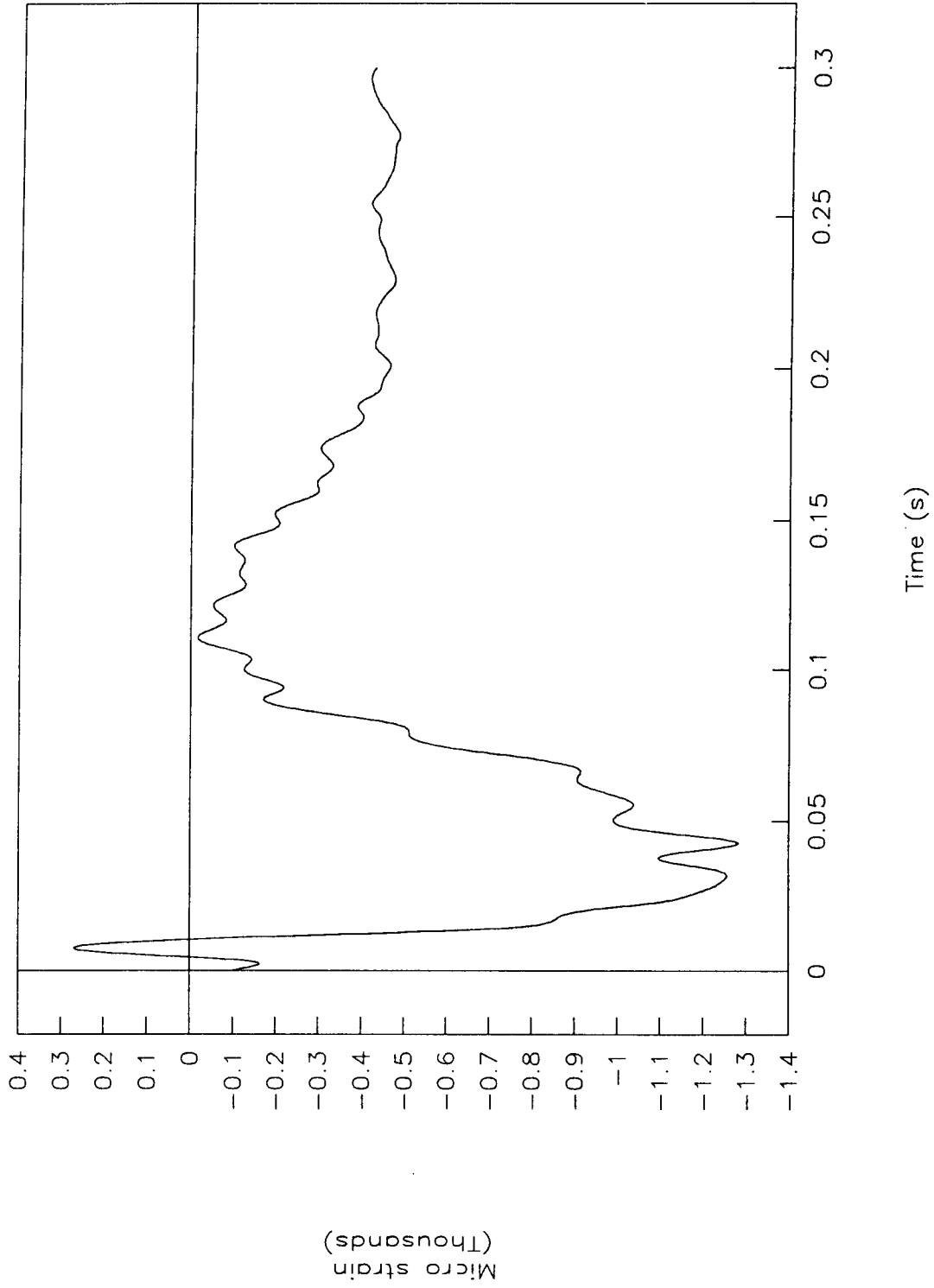


Figure 28. Strain vs. time (left rear), test 96P002.

TEST NO. 96P002
Strain vs. time (right rear)

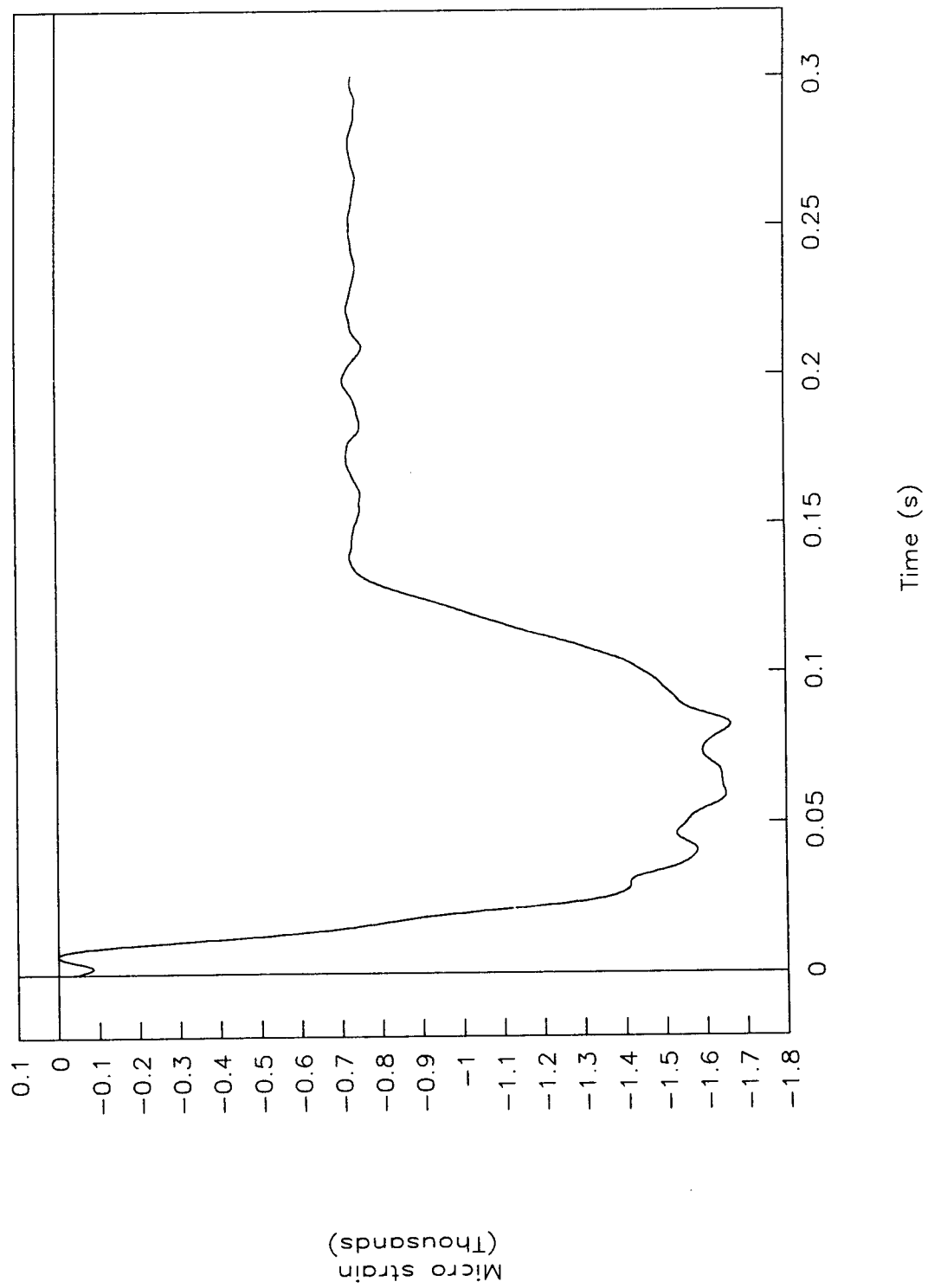


Figure 29. Strain vs. time (right rear), test 96P002.

TEST NO. 96P003

Acceleration vs. time

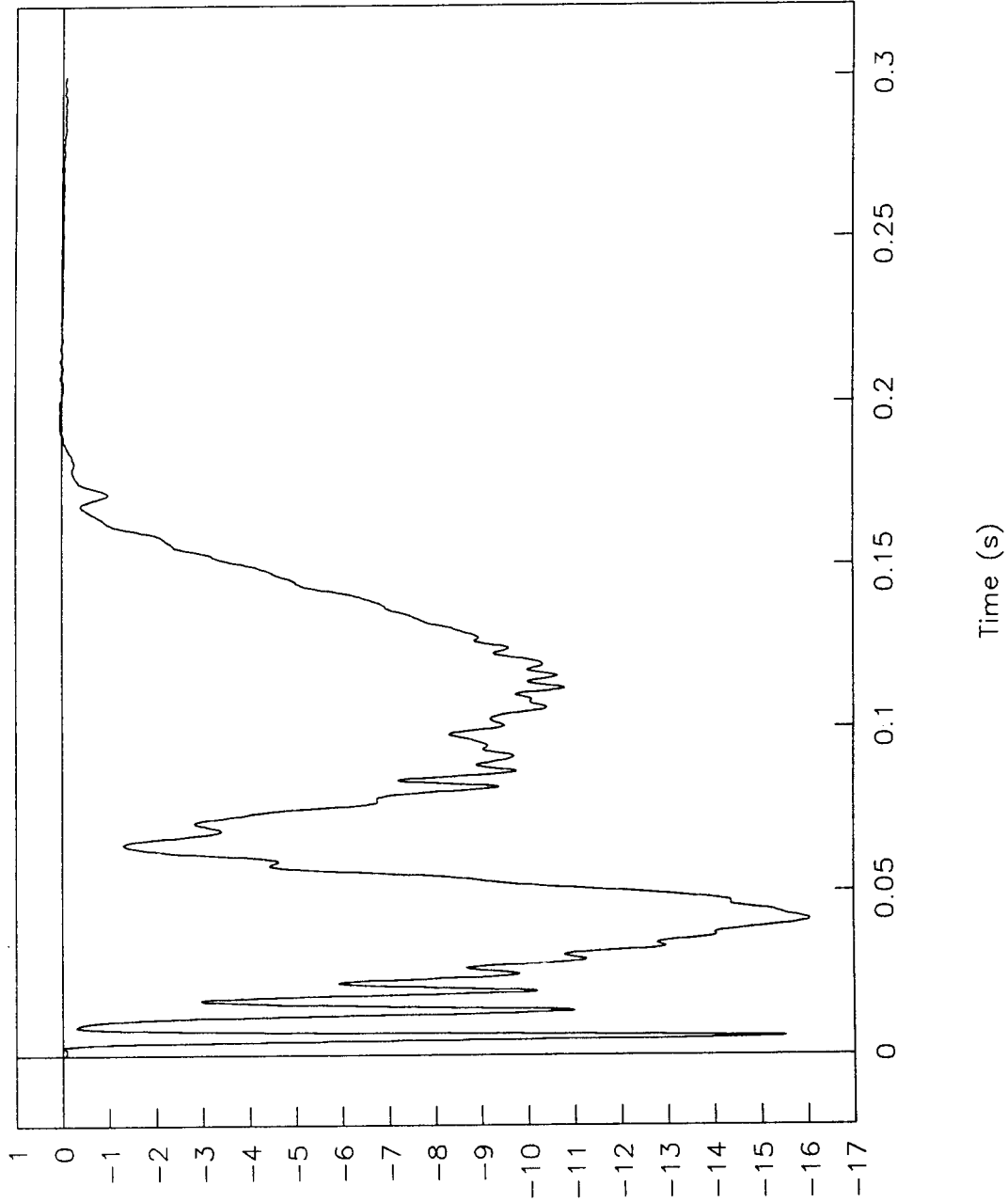


Figure 30. Acceleration vs. time, test 96P003.

TEST NO. 96P003

Velocity vs. time

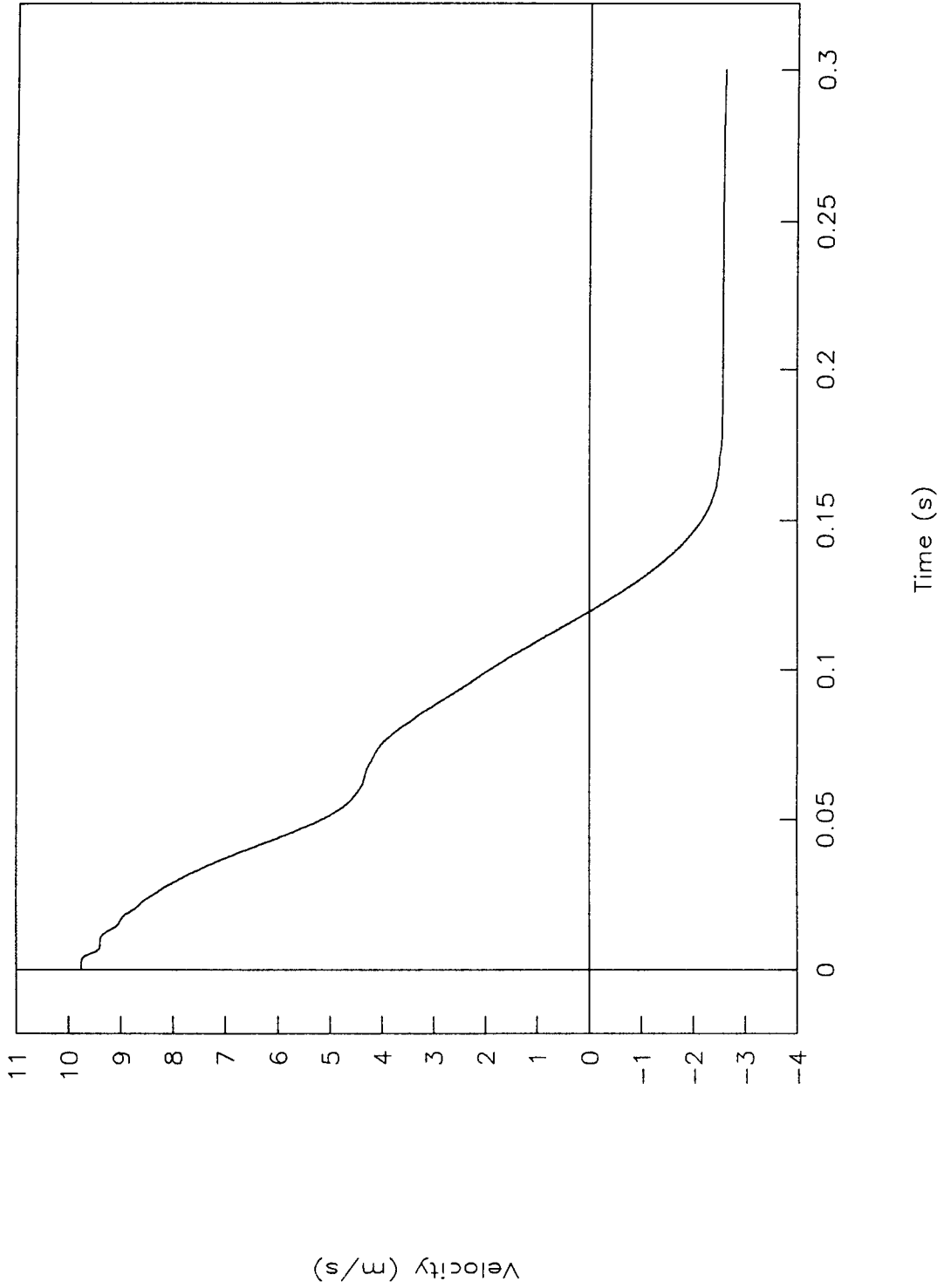


Figure 31. Velocity vs. time, test 96P003.

TEST NO. 96P003

Displacement vs. time

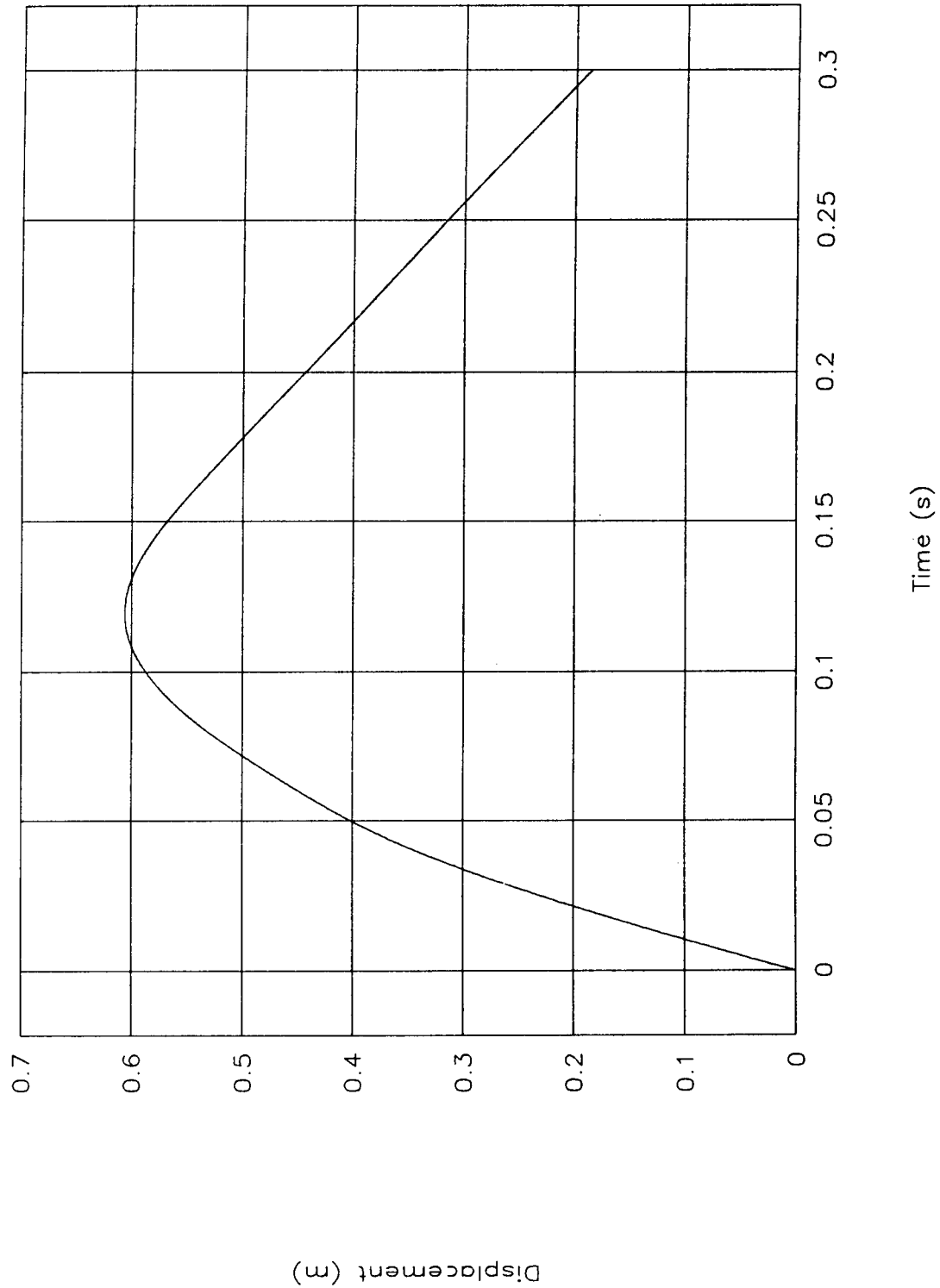


Figure 32. Displacement vs. time, test 96P003.

TEST NO. 96P003

Force vs. time

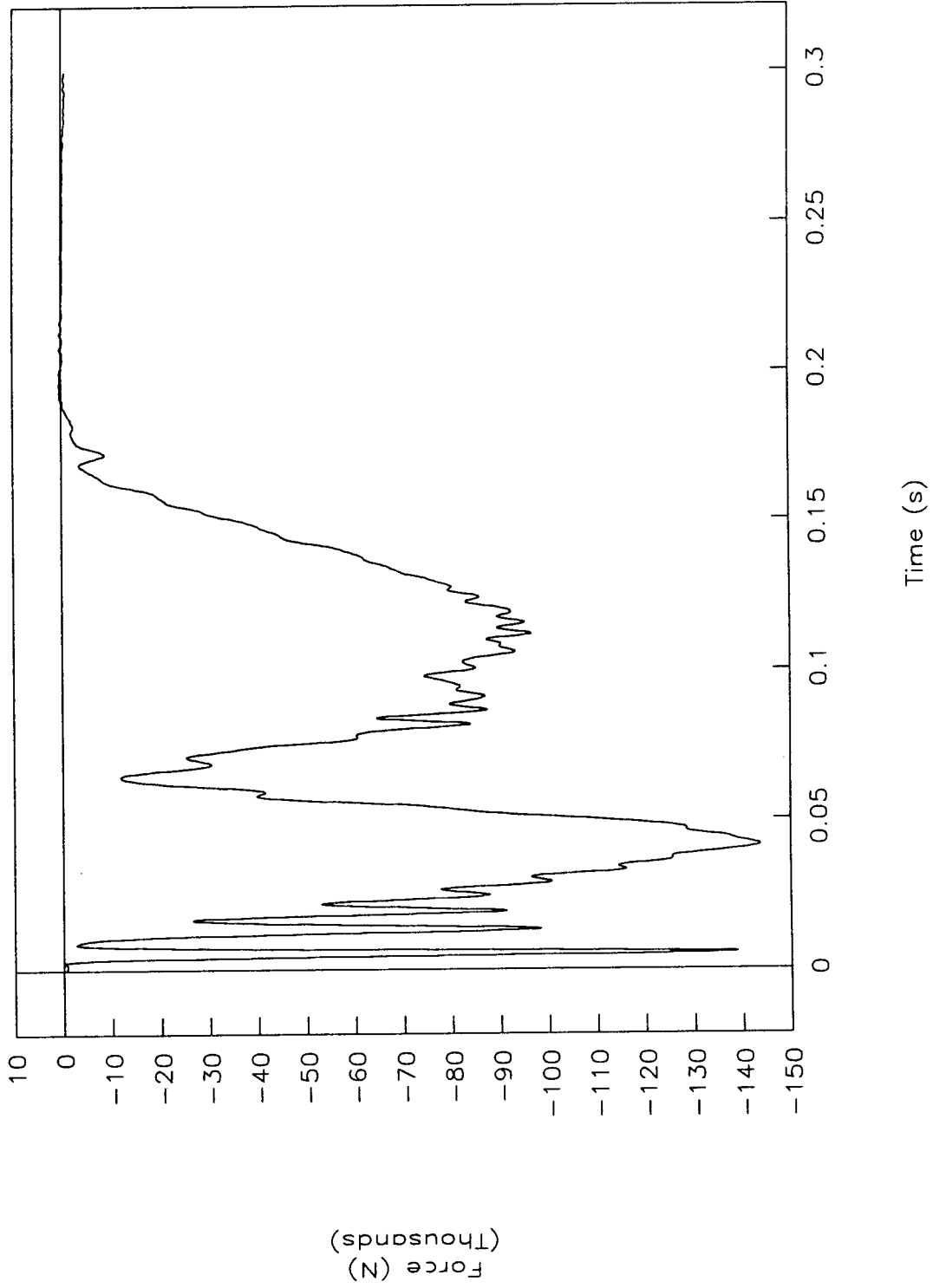


Figure 33. Force vs. time, test 96P003.

TEST NO. 96P003

Force vs. displacement

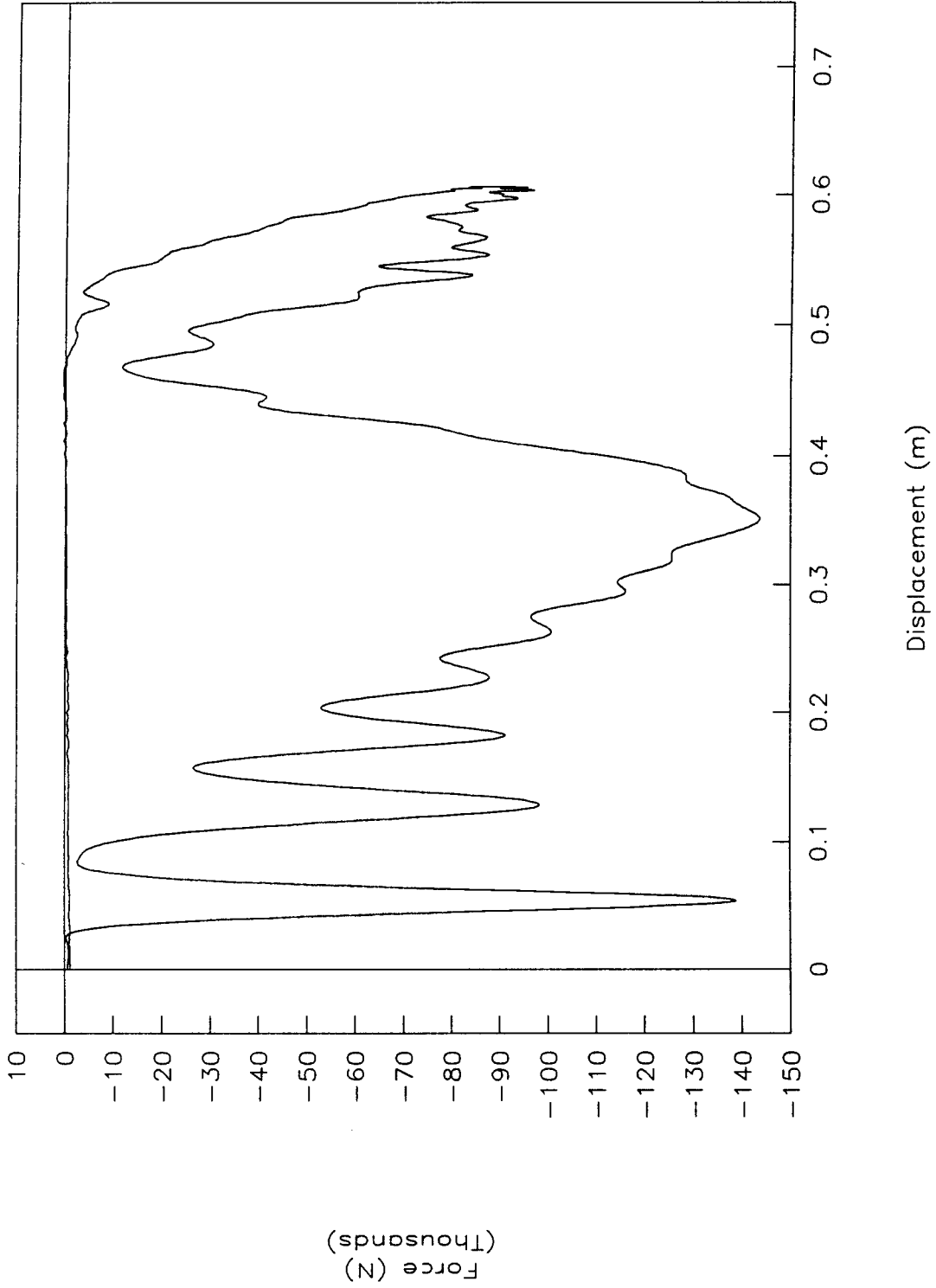


Figure 34. Force vs. displacement, test 96P003.

TEST NO. 96P003

Energy vs. displacement

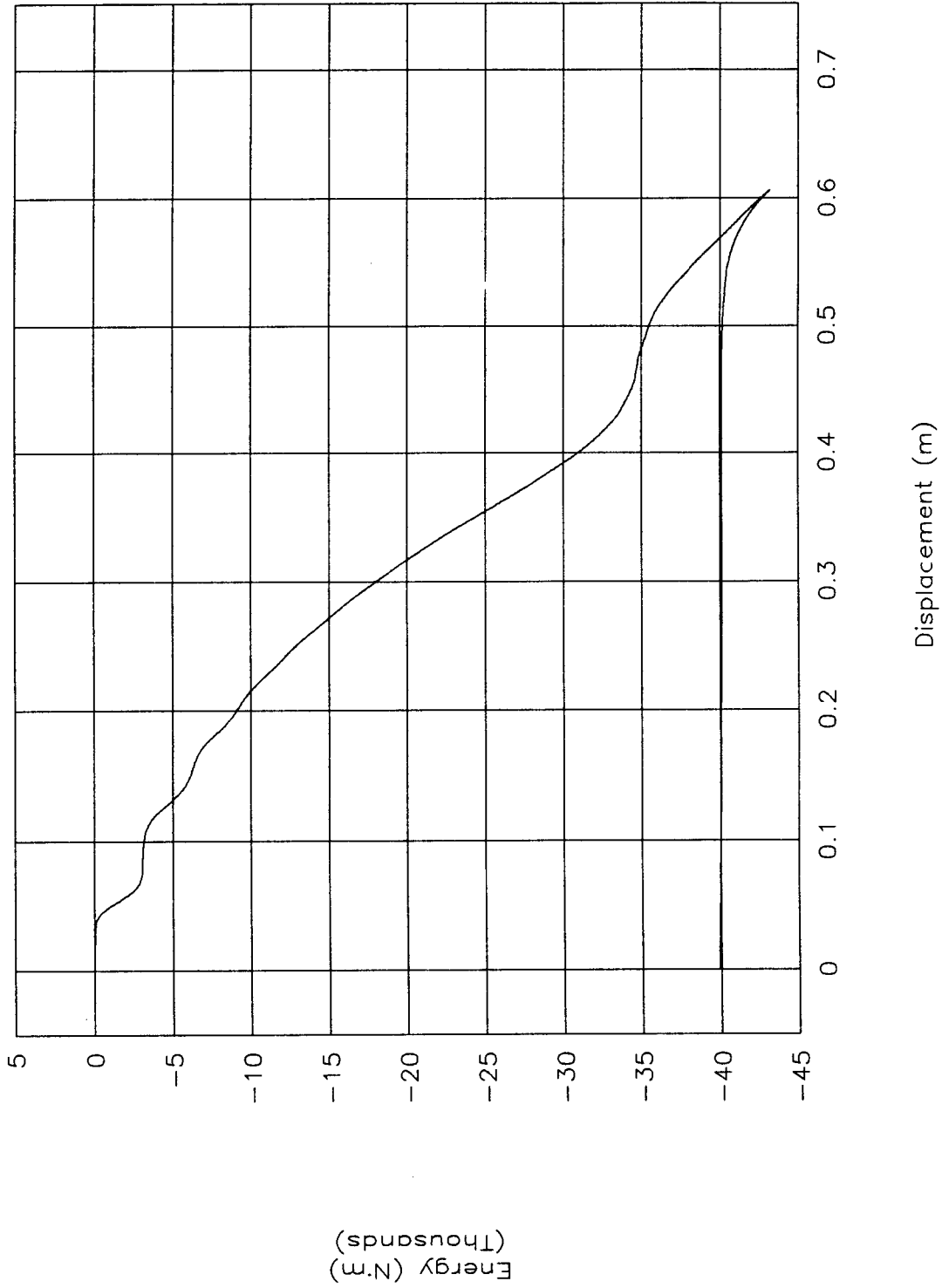


Figure 35. Energy vs. displacement, test 96P003.

TEST NO. 96P003

Strain vs. time (left front)

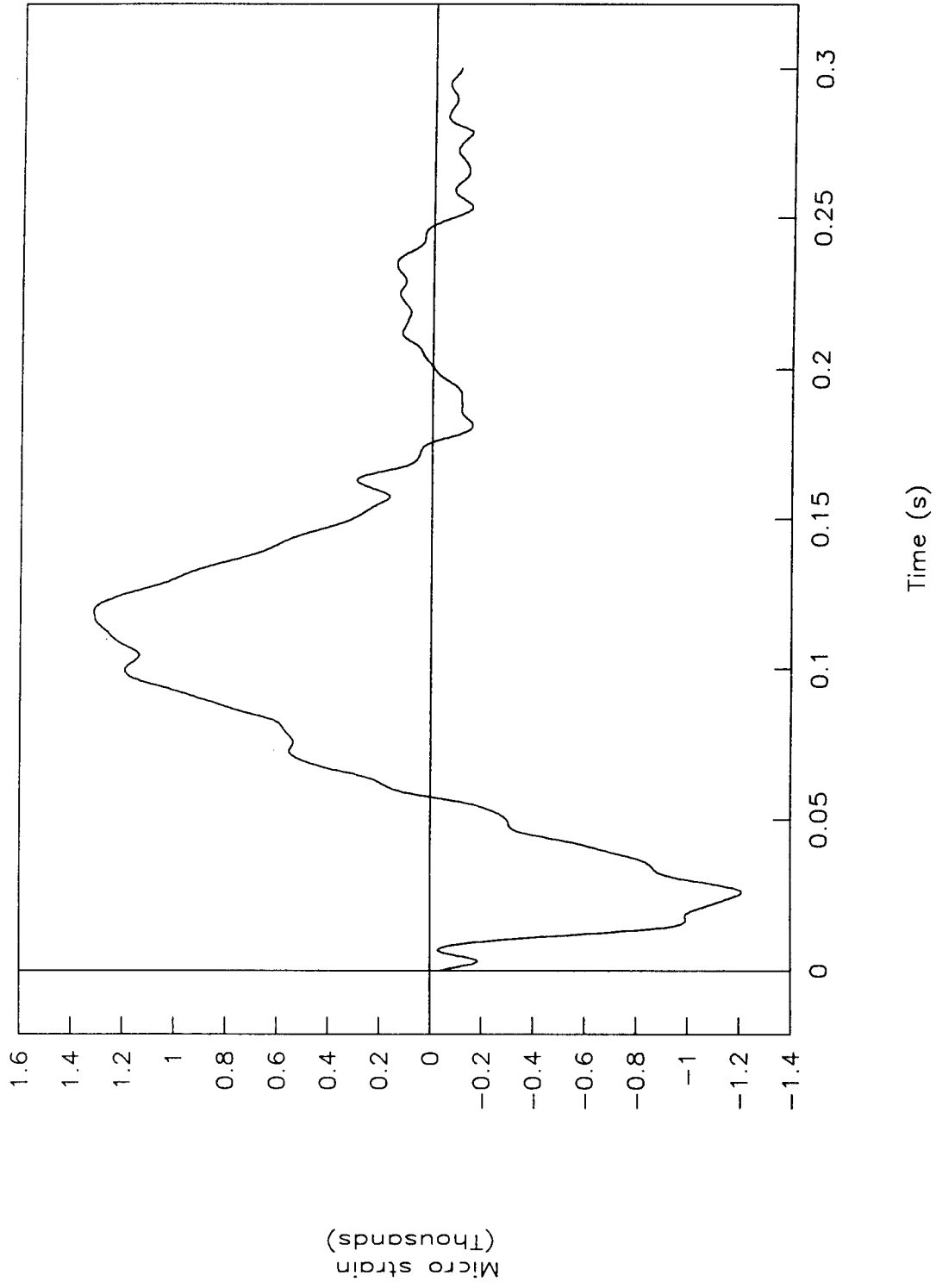


Figure 36. Strain vs. time (left front), test 96P003.

TEST NO. 96P003

Strain vs. time (right front)

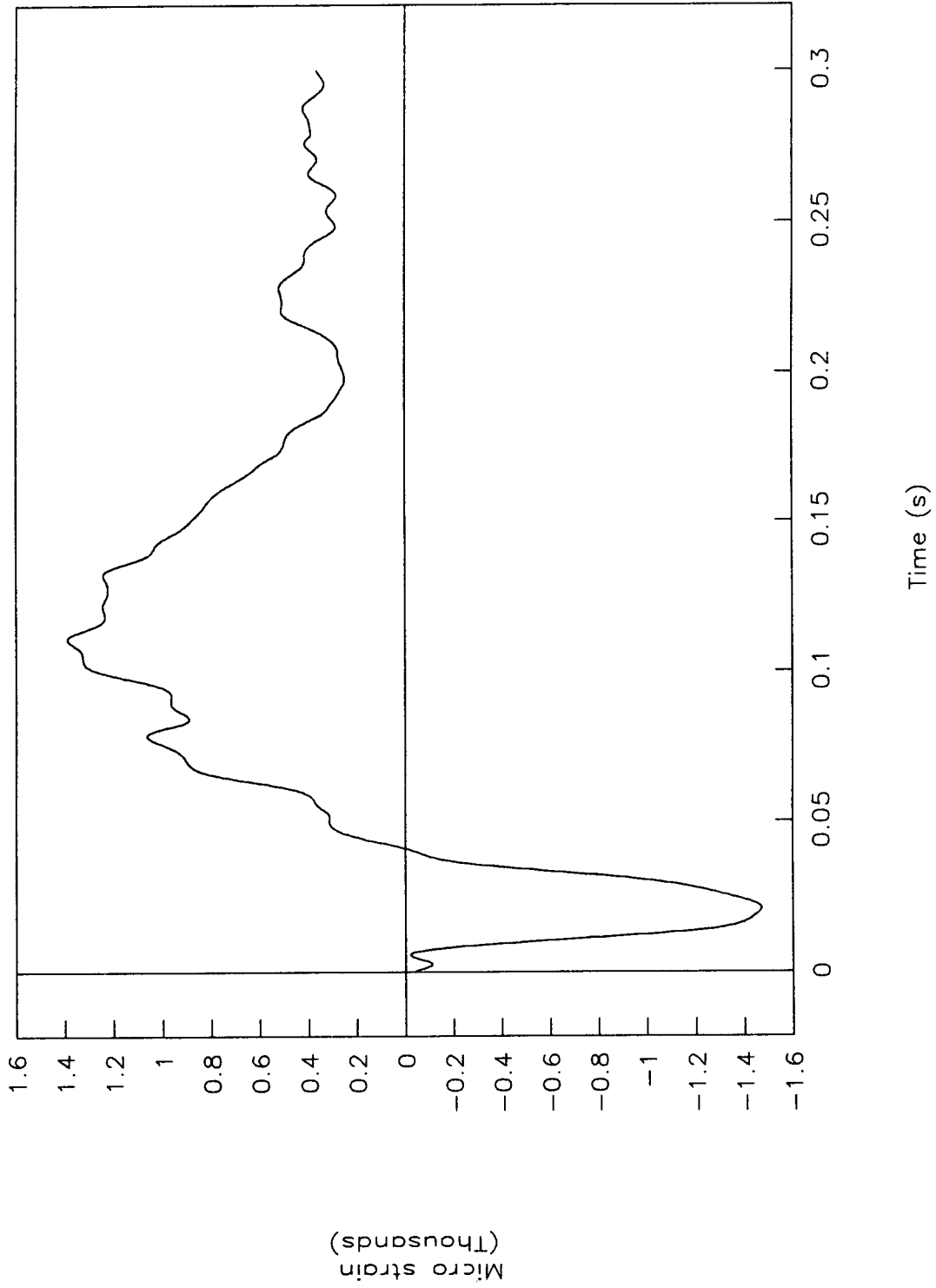


Figure 37. Strain vs. time (right front), test 96P003.

TEST NO. 96P003

Strain vs. time (left rear)

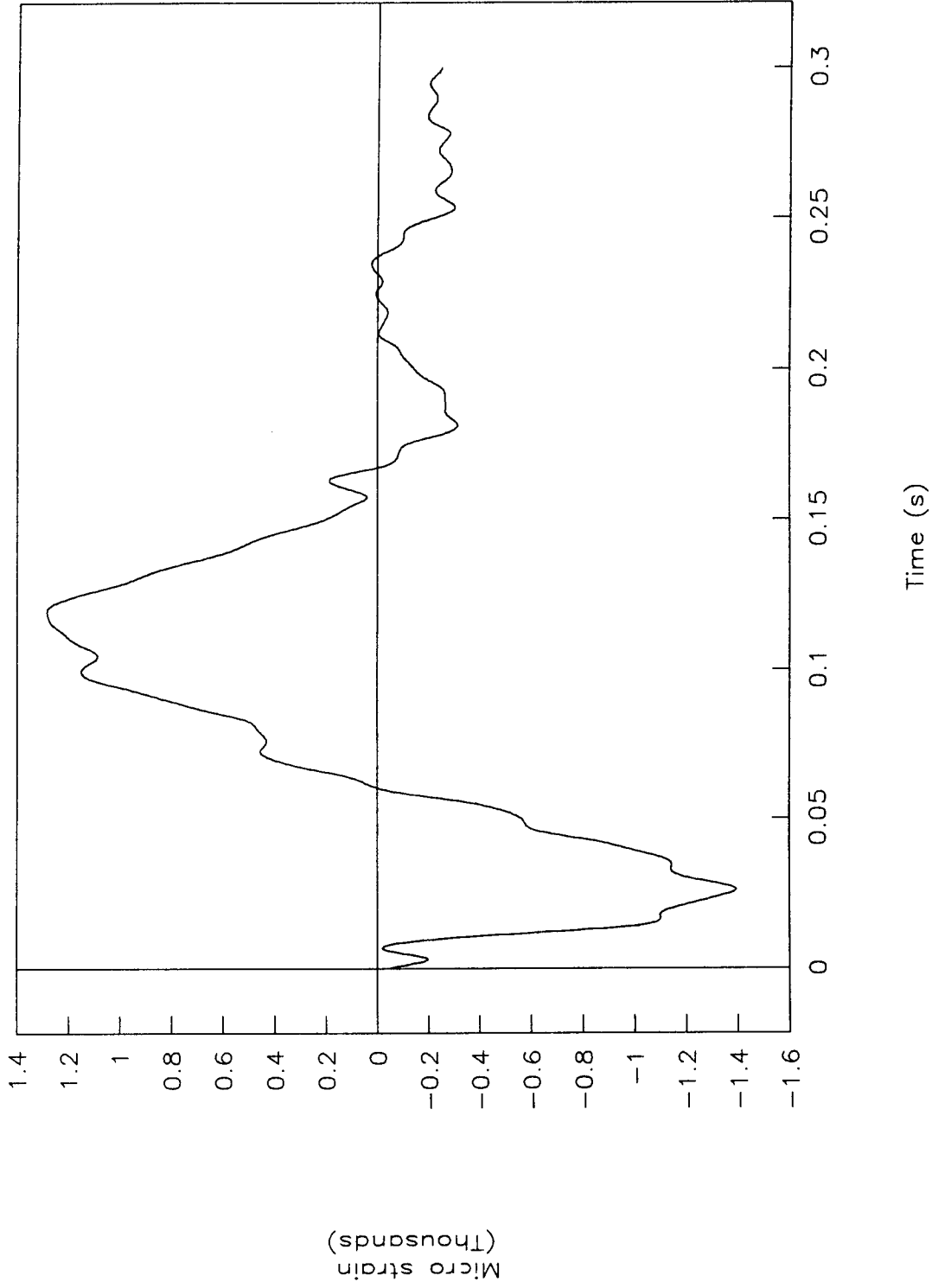


Figure 38. Strain vs. time (left rear), test 96P003.

TEST NO. 96P003

Strain vs. time (right rear)

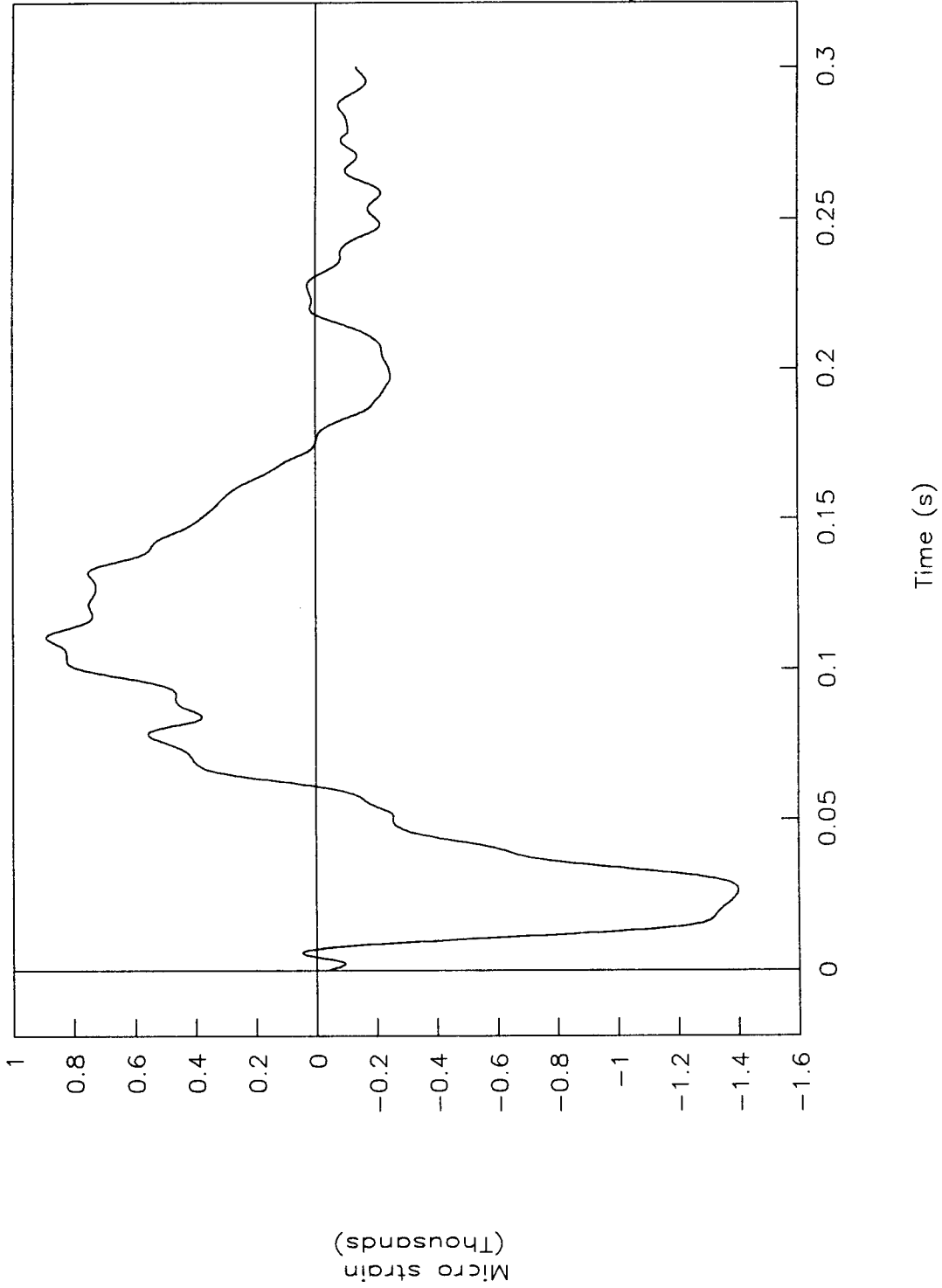


Figure 39. Strain vs. time, (right rear), test 96P003.

TEST NO. 96P004

Acceleration vs. time

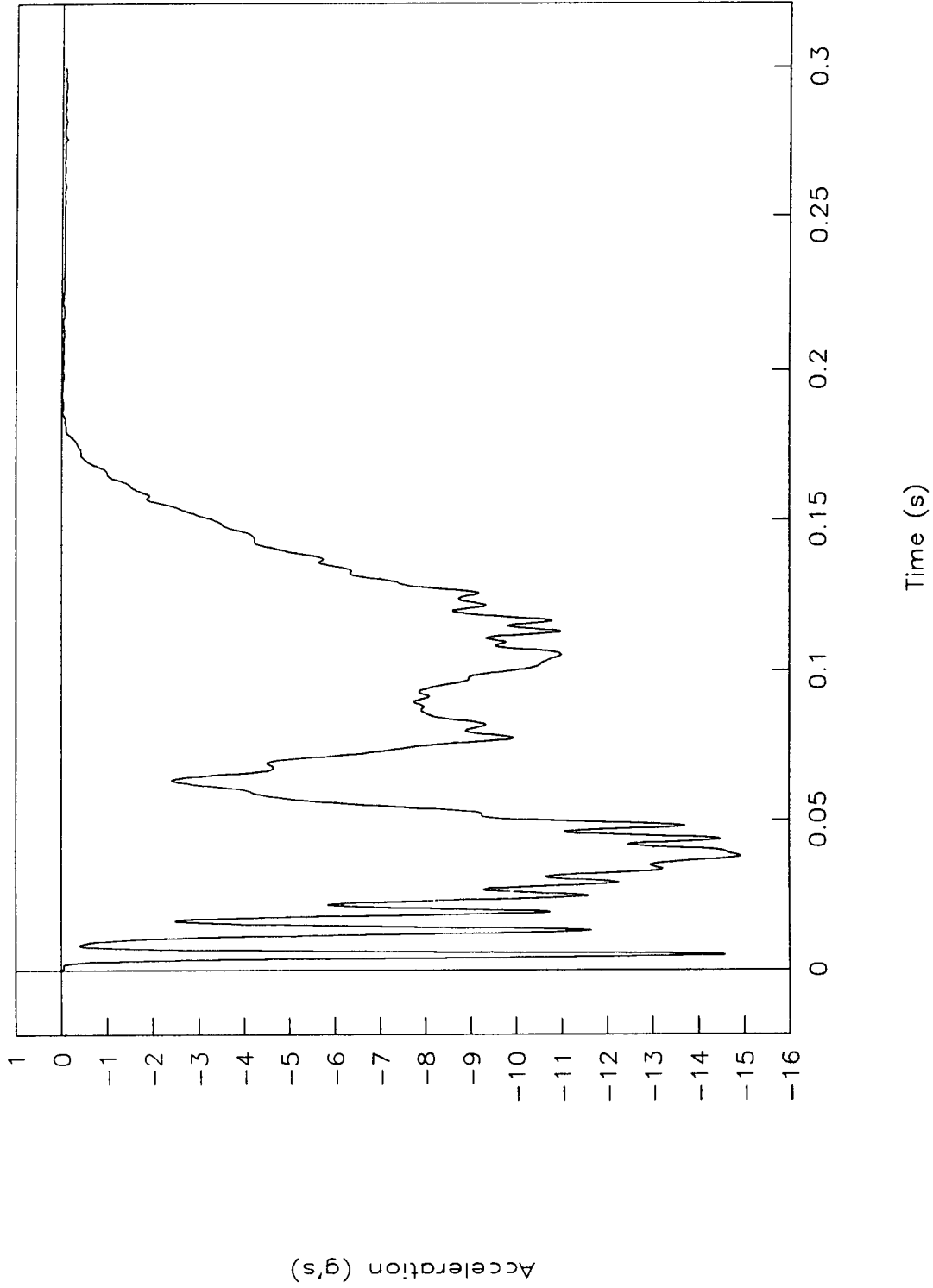


Figure 40. Acceleration vs. time, test 96P004.

TEST NO. 96P004

Velocity vs. time

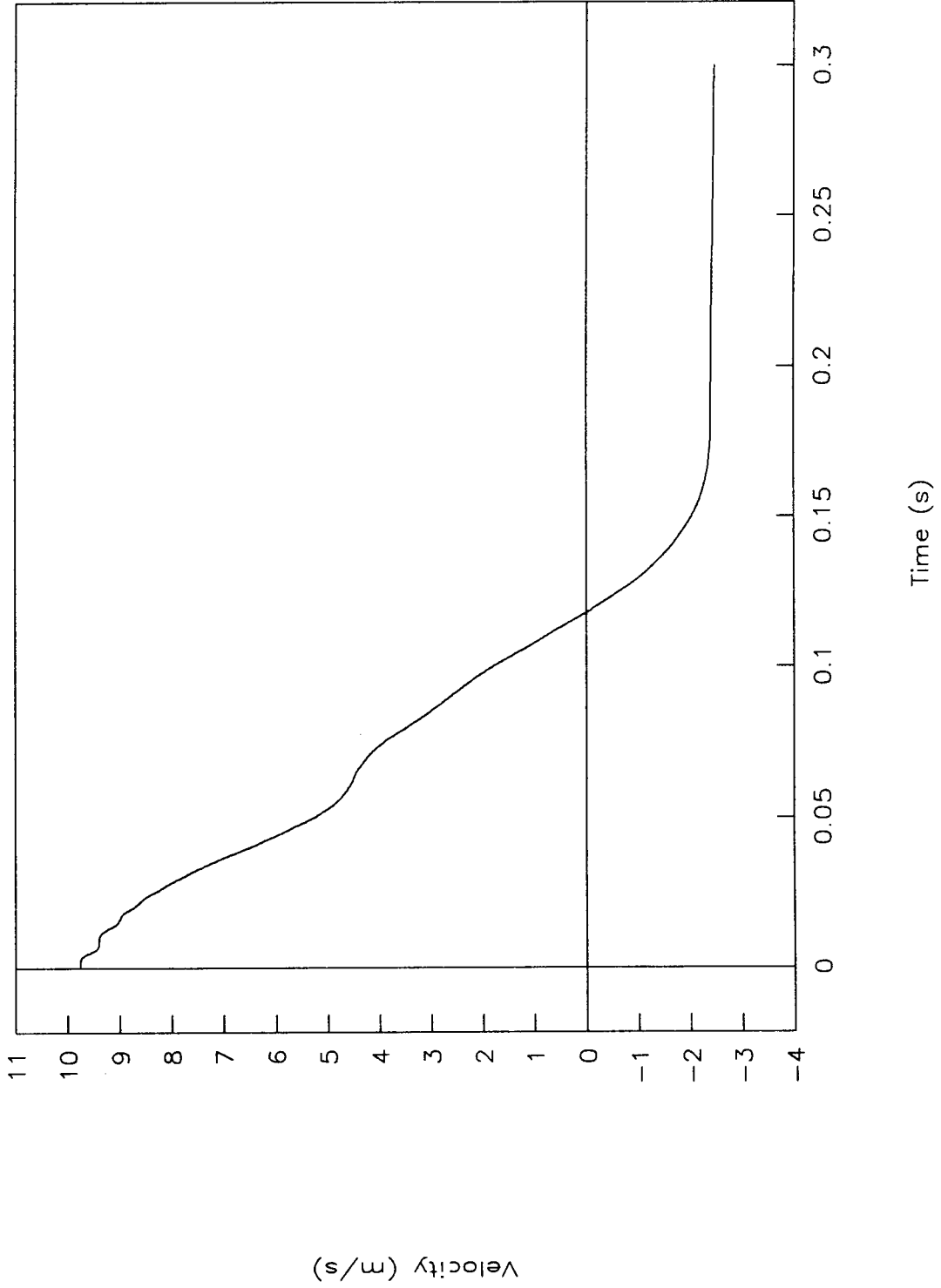


Figure 41. Velocity vs. time, test 96P004.

TEST NO. 96P004

Displacement vs. time

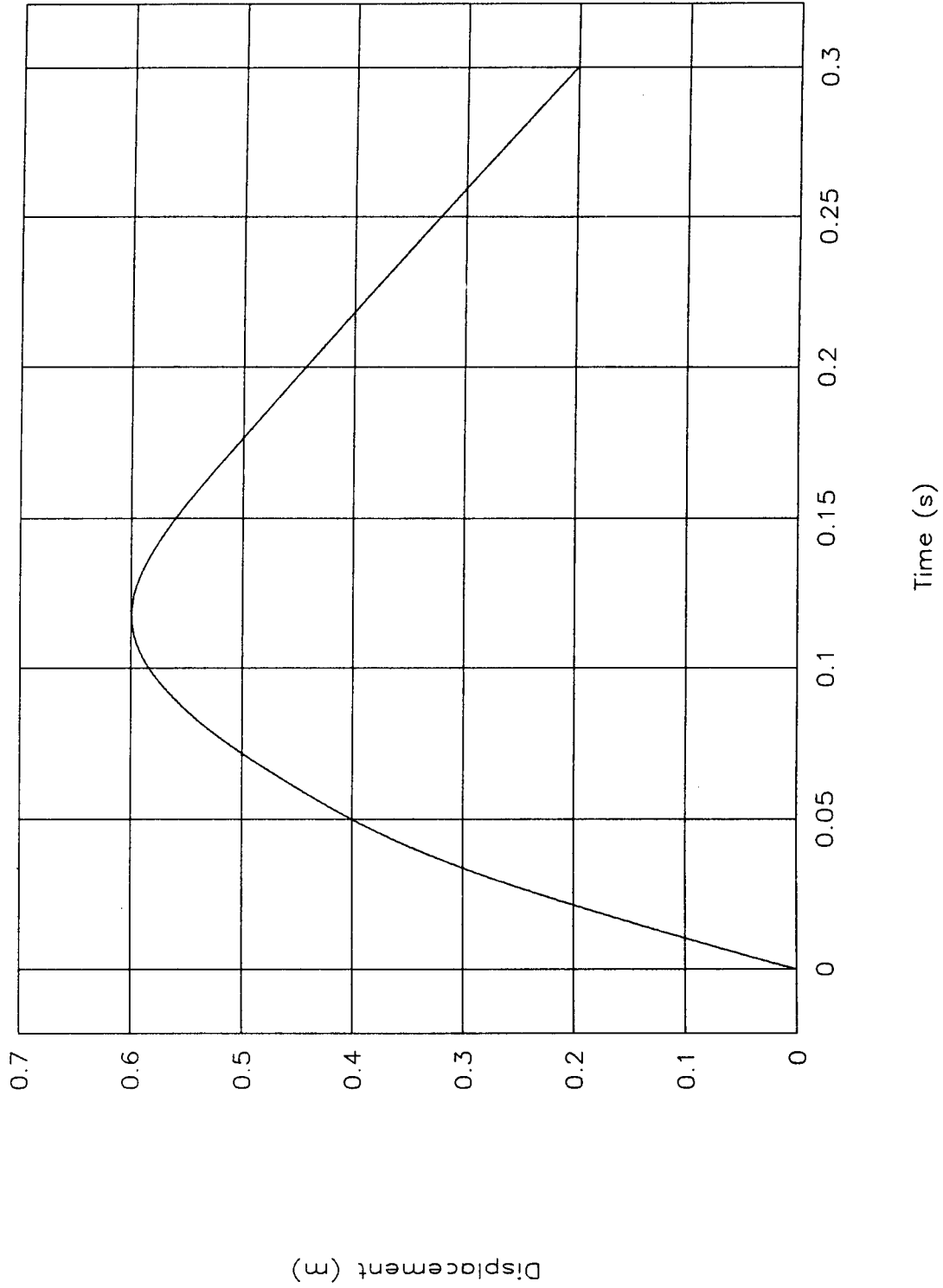


Figure 42. Displacement vs. time, test 96P004.

TEST NO. 96P004

Force vs. time

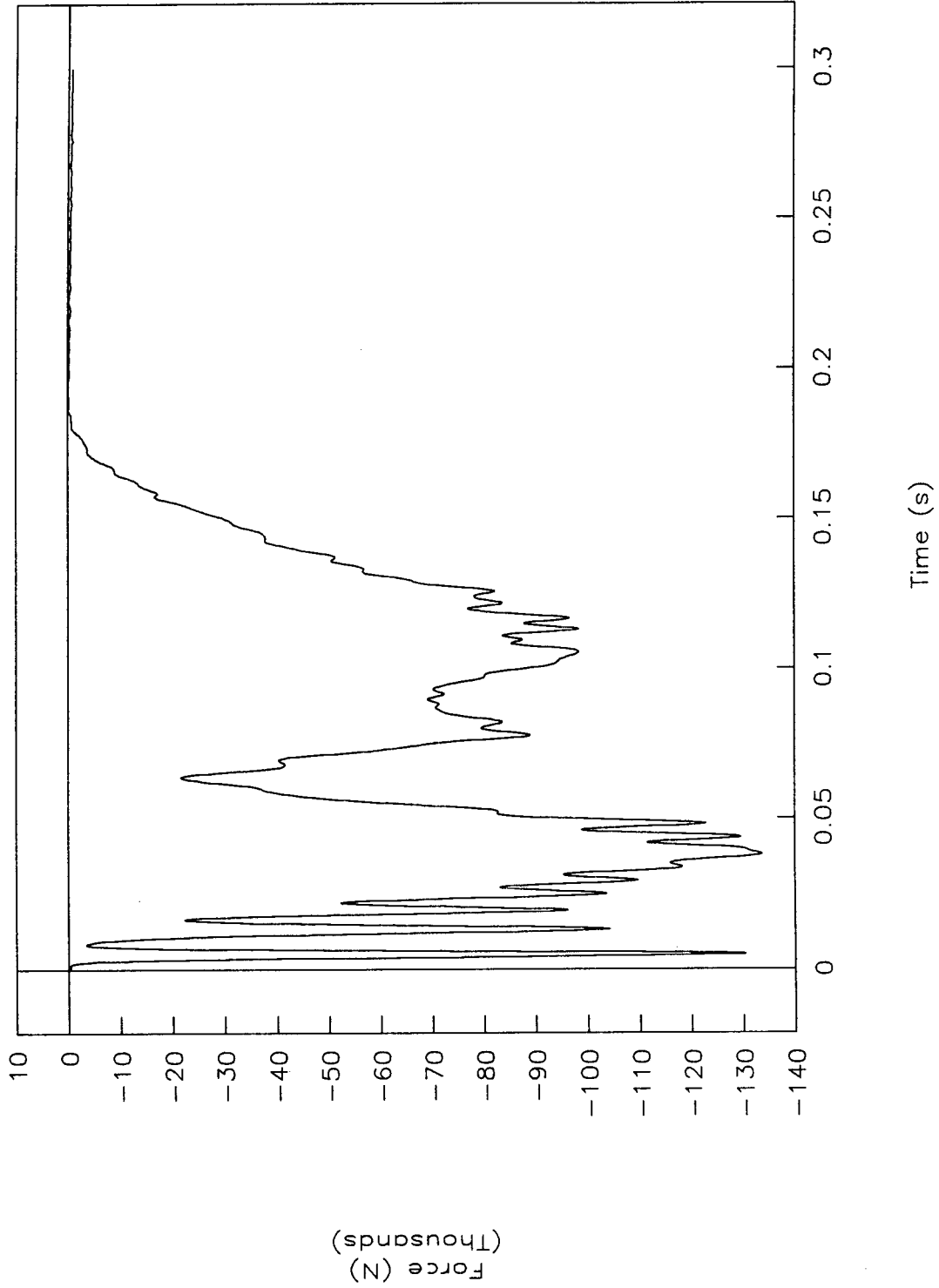


Figure 43. Force vs. time, test 96P004.

TEST NO. 96P004

Force vs. displacement

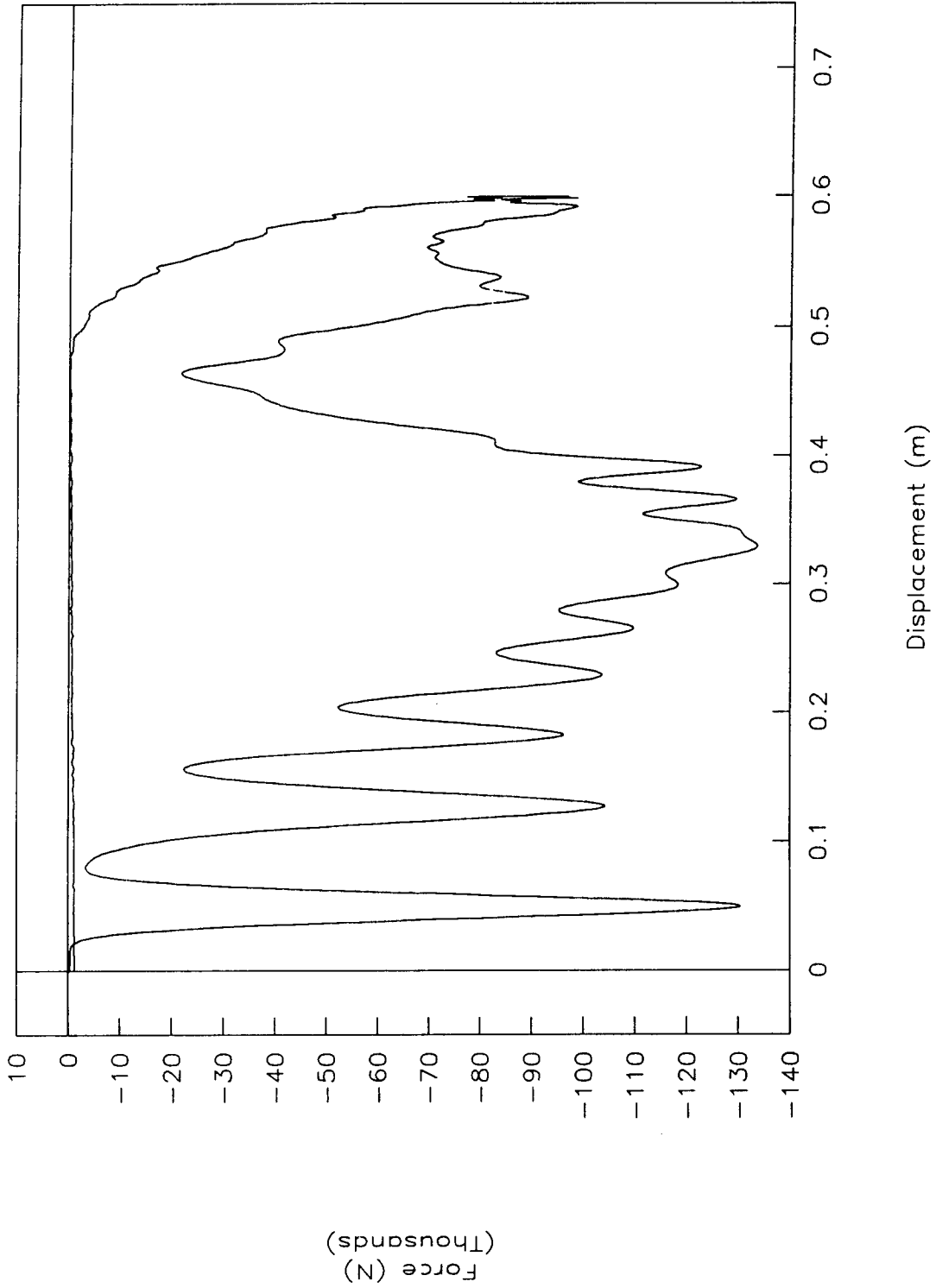


Figure 44. Force vs. displacement, test 96P004.

TEST NO. 96P004

Energy vs. displacement

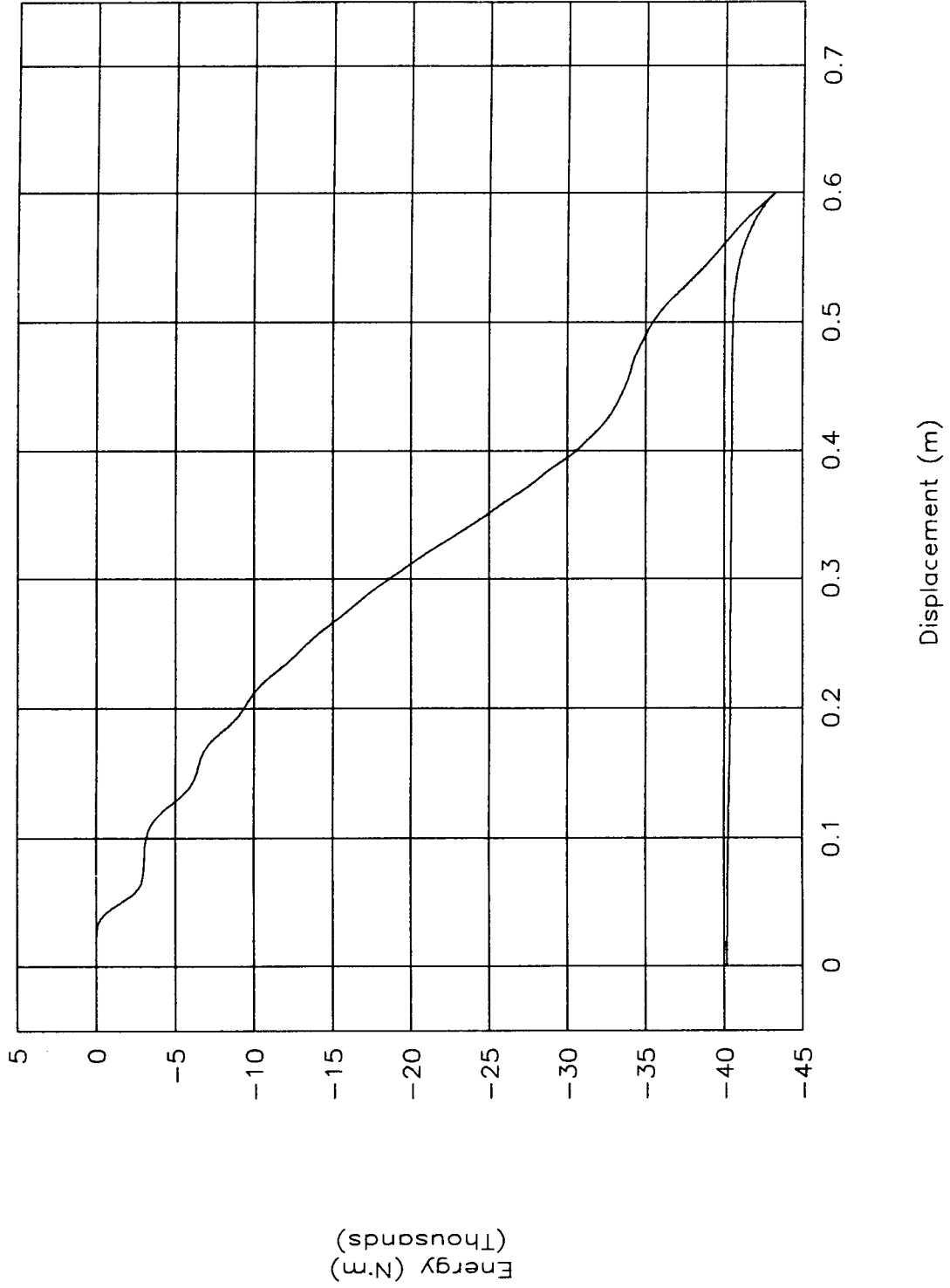


Figure 45. Energy vs. displacement, test 96P004.

TEST NO. 96P004

Strain vs. time (left front)

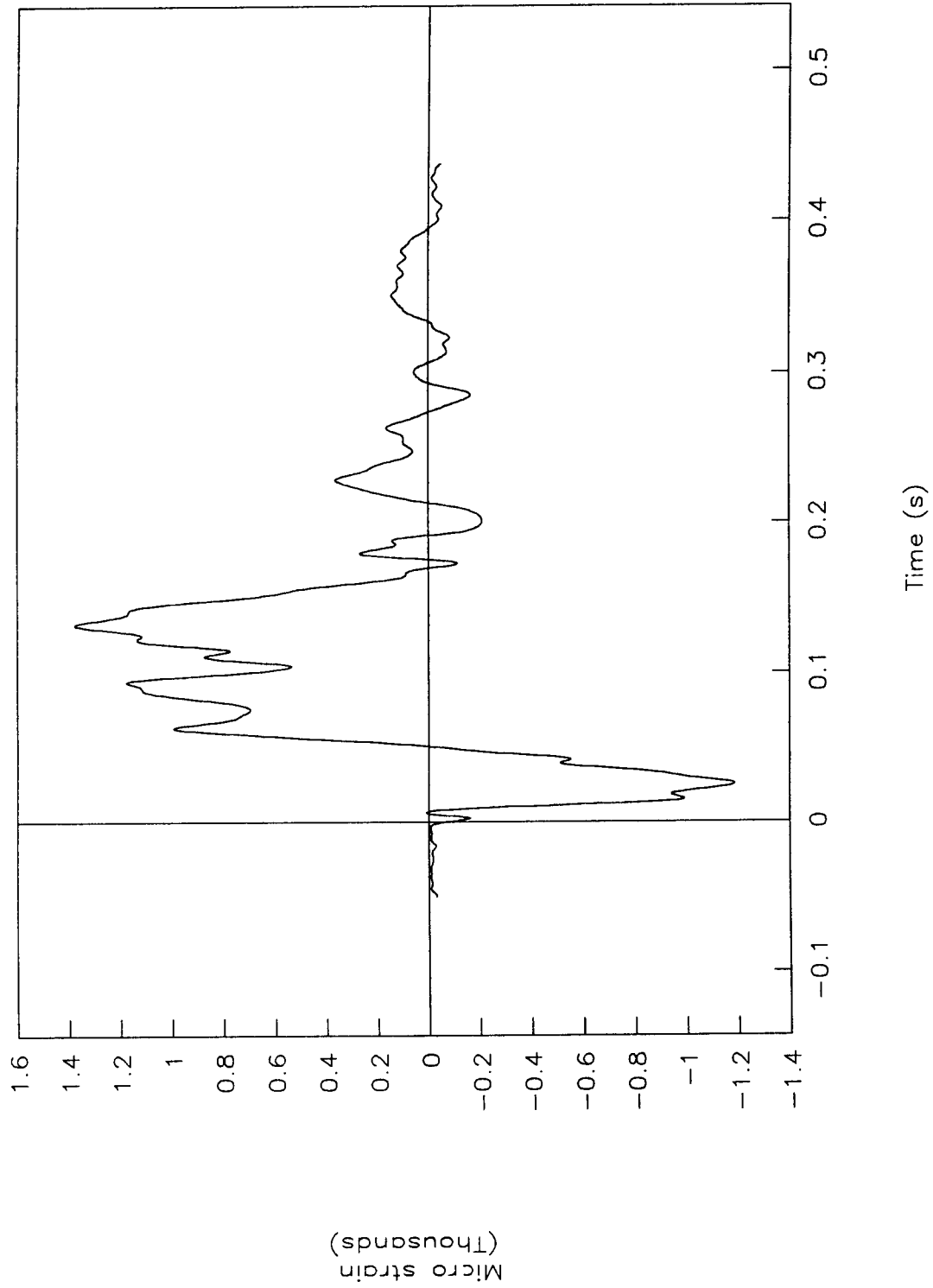


Figure 46. Strain vs. time (left front), test 96P004.

TEST NO. 96P004

Strain vs. time (right front)

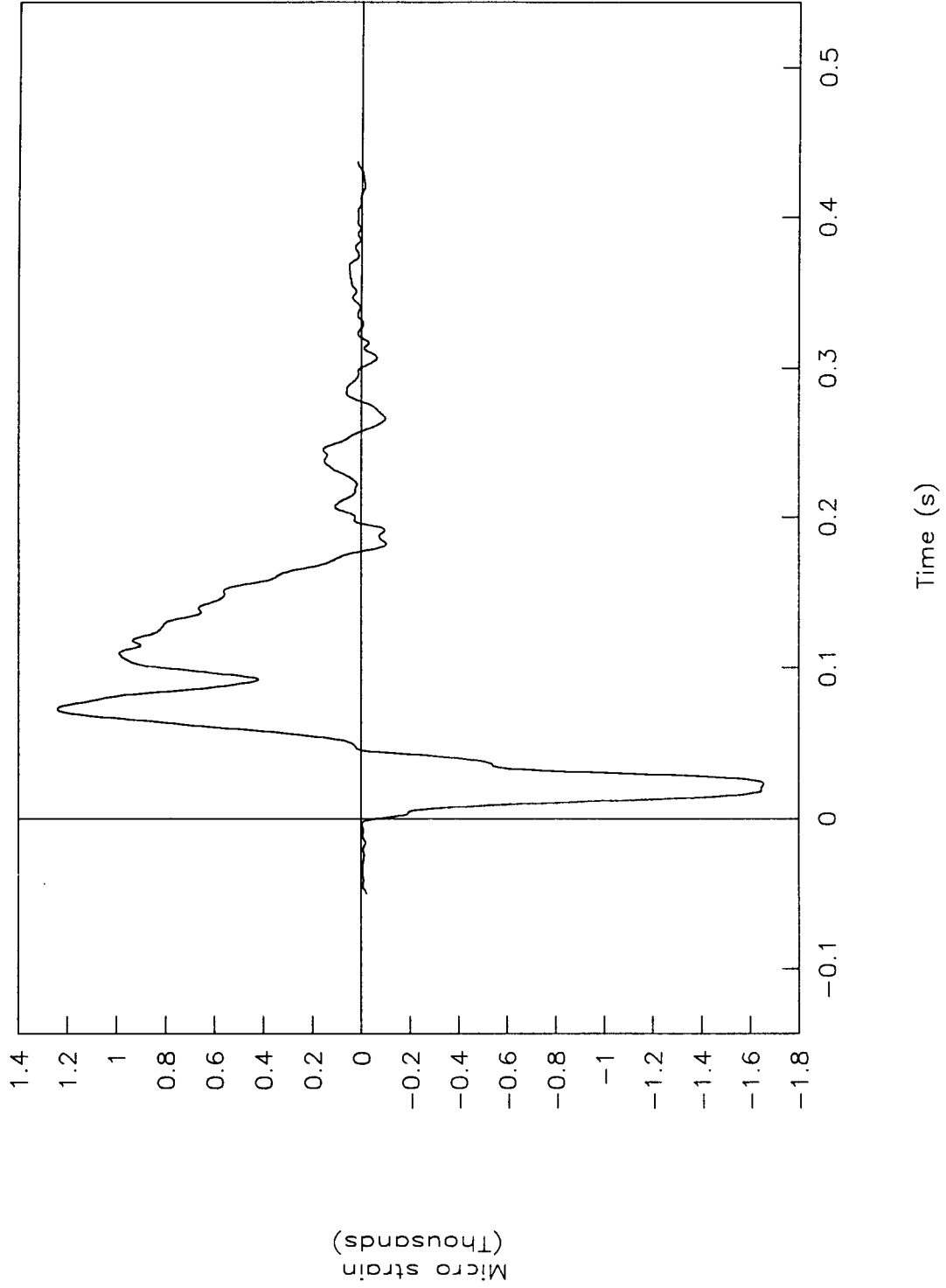


Figure 47. Strain vs. time (right front), test 96P004.

TEST NO. 96P004

Strain vs. time (left rear)

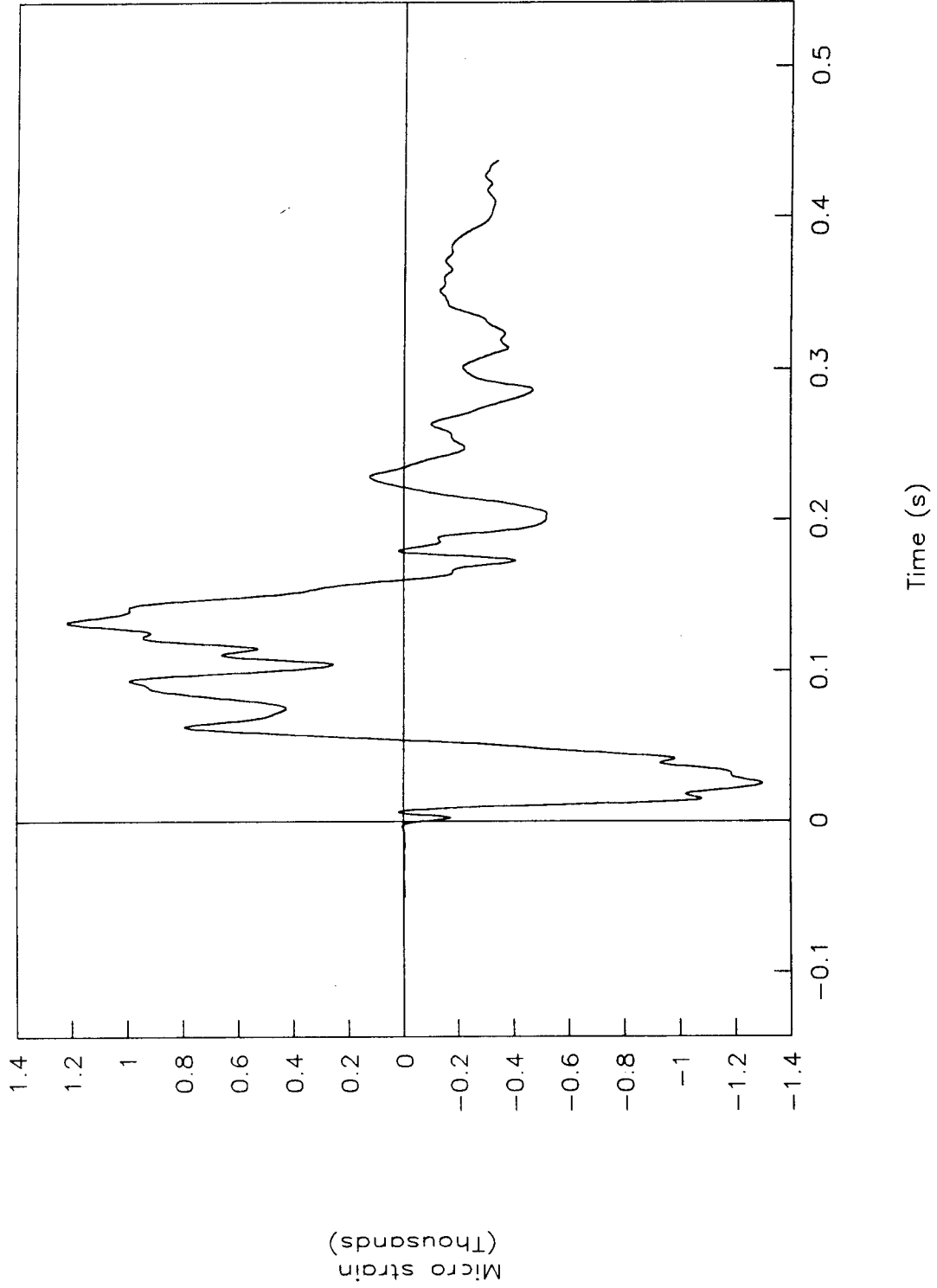


Figure 48. Strain vs. time (left rear), test 96P004.

TEST NO. 96P004

Strain vs. time (right rear)

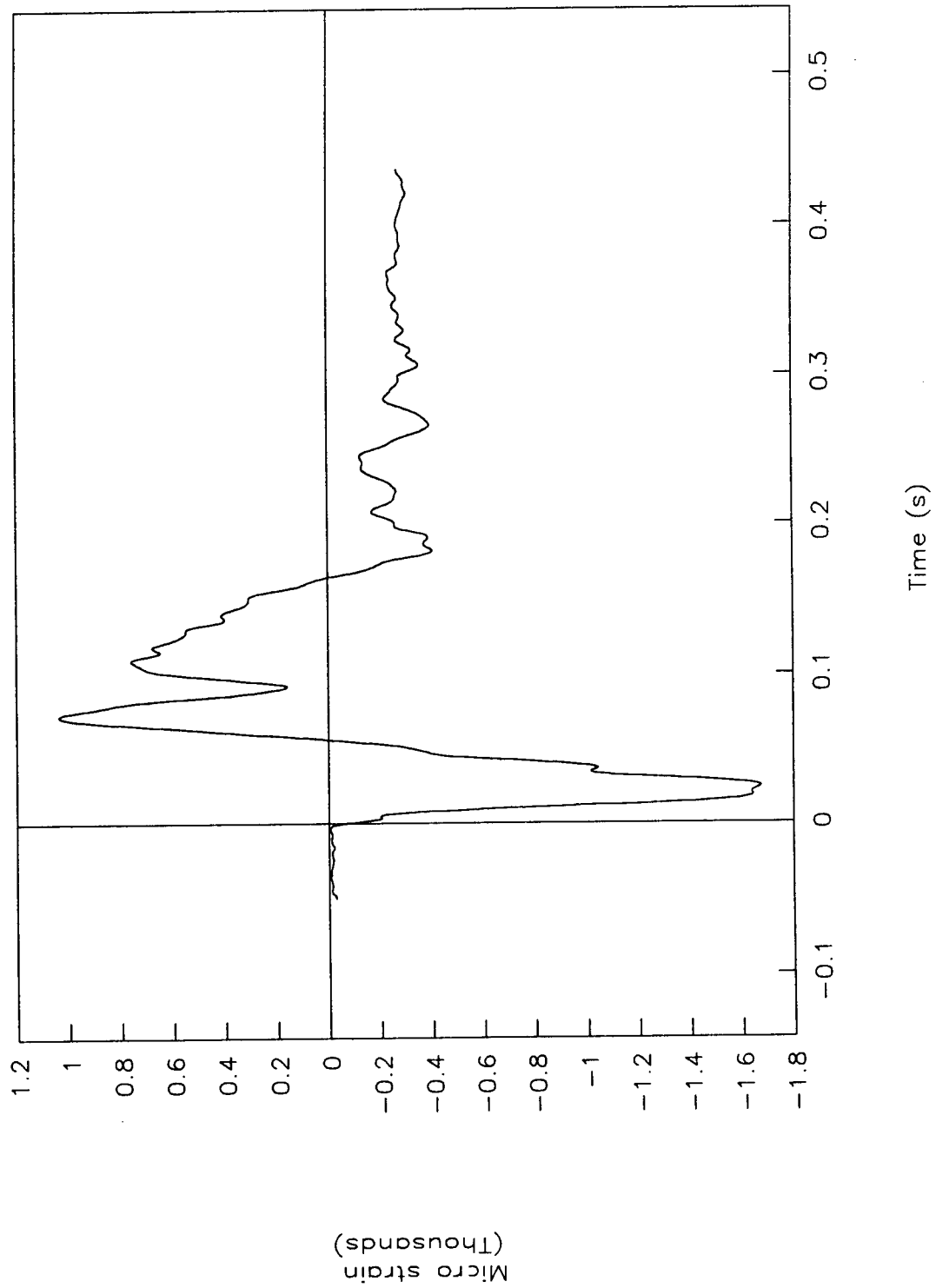


Figure 49. Strain vs. time (right rear), test 96P004.

TEST NO. 96P005

Acceleration vs. time

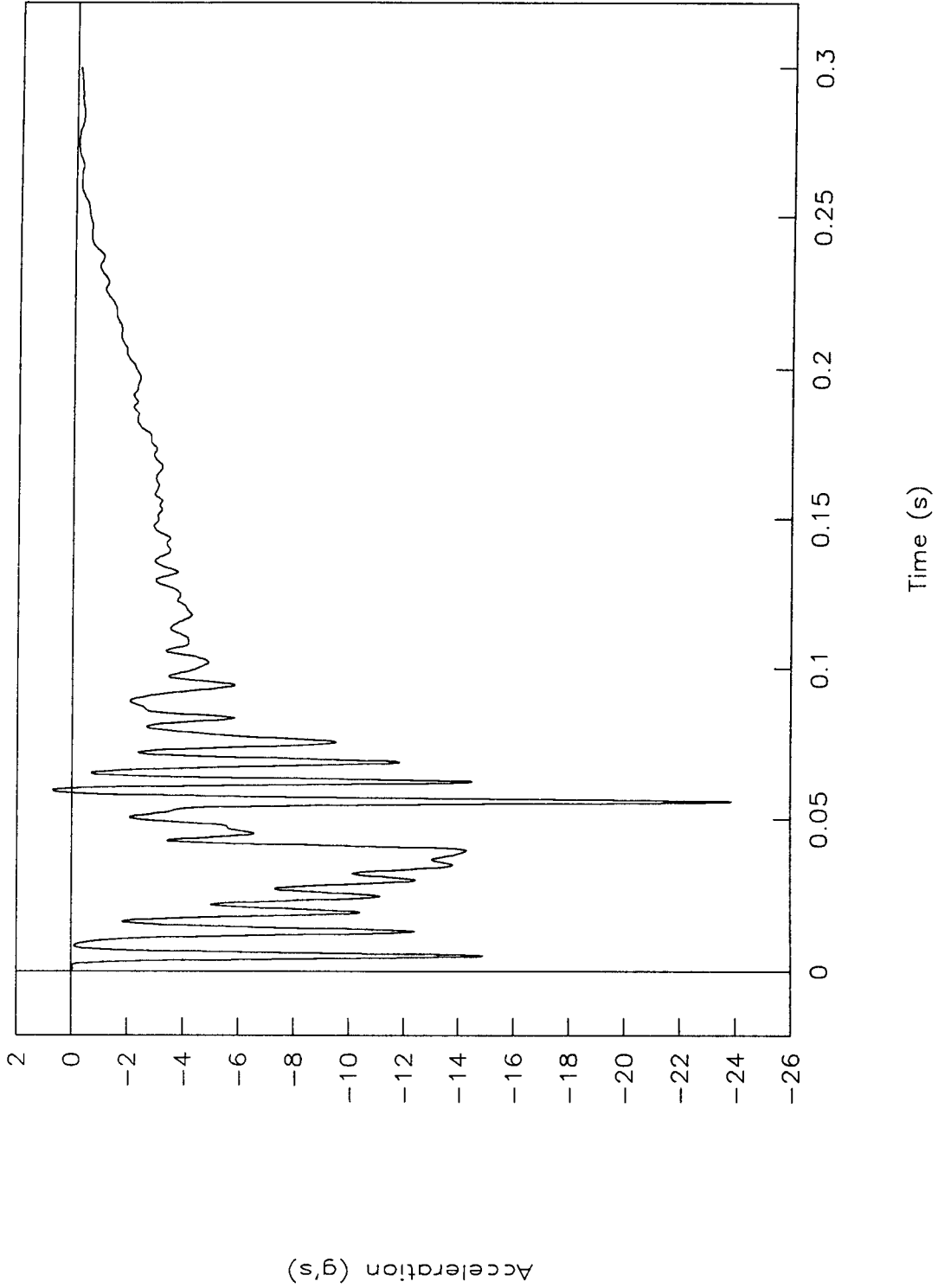


Figure 50. Acceleration vs. time, test 96P005.

TEST NO. 96P005

Velocity vs. time

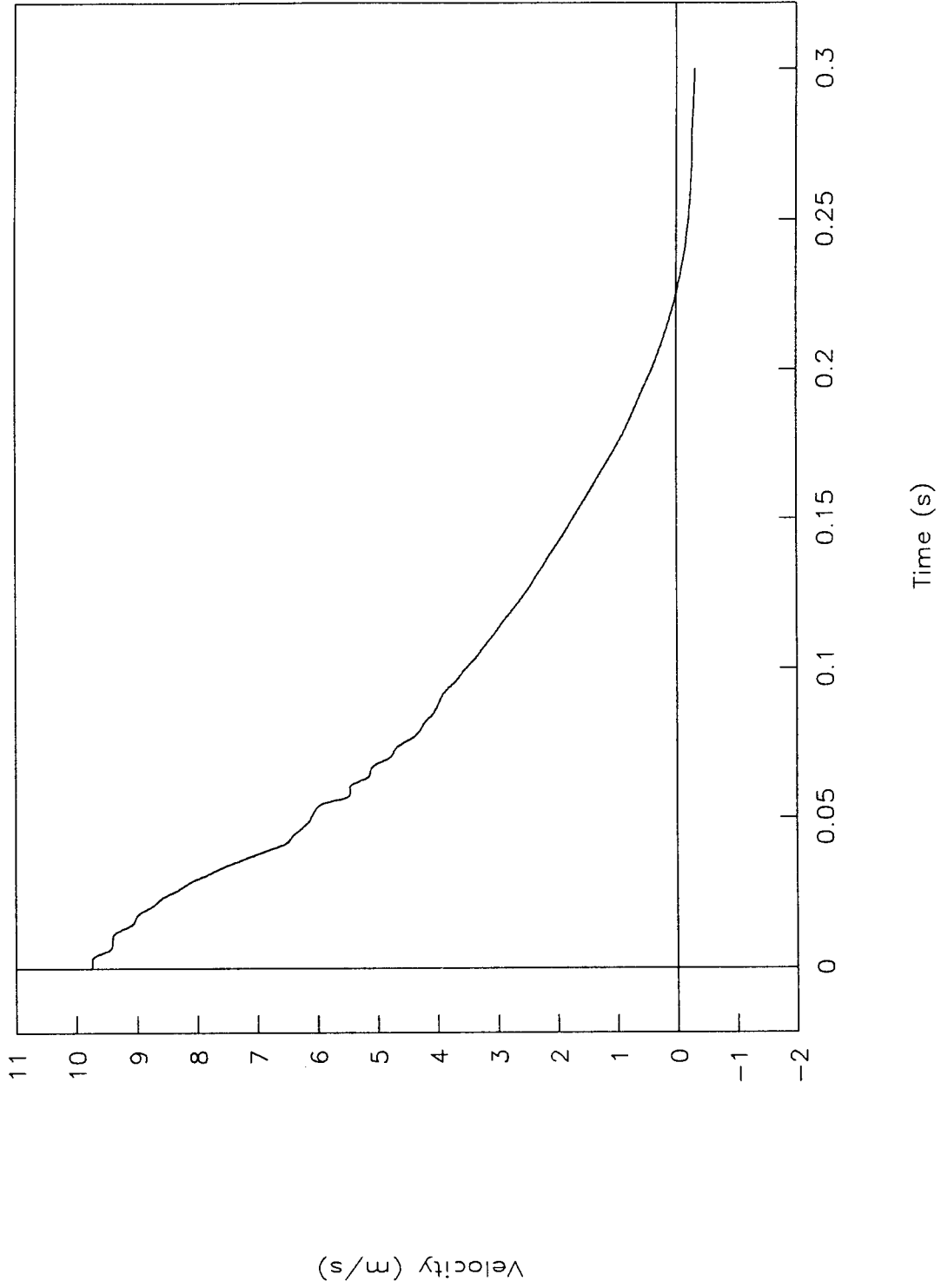


Figure 51. Velocity vs. time, test 96P005.

TEST NO. 96P005

Displacement vs. time

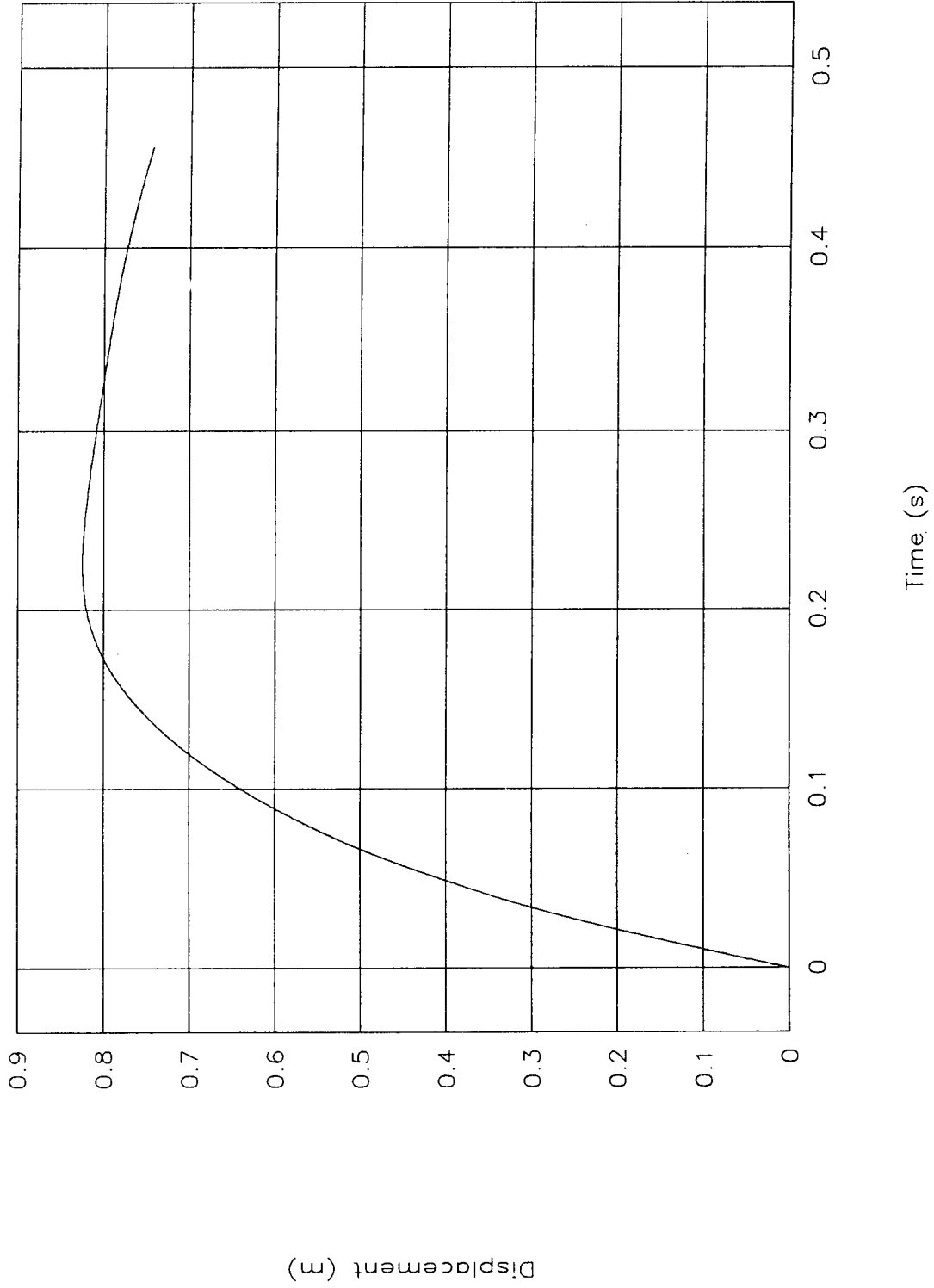


Figure 52. Displacement vs. time, test 96P005.

TEST NO. 96P005

Force vs. time

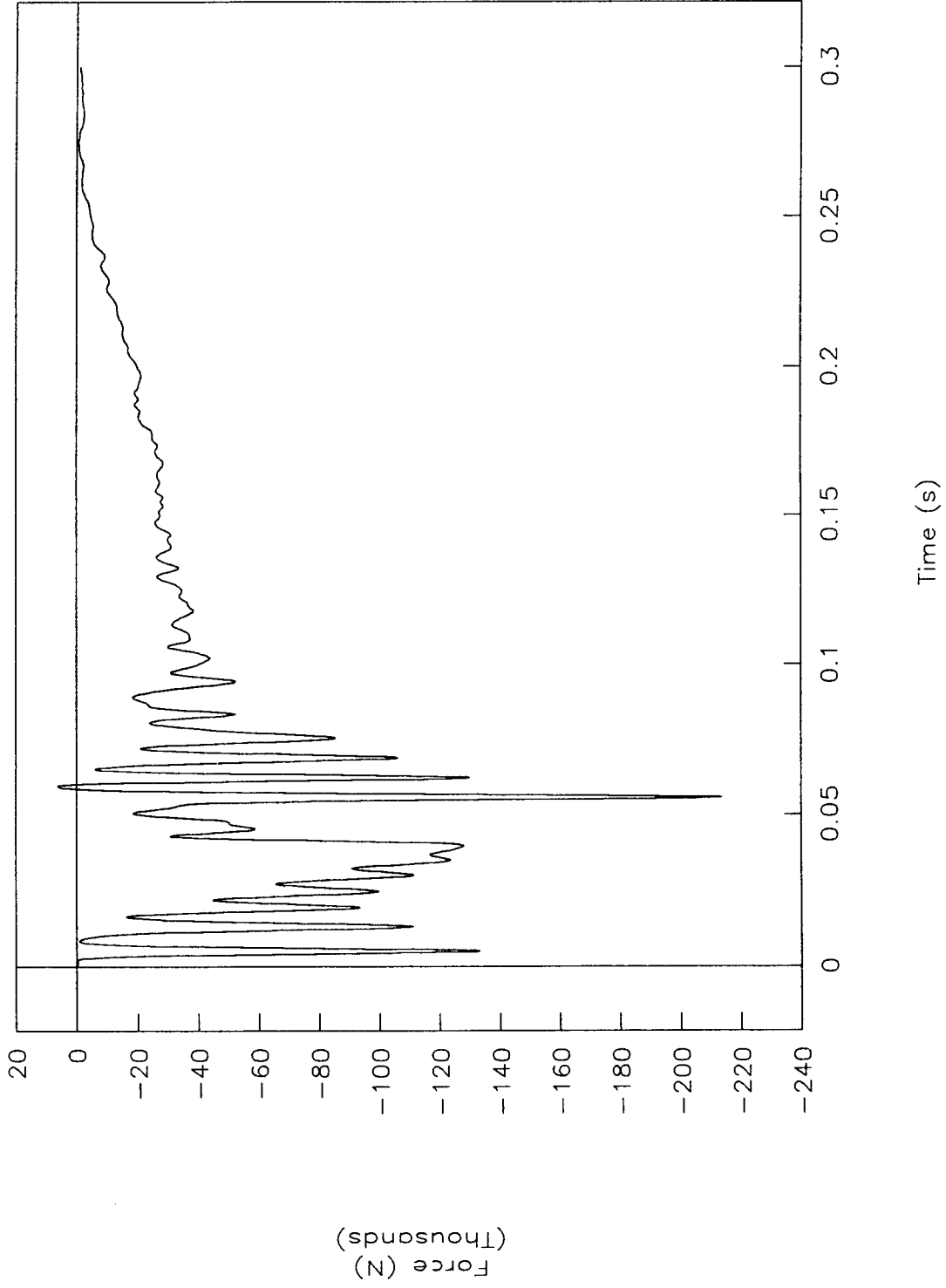


Figure 53. Force vs. time, test 96P005.

TEST NO. 96P005

Force vs. displacement

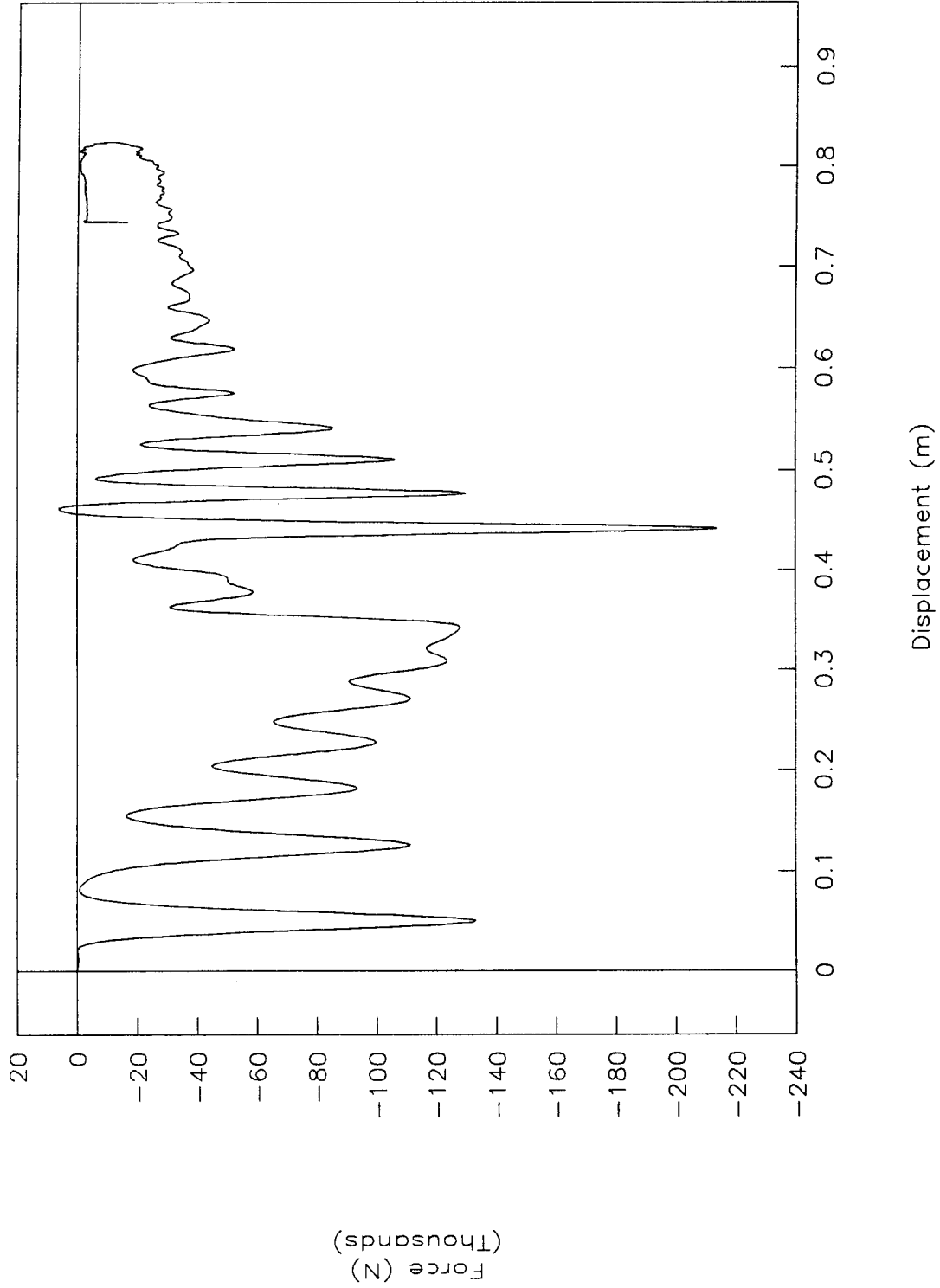


Figure 54. Force vs. displacement, test 96P005.

TEST NO. 96P005

Energy vs. displacement

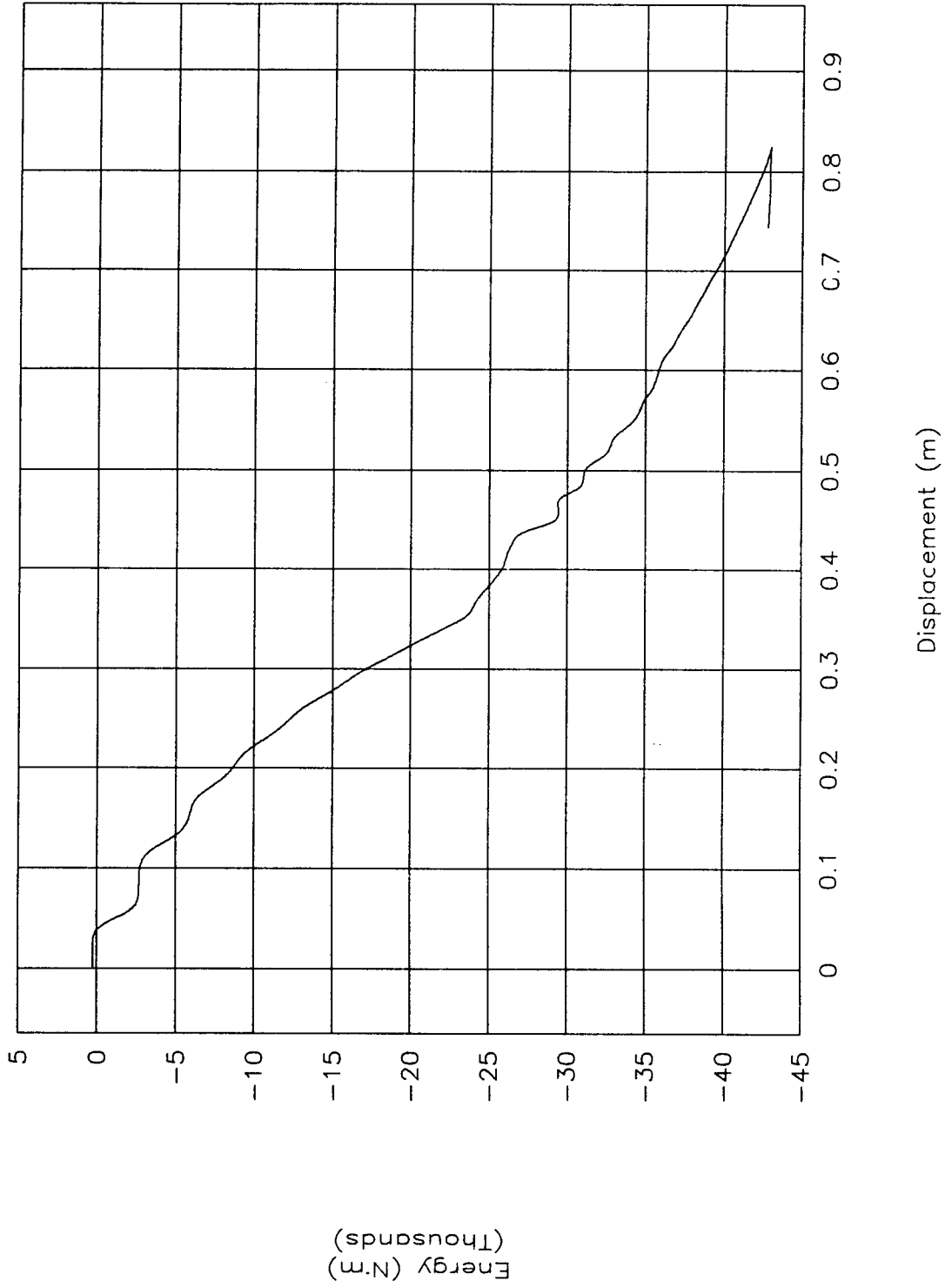


Figure 55. Energy vs. displacement, test 96P005.

TEST NO. 96P005

Strain vs. time (left front)

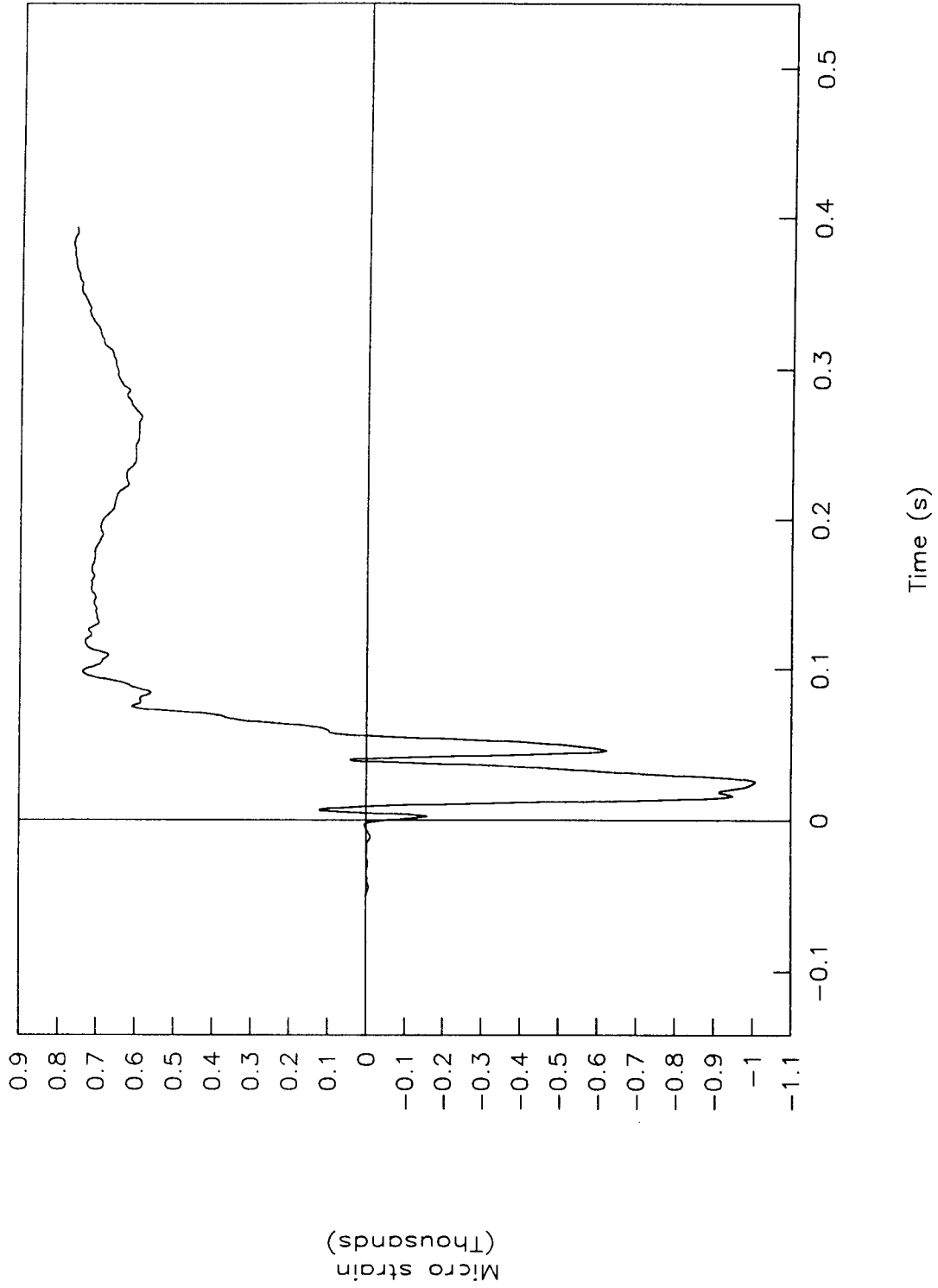


Figure 56. Strain vs. time (left front), test 96P005.

TEST NO. 96P005
Strain vs. time (right front)

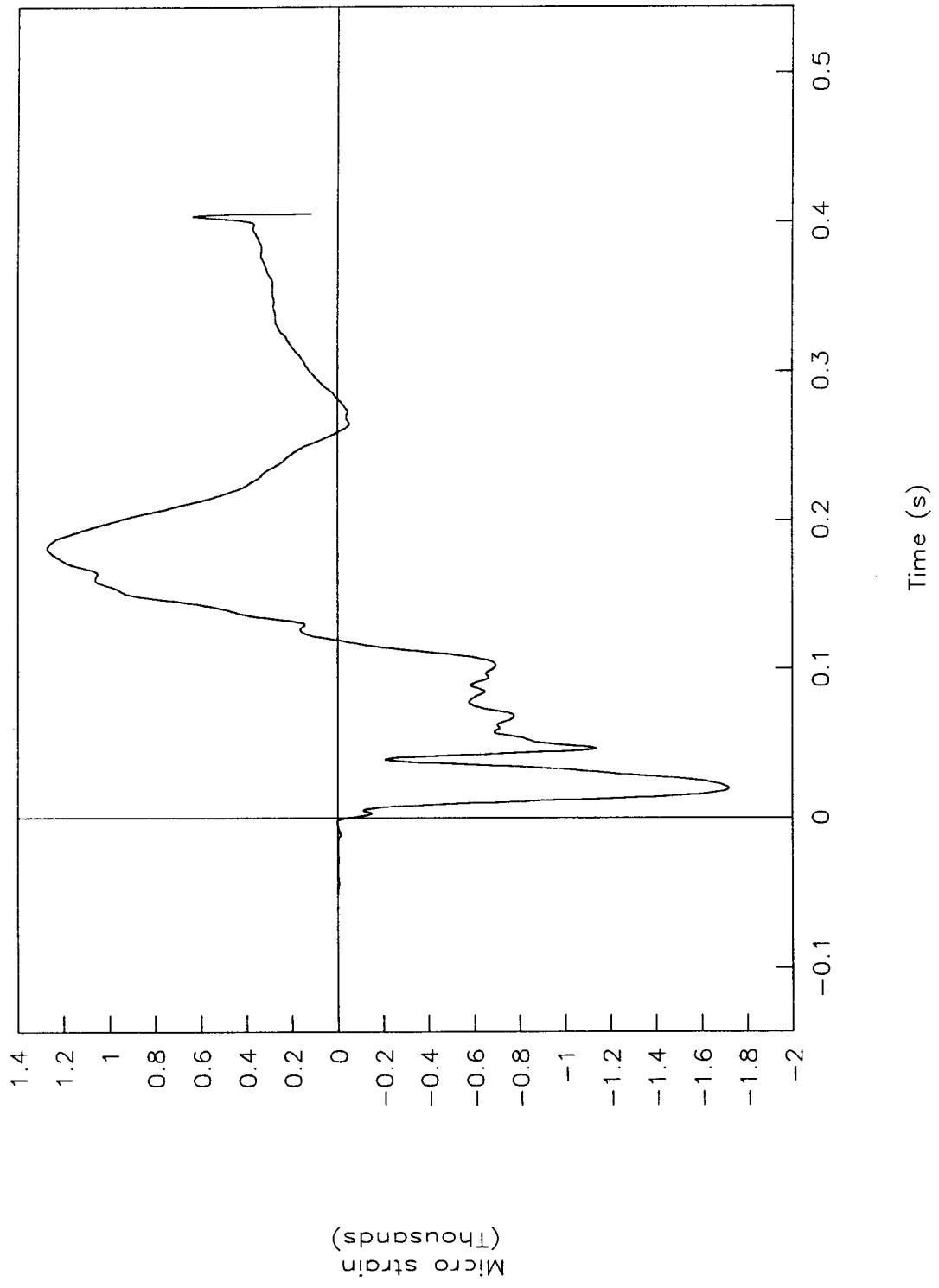


Figure 57. Strain vs. time (right front), test 96P005.

TEST NO. 96P005

Strain vs. time (left rear)

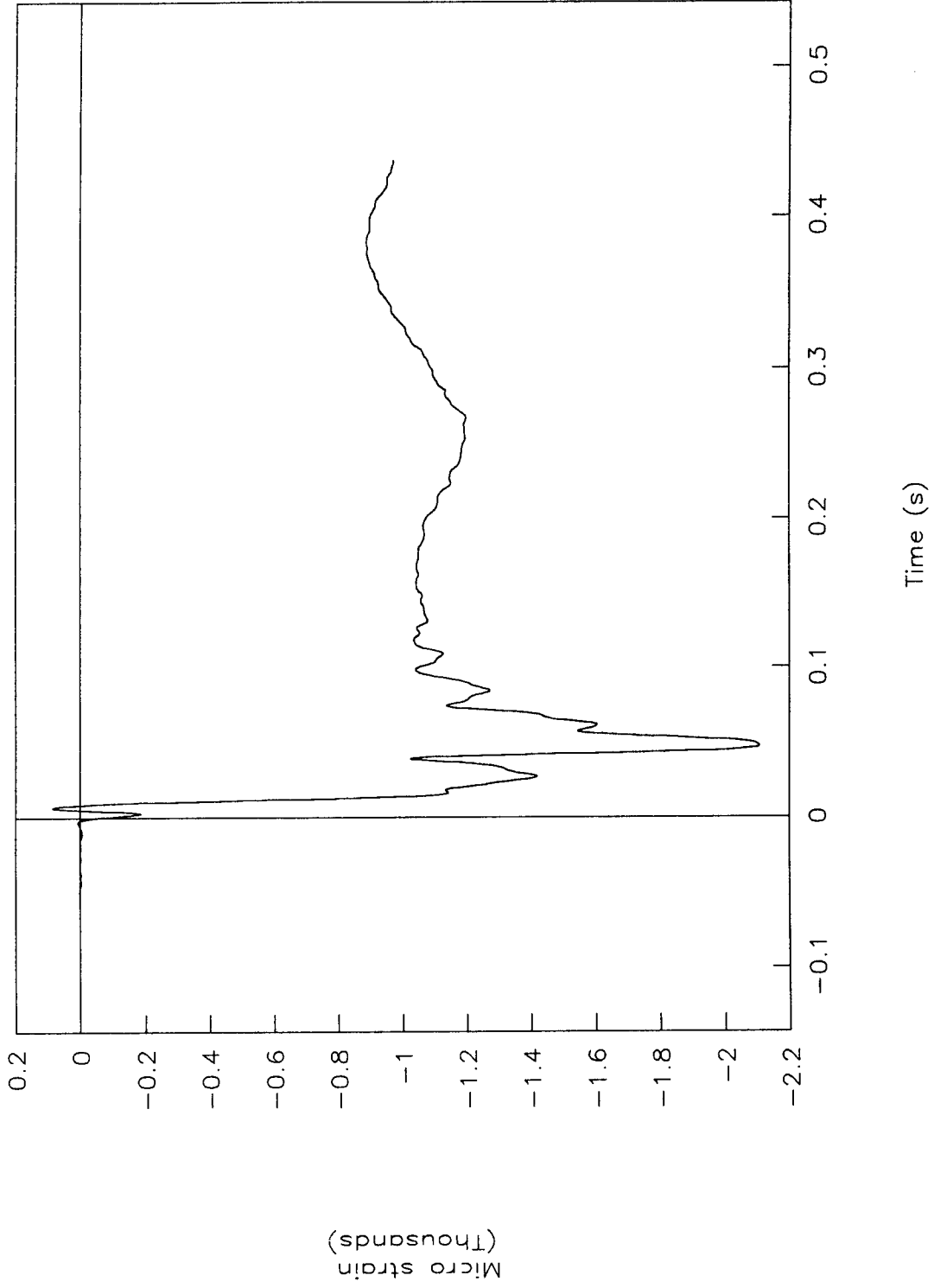


Figure 58. Strain vs. time (left rear), test 96P005.

TEST NO. 96P005

Strain vs. time (right rear)

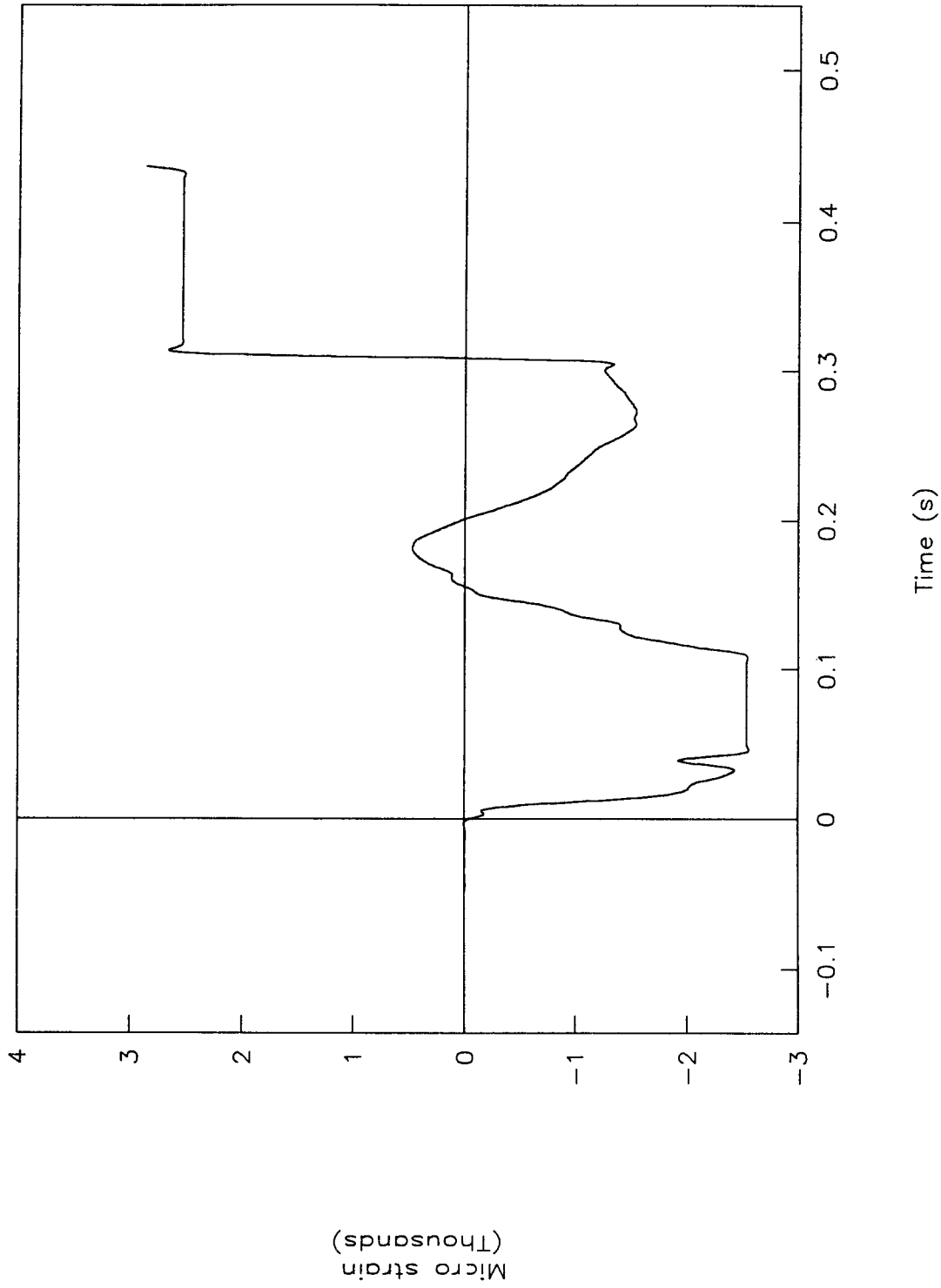


Figure 59. Strain vs. time (right rear), test 96P005.

TEST NO. 96P006

Acceleration vs. time

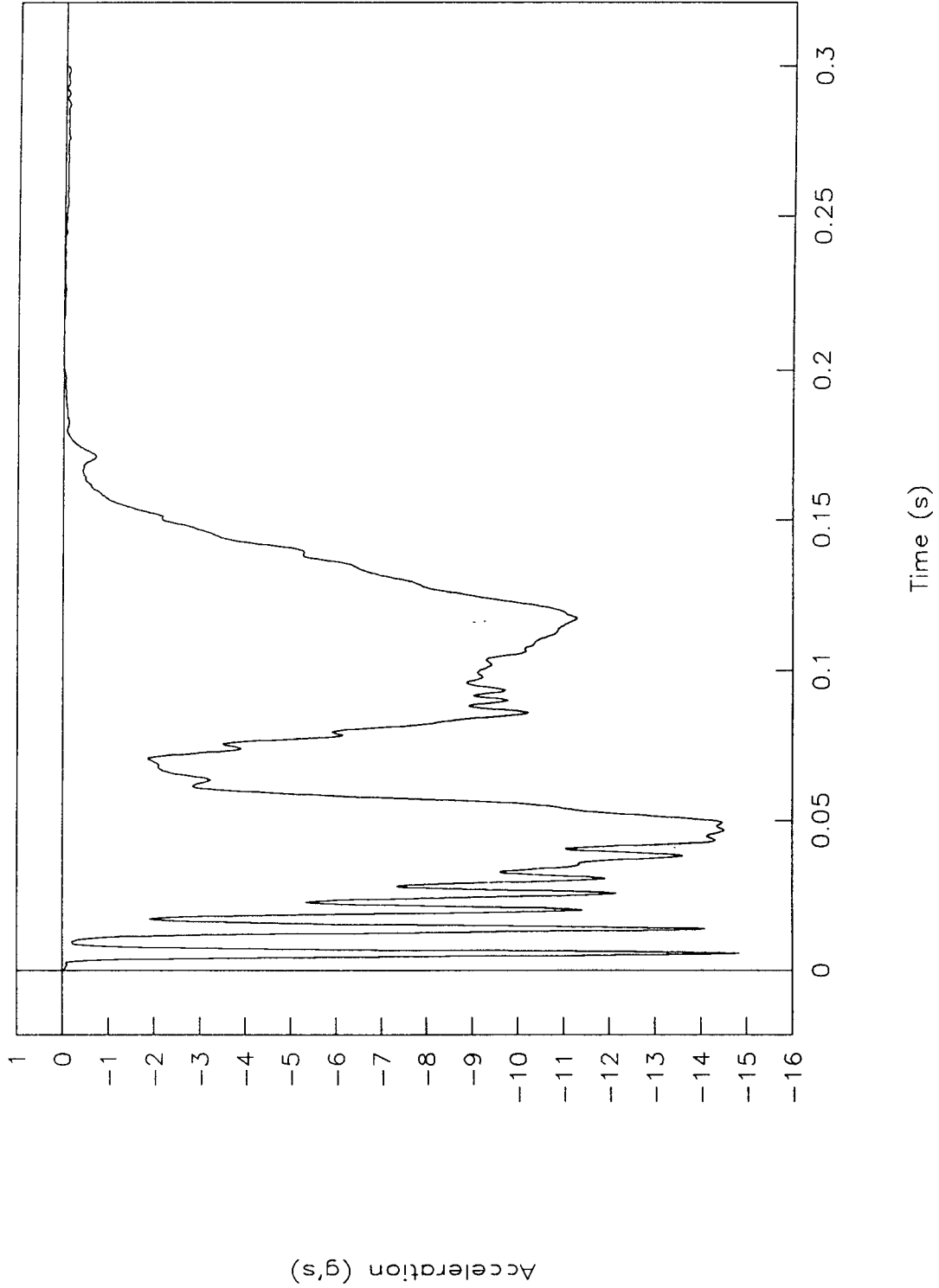


Figure 60. Acceleration vs. time, test 96P006.

TEST NO. 96P006

Velocity vs. time

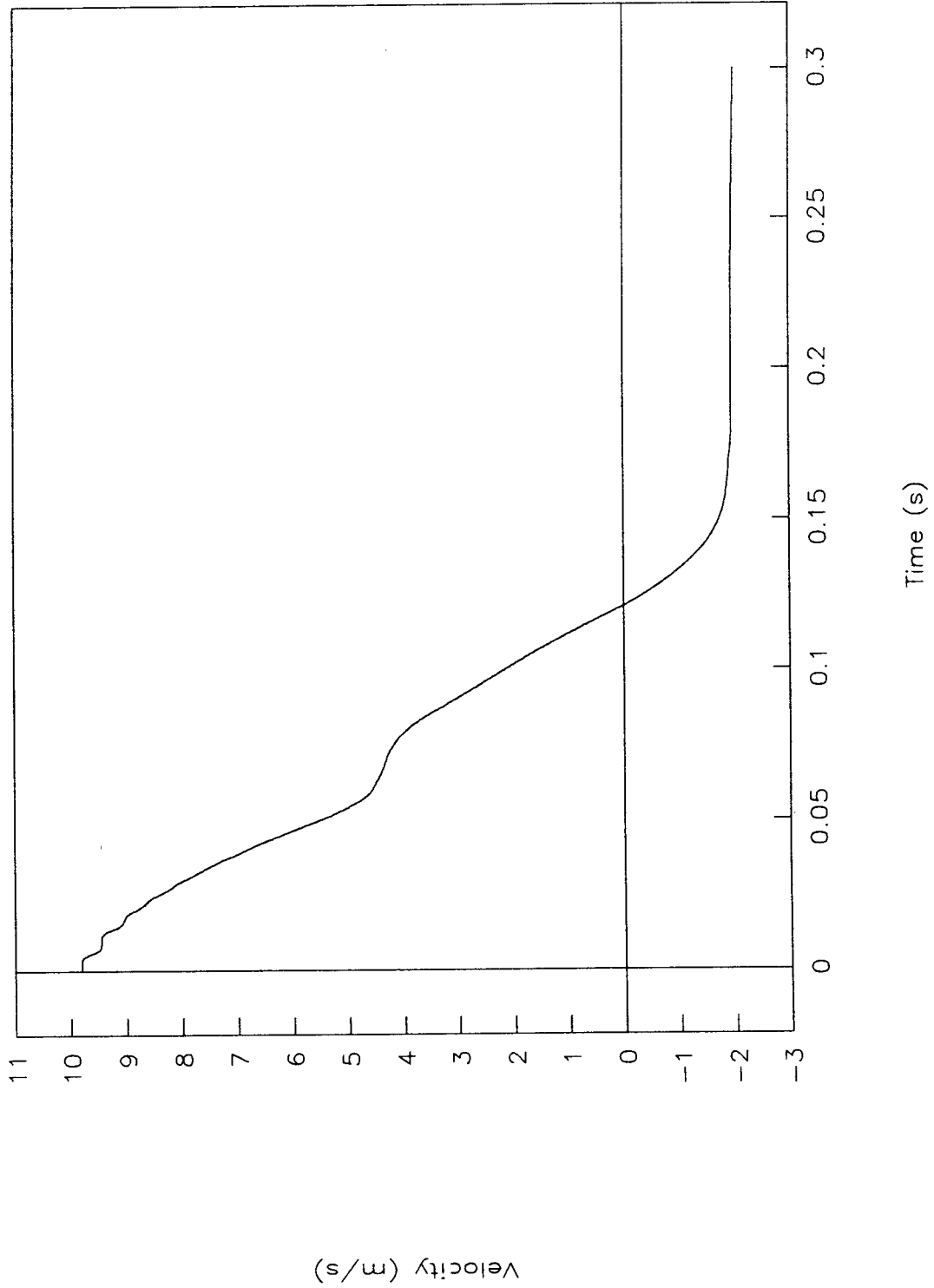


Figure 61. Velocity vs. time, test 96P006.

TEST NO. 96P006

Displacement vs. time

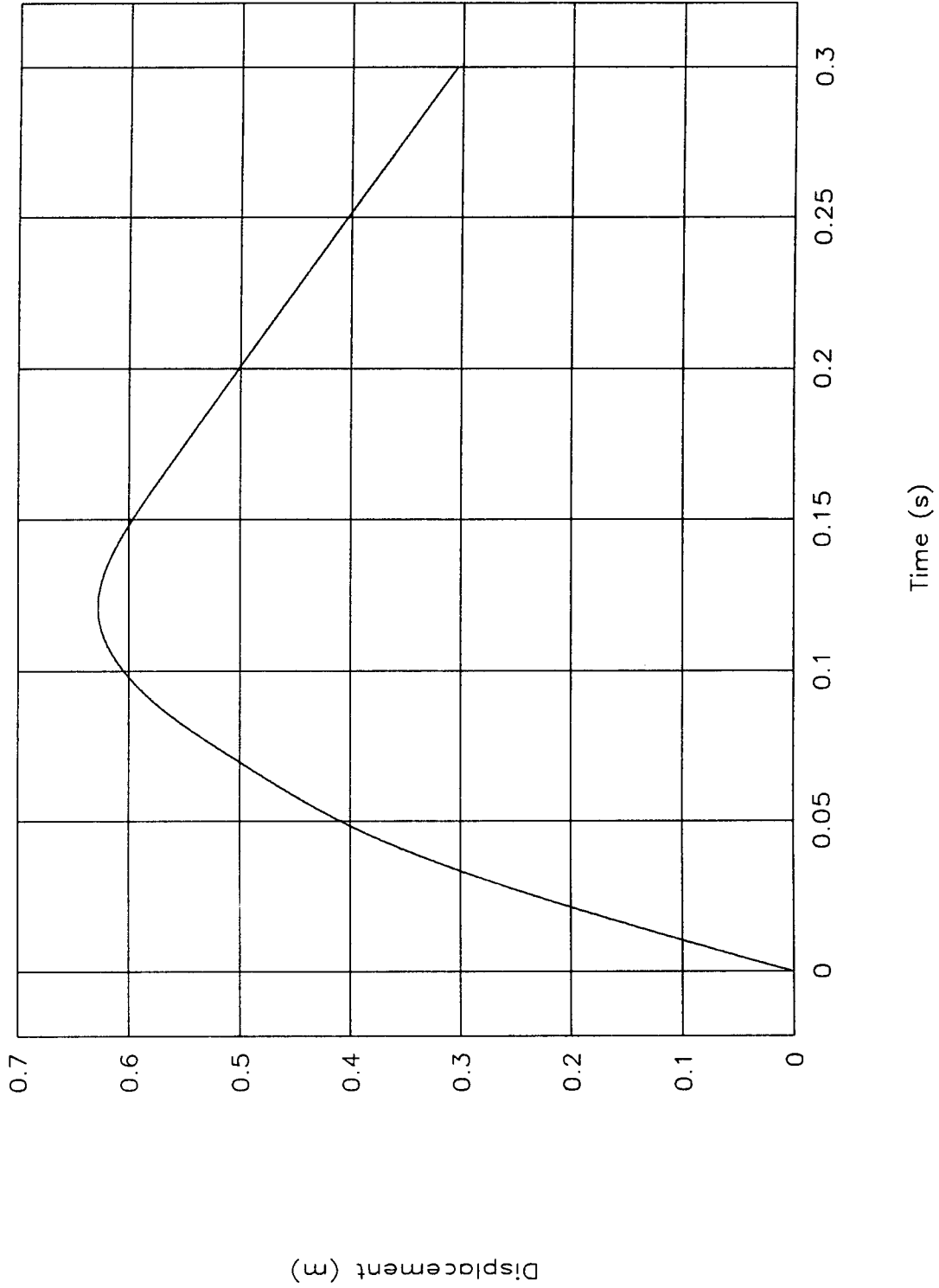


Figure 62. Displacement vs. time, test 96P006.

TEST NO. 96P006

Force vs. time

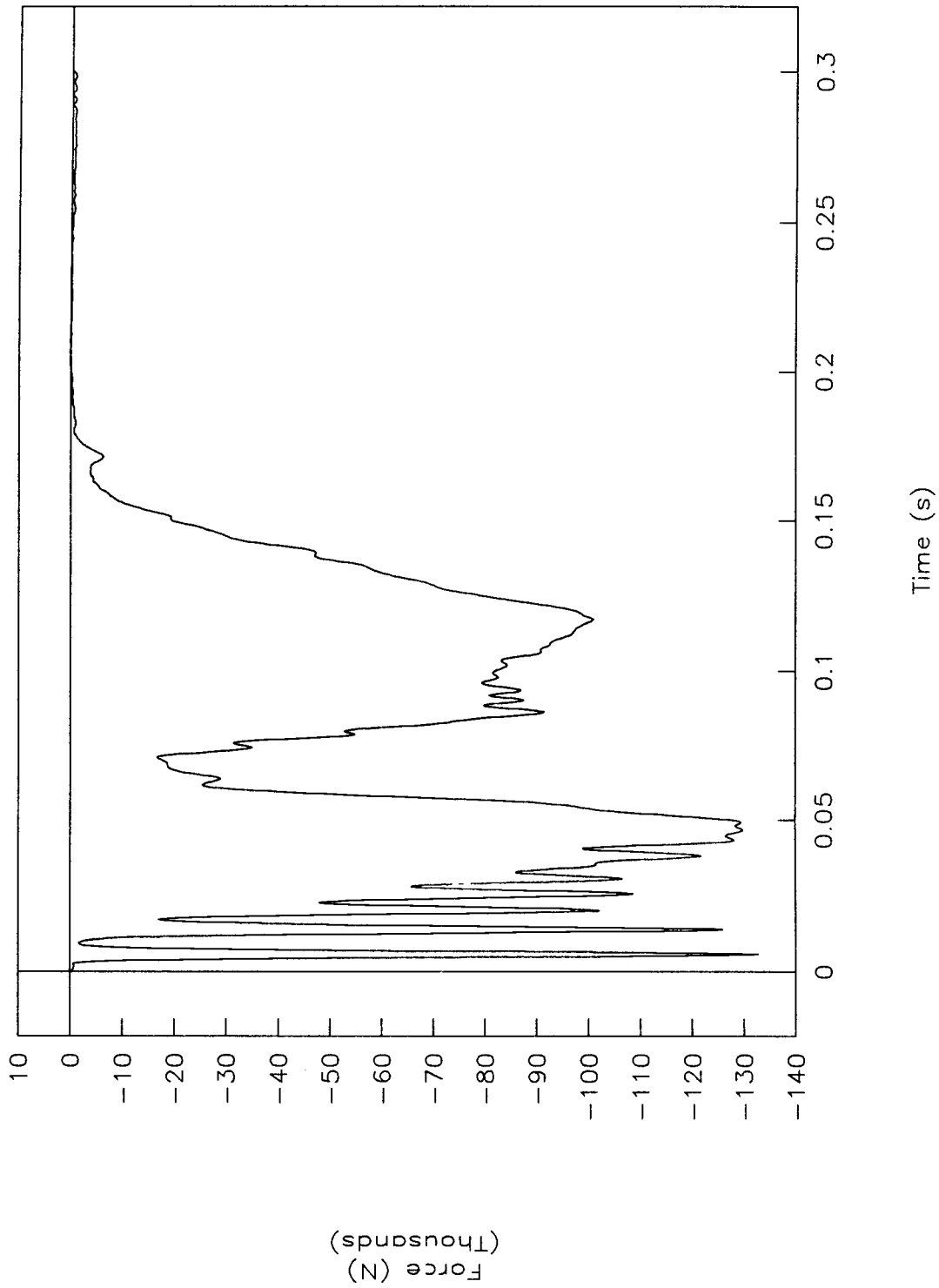


Figure 63. Force vs. time, test 96P006.

TEST NO. 96P006

Force vs. displacement

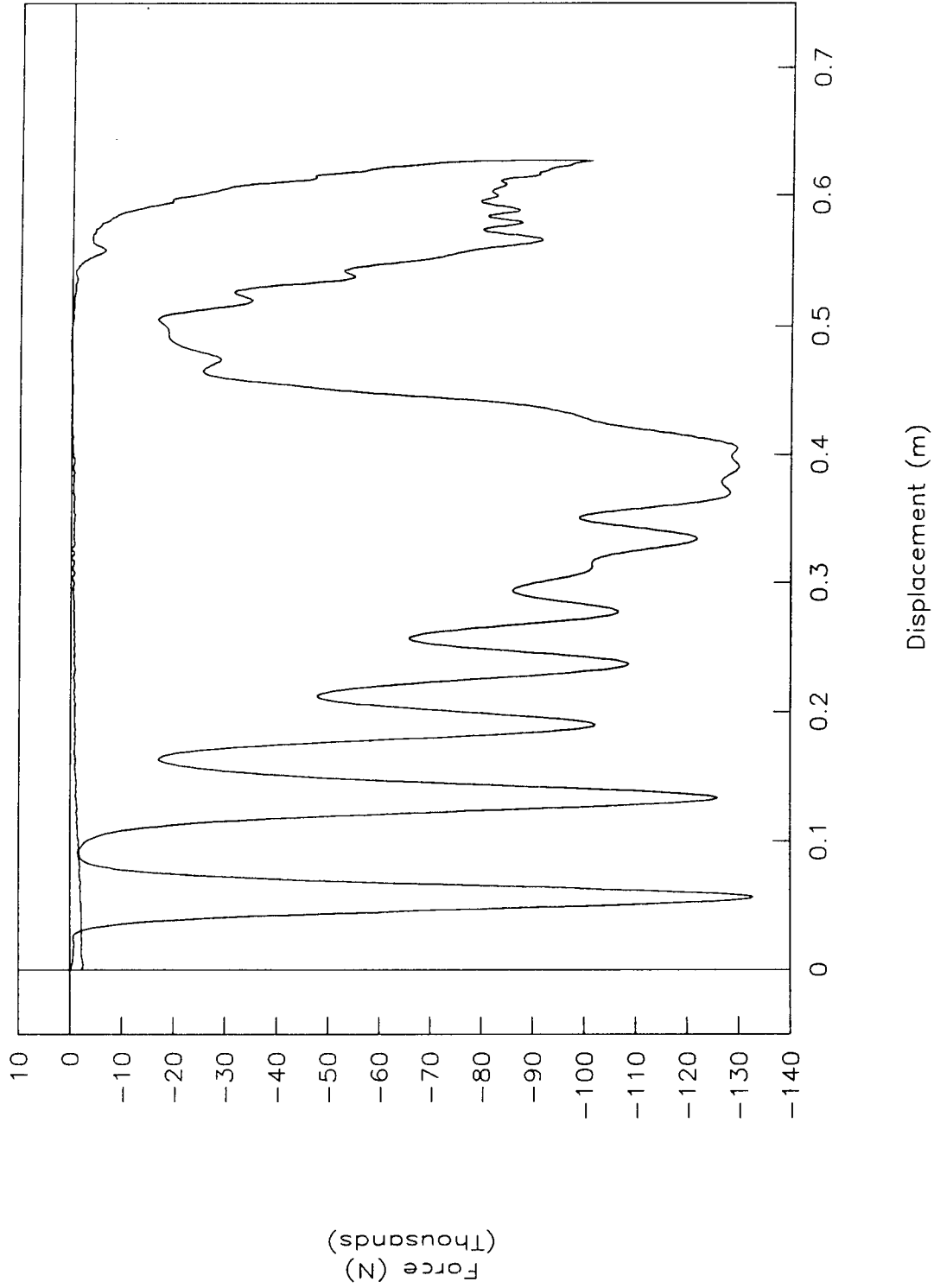


Figure 64. Force vs. displacement, test 96P006.

TEST NO. 96P006

Energy vs. displacement

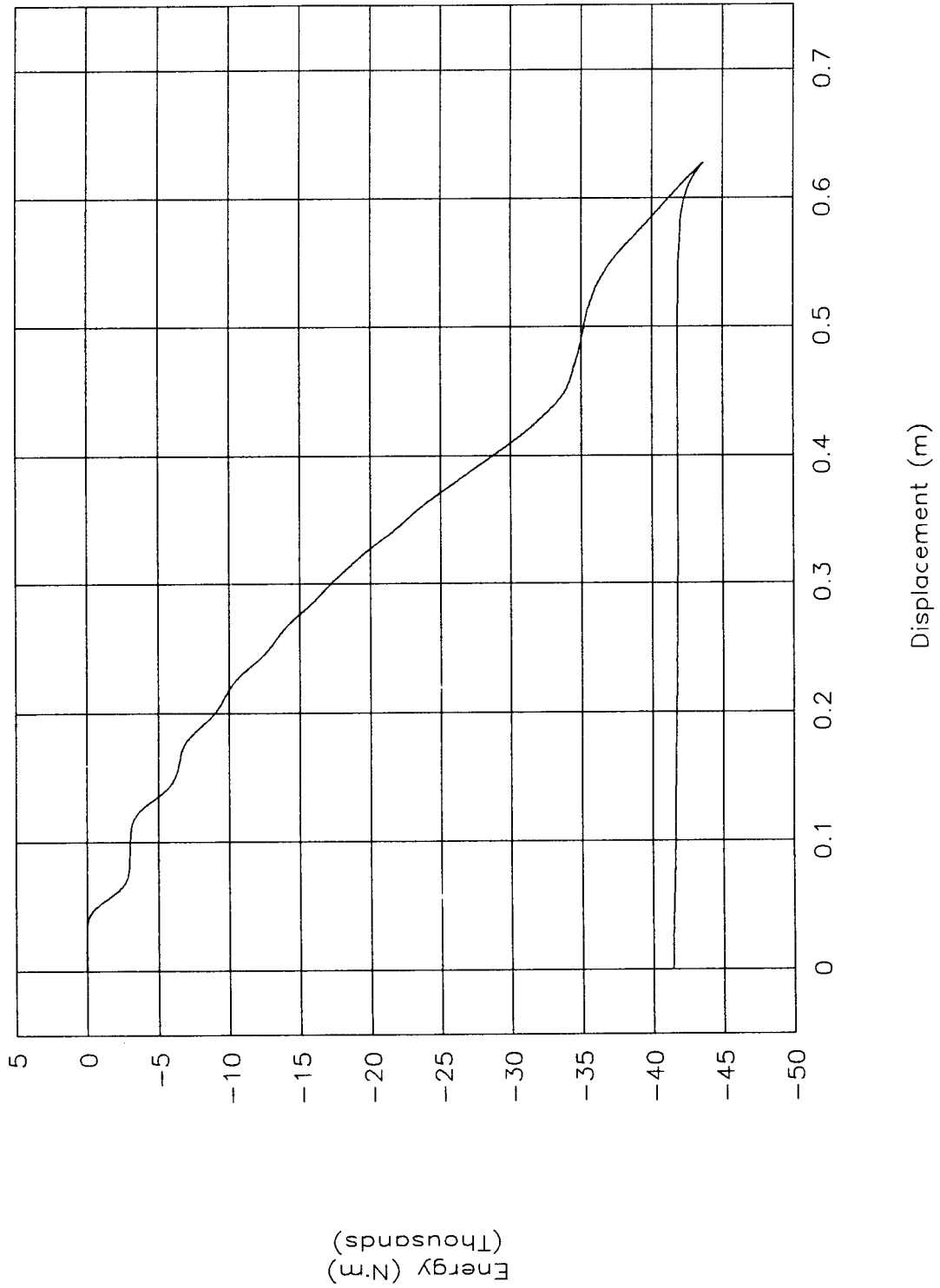


Figure 65. Energy vs. displacement, test 96P006.

TEST NO. 96P006

Strain vs. time (left front)

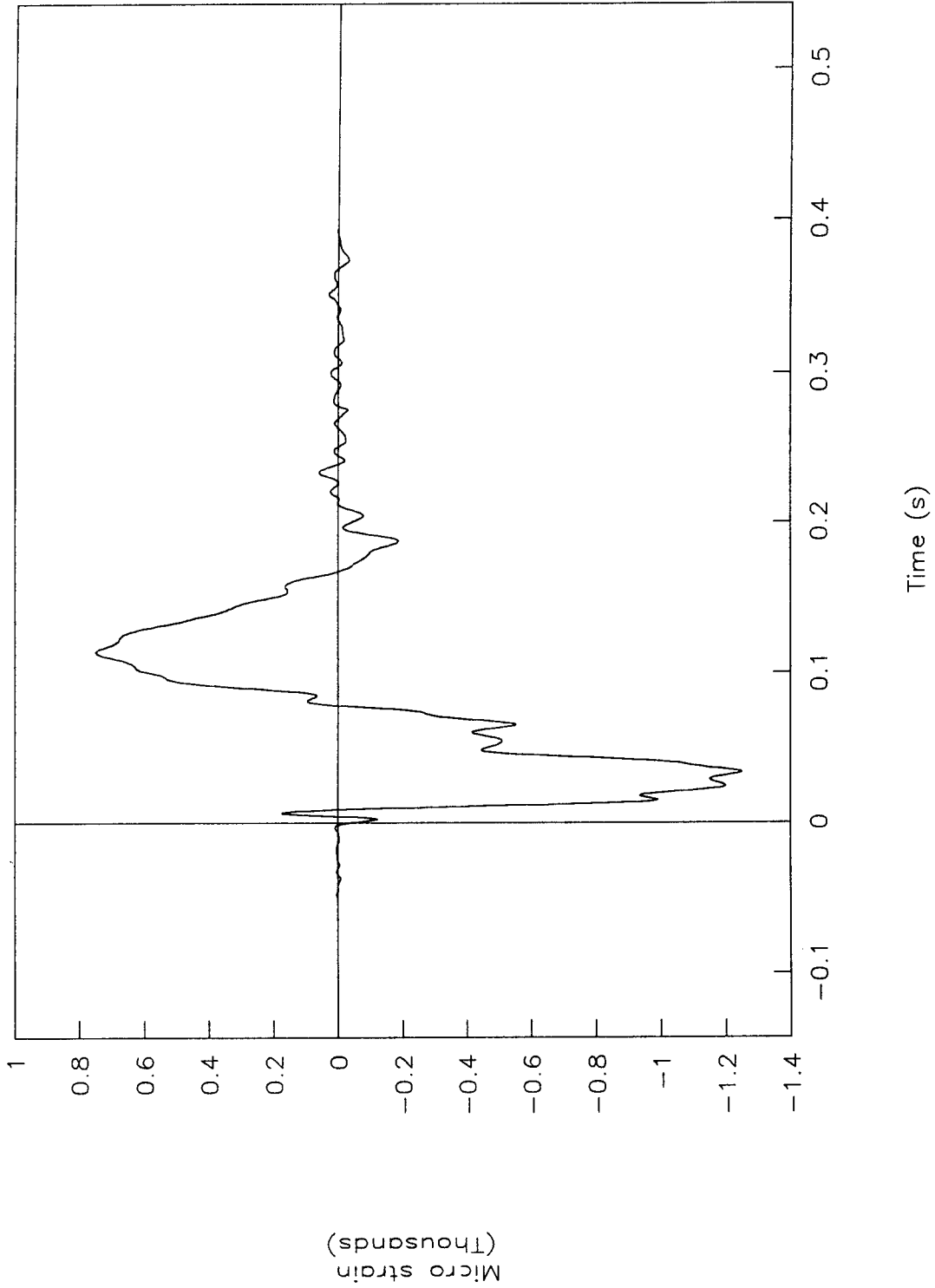


Figure 66. Strain vs. time (left front), test 96P006.

TEST NO. 96P006
Strain vs. time (right front)

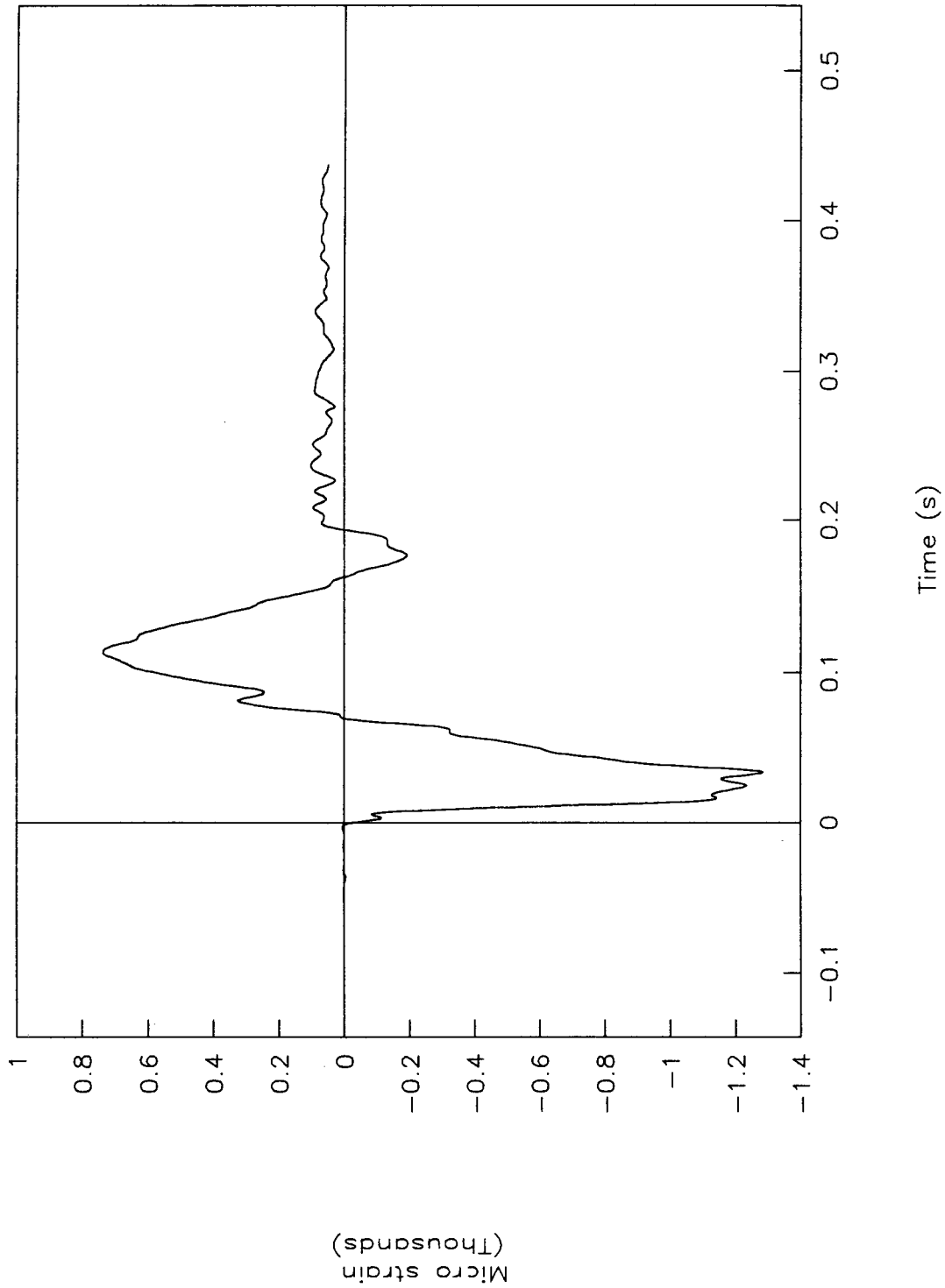


Figure 67. Strain vs. time (right front), test 96P006.

TEST NO. 96P006

Strain vs. time (left rear)

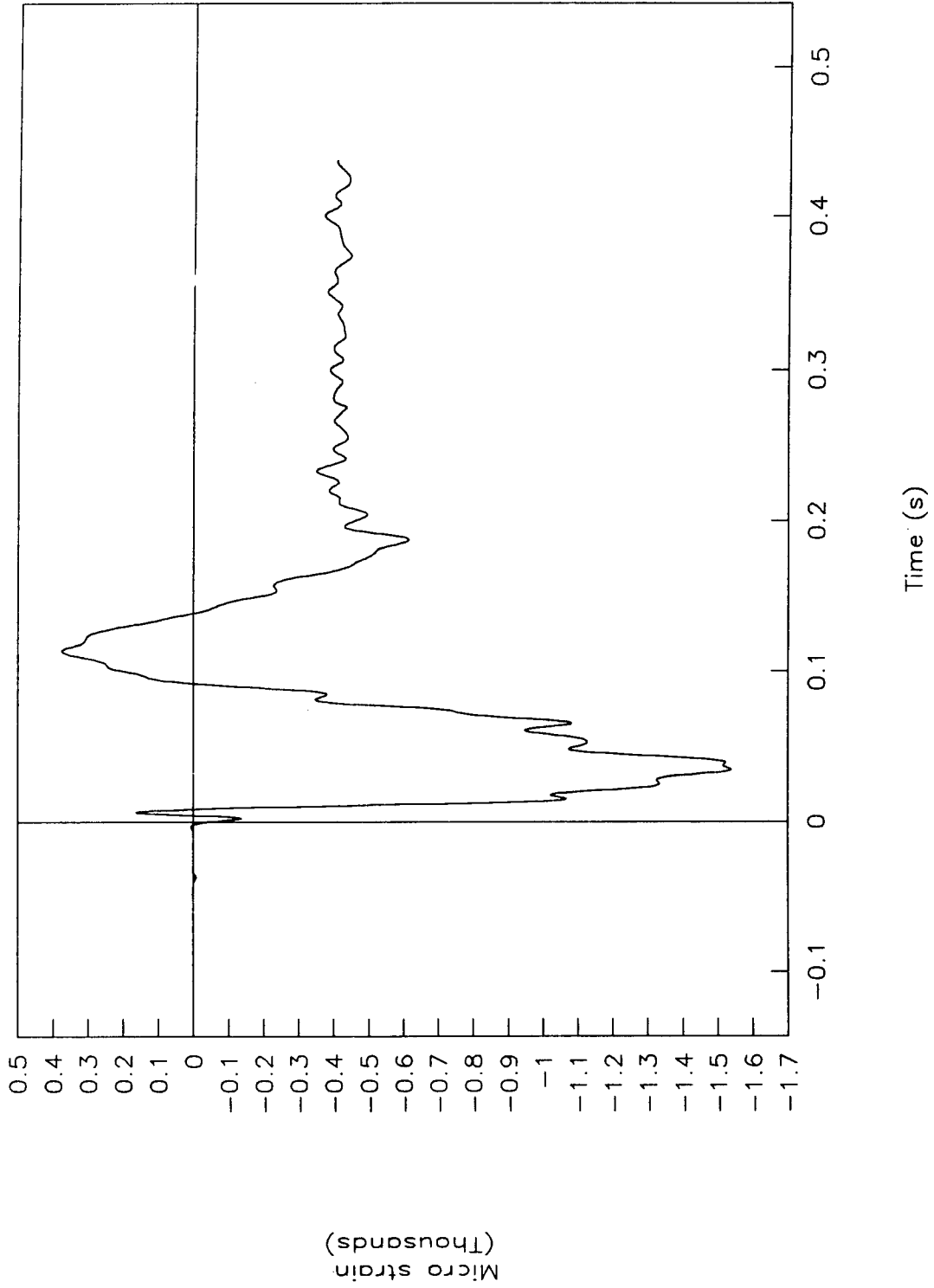


Figure 68. Strain vs. time (left rear), test 96P006.

TEST NO. 96P006

Strain vs. time (right rear)

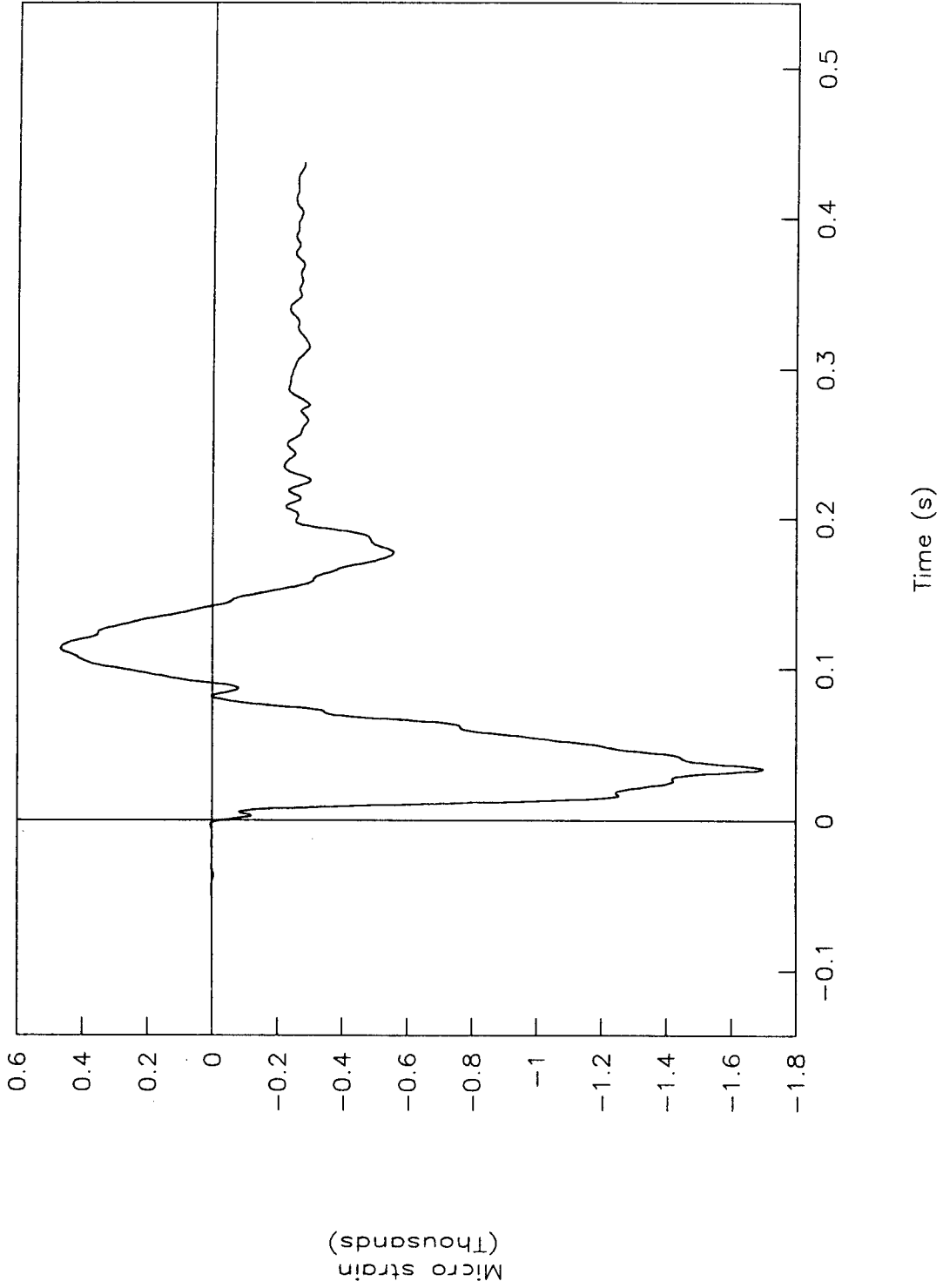


Figure 69. Strain vs. time (right rear), test 96P006.

REFERENCES

- (1) Christopher M. Brown, Alrik L. Svenson, pending report, *Pendulum Impact Testing of Steel W-Beam Guardrail*, Federal Highway Administration, Washington, DC.
- (2) H. E. Ross, Jr., D. L. Sicking, R. A. Zimmer, and J.D. Michie, *Recommended Procedures for the Safety Performance Evaluation of Highway Features*, NCHRP Report 350, National Highway Research Program, Transportation Research Board, Washington, DC, 1993.

☆ U.S. GOVERNMENT PRINTING OFFICE 1997-428-888/60144



HSR-30/6-97(255)QE

NTIS does not permit return of items for credit or refund. A replacement will be provided if an error is made in filling your order, if the item was received in damaged condition, or if the item is defective.

Reproduced by NTIS

National Technical Information Service
Springfield, VA 22161

*This report was printed specifically for your order
from nearly 3 million titles available in our collection.*

For economy and efficiency, NTIS does not maintain stock of its vast collection of technical reports. Rather, most documents are printed for each order. Documents that are not in electronic format are reproduced from master archival copies and are the best possible reproductions available. If you have any questions concerning this document or any order you have placed with NTIS, please call our Customer Service Department at (703) 487-4660.

About NTIS

NTIS collects scientific, technical, engineering, and business related information — then organizes, maintains, and disseminates that information in a variety of formats — from microfiche to online services. The NTIS collection of nearly 3 million titles includes reports describing research conducted or sponsored by federal agencies and their contractors; statistical and business information; U.S. military publications; audiovisual products; computer software and electronic databases developed by federal agencies; training tools; and technical reports prepared by research organizations worldwide. Approximately 100,000 *new* titles are added and indexed into the NTIS collection annually.

For more information about NTIS products and services, call NTIS at (703) 487-4650 and request the free *NTIS Catalog of Products and Services*, PR-827LPG, or visit the NTIS Web site
<http://www.ntis.gov>.

NTIS

*Your indispensable resource for government-sponsored
information—U.S. and worldwide*



U.S. DEPARTMENT OF COMMERCE
Technology Administration
National Technical Information Service
Springfield, VA 22161 (703) 487-4650
